Proceedings of the

Sixth International Symposium on the Vibrations of Continuous Systems

PlumpJack Squaw Valley Inn
Olympic Valley, California
July 23-27, 2007

PREFACE

The International Symposium on Vibrations of Continuous Systems is a forum for leading researchers from across the globe to meet with their colleagues and present both old and new ideas on the field. Each participant has been encouraged to either present results of recent, significant research or to reflect on some aspect of the vibration of continuous systems which is particularly interesting, unexpected, or unusual. This latter type of presentation was proposed to encourage participants to draw on understanding obtained through – in many cases – decades of research. In addition to the technical sessions, there is ample opportunity for the participants to meet in a very informal manner during excursions and hikes, when it is found that both technical and non technical discussions take place, with the researchers benefiting enormously from getting to know their colleagues from around the world at a level not accomplished during normal conference settings.

The Sixth ISVCS takes place July 22-27, 2007 at the PlumpJack Squaw Valley Inn. The PlumpJack Inn is one of Squaw Valley's original properties dating back to 1959 when it housed the 1960 Olympic delegation. It was fully remodeled and upgraded in 1995 and has a first-rate conference center. Squaw Valley is five miles from Lake Tahoe, one of the most scenic places in the United States, if not in the world. It is located in the Sierra Nevada mountain range on the California-Nevada border about 200 miles east of San Francisco. Lake Tahoe is renowned for the depth and clarity of its water, which produce its beautiful blue hues.

These Proceedings contain 18 summaries of the presentations to be made at the Symposium and short biographical sketches submitted by the participants.

Editorial Chairman
Stuart M. Dickinson

Local Arrangements Chairman
James R. Hutchinson

Registration Chairman
Ali H. Nayfeh

General Chairman
Arthur W. Leissa

CONTENTS

Summaries

Buckling and Oscillations of a Slender Elastic Beam in a Plane – A Systematic Perturbation Analysis ---------- 1
E. W. Brommund

Variational Statements for Vibration Analysis of Multifield Problems and Multilayered Structures ---------- 4
E. Carrera, S. Brischetto, and P. Nali

Predicting Damping in Engineered Structures ---------- 7
M. S. Ewing and W. Liu

A Critical Look at the Dirac Function and its Role in Representing Concentrated Harmonic Forces in Vibration Analysis of Structures ---------- 10
D. J. Gorman

Friction Induced Vibrations of a Rotating Kirchhoff Plate: An Excitation Mechanism of Disk Brake Squeal ---------- 13
D. Hochlenert and P. Hagedorn

Vibration of Sectorial and Skew Mindlin Plates with Corner Stress Singularities ---------- 16
C. S. Huang and M. J. Chang

Axisymmetric Vibrations of Thick Clamped Circular Plates Revisited ---------- 19
J. R. Hutchinson

Bounded Eigenvalues of Completely Free Rectangular Plates ---------- 22
Y. Mochida and **S. Ilanko**

On Meaningless Vibration Analysis for Bodies Having Elastic Constraints ---------- 25
A. Leissa

Symplectic Elasticity Approach for Free Vibration of Rectangular Thin Plates ---------- 28
C. W. Lim

A Theory of Stability of a Moving Oscillator on an Infinitely Long, Flexibly Supported Beam ---------- 31
A. V. Metrikine

Experiments on Chaotic Vibrations of a Post-Buckled Rectangular Plate under Compression Normal to Clamped Edges ---------- 34
K. Nagai, S. Maruyama, M. Kurosawa, and T. Yamaguchi

Free Vibration of Shallow Shells with General Surfaces Expressed in Cubic Polyonomial Function ---------- 37
Y. Narita and D. Narita

Resonant Vibration of Planetary Gears Having an Elastic Continuum Ring Gear Excited by Mesh Stiffness Fluctuations ---------- 40
X. Wu and **R. G. Parker**

Dynamics of Circular Cylindrical Shells ---------- 43
F. Pellicano

Oscillation of a Sheet of Falling Water ---------- 46
Y. Sato

Vibration Analysis Of Open Shells Of Revolution ---------- 49
A.V. Singh and Selvakumar Kandasamy

On Bending-Torsional Flutter of a Cantilever with Tip Fluid Jet ---------- 52
J. Wauer and F. C. Moon

Biographical Sketches of Participants

Brommundt, E. ----------57
Carrera, E. ----------58
Dickinson, S.M. ----------59
Ewing, M.S. ----------60
Gorman, D.J. ----------61
Hagedorn, P. ----------62
Hochlenert, D. ----------63
Huang, C.S. ----------64
Hutchinson, J.R. ----------65
Ilanko, S. ----------66
Leissa, A.W. ----------67
Lim, C.W. ----------68
Metrikine, A.V. ----------69
Nagai, K ----------70
Narita, Y. ----------71
Parker, R.G. ----------72
Pellicano, F. ----------73
Sato, Y. ----------74
Seemann, W. ----------75
Singh, A.V. ----------76
Spelsberg-Korspeter, G. ----77
Wauer, J. ----------78

Buckling and Oscillations of a Slender Elastic Beam in a Plane - A Systematic Perturbation Analysis

Eberhard W. Brommundt,
Institut für Dynamik und Schwingungen, Technische Universität Braunschweig,
PF 3329, D-38023 Braunschweig, Germany, E.Brommundt@tu-bs.de

The idea for this investigation stems from the paper by Nayfeh and Kreider [1], which studies analytically the vibrational modes of buckled beams for various boundary conditions. For the case of a fixed-fixed buckled beam, see Fig.1, the analytical results agree very well with experimental results also reported in the paper. The analysis of the buckling and the oscillations is based on a non-linear partial differential equation which, surprisingly, does not permit the transition $EI/(EA\cdot L^2)\to 0$, where EA = longitudinal stiffness, EI = bending stiffness, and L = length of the beam, see Fig.1. The question arises: shouldn't the effects of the longitudinal compressibility of the beam vanish for very thin beams?

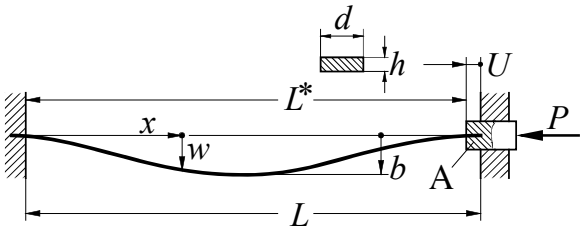

Fig.1: Buckled beam, U – fixed

The goal of the presentation will be, first, a set of nonlinear equations for the motions of an initially straight slender elastic beam in a plane that permits the transition $EI/(EA\cdot L^2)\to 0$. On the basis of these equations, secondly, we study buckling and oscillations by systematic perturbation procedures with respect to the small parameter $\nu = b/L$, where b = nominal sag, and compare the results with those of reference [1]. Here, we introduce briefly the equations of motion and prepare them for the perturbation scheme.

Let the central axis of the beam be placed on the horizontal s-axis of a Cartesian coordinate system, see Fig.2a. Let s be the material (Lagrange) coordinate along the beam. Let $u(s,t)$ and $w(s,t)$ measure its displacements in the horizontal and the vertical (downwards positive) direction, respectively, see Fig.2b; (t = time, $(\cdot)' = \delta_s(\cdot)$, $(\cdot)^{\cdot} = \delta_t(\cdot)$). From Fig.2b we read the axial strain

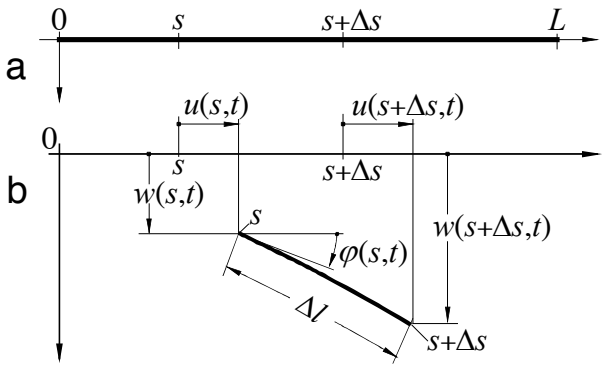

Fig.2: The coordinates and displacements

$$\varepsilon_a = R - 1, \tag{1}$$

where R denotes the square root

$$R = \sqrt{(1+u')^2 + w'^2}. \tag{2}$$

The slope angle $\varphi(s,t)$ satisfies

$$\sin\varphi = w'/R,\ \cos\varphi = (1+u')/R. \tag{3}$$

For convenience we restrict φ to $|\varphi| < \pi/2$. We assume small strains, $|\varepsilon_a| \ll 1, |\varphi'\cdot h| \ll 1$, and neglect shear deformation.

For the axial force F_a, see Fig.3a,

$$F_a = EA\,\varepsilon_a, \tag{4}$$

where E = modulus of elasticity and A = cross-sectional area. The bending moment M is given by

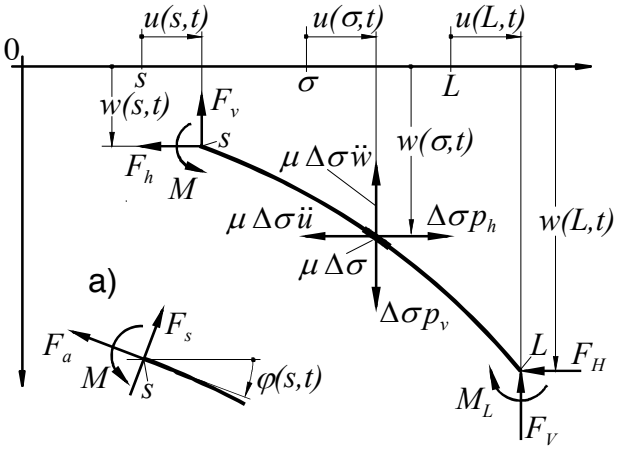

Fig.3: Forces and moments applying at the segment $s \le \sigma \le L$ of the beam

$$M = EI{\cdot}R/\rho = EI\,\varphi', \tag{5}$$

where I = second moment of the cross-sectional area, $1/\rho$ = curvature of the center-line.

Fig.3 shows the segment $s \le \sigma \le L$ of the beam with the applying forces, where $\sigma =$ auxiliary coordinate. At the cut *s*, the bending moment M and the forces $F_h, F_v,$ horizontally and vertically, respectively, exist, with positive orientations against the displacements. At the beam's end, $\sigma = L,$ these quantities are $M_L,$ $F_H, F_V.$ The distributed loads p_h, p_v act along the length of the beam, positively in the direction of the displacements, with the inertia forces $\mu\ddot{u}, \mu\ddot{w},$ (μ = distributed mass); the distributed rotary inertia is neglected.

The forces F_h, F_v at the cut *s* are transformed to the axial force F_a and the shear force $F_s,$ cf. Fig.3/3a:

$$F_a = F_h\cos\varphi + F_v\sin\varphi,\; F_s = -F_h\sin\varphi + F_v\cos\varphi. \tag{6}$$

The conditions for force equilibrium at the displaced beam segment shown in Fig.3 lead to the forces $F_h, F_v,$ and the moment equilibrium about the point *s* of the beam yields the bending moment *M*.

Then from $(6)_1$ and the formulae (1) to (5), after some manipulation, the two integro-differential equations result:

$$\begin{aligned}(R-1)\,EA = &-\frac{1+u'}{R}\left\{F_H + \int_{\sigma=s}^{L}\left(\mu\ddot{u}(\sigma,t) - p_h(\sigma,t)\right)\mathrm{d}\sigma\right\}\\ &-\frac{w'}{R}\left\{F_V + \int_{\sigma=s}^{L}\left(\mu\ddot{w}(\sigma,t) - p_v(\sigma,t)\right)\mathrm{d}\sigma\right\},\end{aligned} \tag{7}$$

$$\begin{aligned}\frac{(1+u')\,w'' - u''\;w'}{R^2}EI = {} & M_L + F_H\left[w(L,t) - w(s,t)\right] - F_V\left[\left(L\;+\;u(L,t)\right) - \left(s\;+\;u(s,t)\right)\right]\\ &+\int_{\sigma=s}^{L}\left[w(\sigma,t) - w(s,t)\right]\left(\mu\ddot{u}(\sigma,t) - p_h(\sigma,t)\right)\mathrm{d}\sigma\\ &-\int_{\sigma=s}^{L}\left[\left(\sigma + u(\sigma,t)\right) - \left(s + u(s,t)\right)\right]\left(\mu\ddot{w}(\sigma,t) - p_v(\sigma,t)\right)\mathrm{d}\sigma.\end{aligned} \tag{8}$$

To complete the above equations of motion, a set of six boundary conditions is necessary (we will neglect here the initial conditions). For the beam of Fig.1 the following equations apply, when a fixed displacement is *U* given:

$$\begin{aligned}&\text{at } s = 0\text{: } u(0,t) = \;\; 0,\; w(0,t) = 0, \varphi(0,t) = 0,\\ &\text{at } s = L\text{: } u(L,t) = -U, w(L,t) = 0, \varphi(L,t) = 0.\end{aligned} \tag{9}$$

Instead of $u(L,t) = -U$ the conditions $u(L,t) = -U(t)$ or $F_H = P(t),$ with given $U(t), P(t),$ respectively, might be of interest for the shown beam.

We work on the basis of the integro-differential equations (7), (8), for their individual terms have immediate physical meaning. For example, division of equation (7) by EA and transition $EA \to \infty$ leads to $R = 1$, i.e., for the inextensible beam the equation (7) is replaced by

$$2u' + u'^2 + w'^2 = 0. \tag{10}$$

It is easy to solve the integrals of the equations (7), (8) by proper differentiations; but the terms of the equations will become more intricate. However, even after such differentiations there will remain products of inertia terms (accelerations) and displacements or displacement derivatives. Is this a characteristic of the system?

For an answer we look at Hamilton's Principle (no calculations are necessary): The kinetic energy T and the elastic potential V of the beam, which enter the principle, have the forms

$$T = \tfrac{1}{2}\int_{s=0}^{L} \left(\dot{u}^2 + \dot{w}^2\right)\mu \, ds, \; V = \tfrac{1}{2}\int_{s=0}^{L} \left(EA\,\varepsilon_a^2 + EI\varphi'^2\right) ds, \tag{11}$$

where ε_a and φ' are calculated from (1) and (3). The standard manipulations to get the equations of motion by the principle require partial integrations only. Thus, no products of accelerations and displacements will result but the terms that cover the elastic behavior will become involved.

The perturbation procedure is done for the dimensions of the beam of [1]. They are (in metric form): $L = 279.17$ mm, $h = 0.831$ mm, $b \approx 2.5$ mm, d – cancels. We choose the reference quantities length: $L_R = L,$ force: $F_R = EI/L^2,$ frequency: $\omega_R = \sqrt{EI/(\mu L^2)},$ and the small parameter $\nu = b/L_R \approx 0.01.$ A comparison of the magnitudes of the individual quantities and terms of the equations leads to the following normalized variables, marked by a tilde:

$$\tilde{s} = s/L_R, \tilde{\sigma} = \sigma/L_R, \tilde{t} = \omega_R\, t, u(s,t) = \nu^2 L_R\, \tilde{u}(\tilde{s},\tilde{t}), w(s,t) = \nu L_R\, \tilde{w}(\tilde{s},\tilde{t}), p_v(s,t) = F_R/L_R \cdot \nu\, \tilde{p}_v(\tilde{s},\tilde{t}),$$
$$p_h \equiv 0, F_H = F_R\, \tilde{F}_H, F_V = \nu F_R\, \tilde{F}_V, M_L = \nu L_R\, F_R \tilde{M}_L; EI/EA = r_I^2, r_I/L_R = 8.59 \cdot 10^{-4} =: \nu\, \tilde{r}_I.$$

The normalized equations of motion read

$$\frac{2\tilde{u}' + \varepsilon\tilde{u}'^2 + \tilde{w}'^2}{1+\tilde{R}} = -\tilde{r}_I^2 \frac{1+\varepsilon\tilde{u}'}{\tilde{R}} \left\{ \tilde{F}_H + \varepsilon \int_{\tilde{s}}^{\tilde{L}} \ddot{\tilde{u}}(\tilde{\sigma},\tilde{t})\, \mathrm{d}\tilde{\sigma} \right\} - \tilde{r}_I^2 \frac{\varepsilon\tilde{w}'}{\tilde{R}} \left\{ \tilde{F}_V + \int_{\tilde{s}}^{\tilde{L}} \left(\ddot{\tilde{w}}(\tilde{\sigma},\tilde{t}) - \tilde{p}_v(\tilde{\sigma},\tilde{t}) \right) \mathrm{d}\tilde{\sigma} \right\}, \tag{12}$$

$$\begin{aligned} \frac{(1+\varepsilon\tilde{u}')\tilde{w}'' - \varepsilon\tilde{u}''\tilde{w}'}{\tilde{R}^2} = {} & \tilde{M}_L + \tilde{F}_H \left[\tilde{w}(\tilde{L},\tilde{t}) - \tilde{w}(\tilde{s},\tilde{t}) \right] - \tilde{F}_V \left[\left(\tilde{L} + \varepsilon\tilde{u}(\tilde{L},\tilde{t}) \right) - \left(\tilde{s} + \varepsilon\tilde{u}(\tilde{s},\tilde{t}) \right) \right] \\ & + \varepsilon \int_{\tilde{s}}^{\tilde{L}} \left[\tilde{w}(\tilde{\sigma},\tilde{t}) - \tilde{w}(\tilde{s}\ \ddot{\tilde{u}}(\tilde{\sigma},\tilde{t}),\tilde{t}) \right] \mathrm{d}\tilde{\sigma} \\ & - \int_{\tilde{s}}^{\tilde{L}} \left[\left(\tilde{\sigma} + \varepsilon\tilde{u}(\tilde{\sigma},\ \tilde{t}) \right) - \left(\tilde{s} + \varepsilon\tilde{u}(\tilde{s},\tilde{t}) \right) \right] \left(\ddot{\tilde{w}}(\hat{\sigma},\tilde{t}) - \tilde{p}_v(\hat{\sigma},\tilde{t}) \right) \mathrm{d}\tilde{\sigma}, \end{aligned} \tag{13}$$

where the derivatives are to be taken with respect to $\tilde{s}$ and $\tilde{t},$ and

$$\varepsilon := \nu^2 \approx 0.0001, \;\; \tilde{R} := \sqrt{(1+\varepsilon\tilde{u}')^2 + \varepsilon\tilde{w}'^2}. \tag{14}$$

The boundary conditions (9) are normalized likewise.

These equations and parameters will be the starting point of the perturbation procedures.

Reference:

[1] A.H. Nayfeh, W. Kreider: Investigations of natural frequencies and mode shapes of buckled beams. AIAA Journal, 33 (1995), pp. 1121 - 1126

Variational Statements for Vibration Analysis of Multifield Problems and Multilayered Structures

E. Carrera, S. Brischetto, P. Nali
Aerospace Department, Politecnico di Torino, Italy
e.mail: erasmo.carrera@polito.it

It is widely believed that much of next generation aircraft and spacecraft will be manufactured as multilayered structures (MLS) under the action of a combination of two or more of fields such as mechanical, thermal, electrical and magnetical fields. Two examples of multi-field problem (MFP) application are: the so called 'smart structures' in which layers of piezo-electric or piezo-magnetical materials are used as sensor or actuators to develop electro-magnetical fields able to counteract thermo-mechanical deformation; inflatable structures that have been planned to be used for the future space exploration mission, which consist of a very special multilayered-made structure subject to thermo-mechanical loadings and in some cases to electric-magnetical loadings as well. These two examples show that structures that are typically employed in MFP appear as assemblies of flat or curved MLS. Vibration response of these structures is one of the topics that should be considered for their use. A number of requirements must be taken into account for accurate vibration analysis of MFP/MLS. In particular, appropriate variational statements and kinematic description of the various fields in the thickness plate/shell direction must be employed to accurately describe the various couplings among the applied fields. These two points are dealt with in the present paper.

Constitutive Equations (CE). The derivation of CE is a starting point in the analysis of MFP. In the case of linearity, let's assume as independent variables θ, ϵ, E and H, which represent increments of temperature, strain, electric field and magnetic field, respectively. The relevant thermodynamic function is the Gibbs free energy per unit of volume G [1]:

$$G = U - \theta\eta - \sigma_{ij}\epsilon_{ij} - E_i D_i - H_i B_i, \qquad i,j = 1,2,3 \tag{1}$$

where, $1,2,3$ denote a reference system in the body volume V; U is the internal energy per unit of volume, η is the entropy per unit of volume; σ_{ij} are stress components; D_i are electrical displacement components; B_i are magnetic inductance components. Standard tensor notation is used and Einstein's summation convention is intended over repeated indices. Upon differentiation of the function G and by substituting appropriate material constants, a set of constitutive relations in the coupled four-field system (θ, ϵ, E, H) can be obtained. Explicit forms are given in [2].

Classical Variational Statement (CVS). Governing equations in both weak or strong form of the considered MFP could be conveniently obtained by employing appropriate variational statements. If only primary variables are used as problem unknowns, the extension of the Principle of Virtual Displacement (PVD) in the dynamic case, is written in the following form:

$$\int_V (\eta\delta\theta + \sigma_{ij}\delta\epsilon_{ij} + D_i\delta E_i + B_i\delta H_i)\, dV \; = \delta L_e + \delta L_{in} \tag{2}$$

δL_e is the virtual variation of the work made by the external loads; δL_{in} is the virtual variation of the work made by the inertial loads.

The PVD statement at Eq.(2) can lead to various subcase problems; these all could be obtained by neglecting some of the considered virtual variations. A complete discussion has been provided in [2]. As an example we consider the extreme case in which a pure thermal problem is considered; that is only the temperature $\delta\theta$ is considered as virtual variation. The PVD leads to the following:

$$\int_V \delta\theta \;\; \eta \, dV \;=\; \delta L_e + \delta L_{in}. \tag{3}$$

Mixed Variational Statement (MVT). Multilayered structures are often used in MFP. A number of requirements must be addressed to provide accurate analysis of these structures. Among them, the fulfillment of the continuity of relevant secondary variables in the thickness plate/shell directions (the so called Zig-Zag effect, ZZ, and inter-laminar continuity, IC) at the interface between two adjacent layers are such necessary amendments. In [3] these requisites were referred to by the acronym C_z^0–requirements, which state that some of the MF variables are C^0–continuous functions in the thickness coordinate z.

A valuable variational tool that permits one the 'a priori' fulfillment of the C_z^0-Requirements, is the extended Reissner Mixed variational Theorem, RMVT. RMVT was originally proposed for the pure mechanical case [3]. Its extension to MFP, in the dynamic case, leads to the following variational statement:

$$\begin{aligned}\int_V \delta\boldsymbol{\epsilon}_{pG}^T\boldsymbol{\sigma}_{pH} + \delta\boldsymbol{\epsilon}_{nG}^T\boldsymbol{\sigma}_{nM} + \delta\boldsymbol{\sigma}_{nM}^T(\boldsymbol{\epsilon}_{nG} - \boldsymbol{\epsilon}_{nH}) + \delta\theta_G\eta_H + \delta\boldsymbol{E}_{pG}\boldsymbol{D}_{pH} + \delta\boldsymbol{E}_{nG}\boldsymbol{D}_{nM} + \\ \delta\boldsymbol{D}_{nM}^T(\boldsymbol{E}_{nG} - \boldsymbol{E}_{nH}) + \delta\boldsymbol{H}_{pG}\boldsymbol{B}_{pH} + \delta\boldsymbol{H}_{nG}\boldsymbol{D}_{nM} + \delta\boldsymbol{B}_{nM}^T(\boldsymbol{H}_{nG} - \boldsymbol{H}_{nH})dV = \delta L_e + \delta L_{in}\end{aligned} \tag{4}$$

Bold letters denote array; subscripts p and n denote in-plane and out-of-plane components, respectively. Tranverse normal and shear stresses $\sigma_{33}, \sigma_{13}, \sigma_{23}$, transverse electrical displacement D_3 and magnetical inductance B_3 are considered as independent variables, therefore these last can be assumed continuous at each layer interface. Subscripts H, G and M denote variables from CE, geometrical relations and assumed models, respectively.

Several sub-cases can be obtained by RMVT by considering all the possible combination of virtual variation active in the model, see [2]. For instance, RMVT for the coupled Magneto-Mechanical case, would lead to the following choice for the virtual variations: δu_1, δu_2, δu_3, $\delta\varphi$, $\delta\sigma_{33}$, $\delta\sigma_{13}$, $\delta\sigma_{23}$, δB_n. The related variational statement is,

$$\begin{aligned}\int_V \delta\boldsymbol{\epsilon}_{pG}^T\boldsymbol{\sigma}_{pH} + \delta\boldsymbol{\epsilon}_{nG}^T\boldsymbol{\sigma}_{nM} + \delta\boldsymbol{\sigma}_{nM}^T(\boldsymbol{\epsilon}_{nG} - \boldsymbol{\epsilon}_{nH}) + \delta\boldsymbol{H}_{pG}\boldsymbol{B}_{pH} + \delta\boldsymbol{H}_{nG}\boldsymbol{D}_{nM} + \\ +\delta\boldsymbol{B}_{nM}^T(\boldsymbol{H}_{nG} - \boldsymbol{H}_{nH})dV = \delta L_e + \delta L_{in}\end{aligned} \tag{5}$$

Results. The various CVSs and MVS that have been recently proposed in [2], are in the present work extended to evaluate the vibration response of MLS for MFP. Numerical results are obtained in the framework of Unified Formulation (UF) recently detailed in [4]. UF permits a comprehensive modeling of homogeneous and multilayered plates. Both Layer-Wise (LW) and Equivalent Single Layer (ESL) models have been addressed. Those theories which preserve the number of variables independent of the number of the constitutive layers are herein denoted by ESLM, while those theories in which the same variables are kept independent in each layer are denoted by LWM. Higher order ESLM plate theories formulated on the basis of PVD are compared in Table 1 for the first three modes. The coupled piezo-mechanical problems in [5] are considered, see [5] for details. Errors are quoted. Plate theories with linear, parabolic and cubic expansion in the thickness direction are compared in both thin (a/h=4) and thick plate (a/h=50) geometries. Table 1 clearly shows the possibility of increasing the accuracy by employing higher order kinematic description. PVD results are compared to RMVT ones in the

same Table. Layer-wise plate theories are considered. Two cases of RMVT are given: RMVT-1 and RMVT-2. The 'a priori' IC of transverse electric displacement components at the layer interface is included in the RMVT-2 case. The results clearly show the possibilities of MVS to improve CVS analysis. It is concluded that both variable kinematic models and mixed variational statements could be considered to accurately describe the vibration response of MLS in the MFP framework.

References

[1] Ikeda T, Fundamentals of piezoelectriticy, Oxford University Press, 1996.

[2] Carrera E, Brischetto S, Nali P, 2007, Variational Statements and Computational Models for Multifield Problems, Multilayered Structures, Mechanics of advanced Materials and Structures, in press

[3] Carrera E , 2001, Developments, ideas and evaluations based upon the Reissner's mixed theorem in the modeling of multilayered plates and shells, *Applied Mechanics Review* , vol 54, pp 301–329.

[4] Carrera E , 2003, Theories and Finite Elements for multilayered plates and shells: A Unified compact Formulation with numerical assessment and benchmarking. Archives of Computational Methods in Engineering, State of the art reviews, vol 10, pp 215-296

[5] Heyliger P, Saravanos D A, 1995, Exact free-vibration analysis of laminated plates with embedded piezoelectric layers, Journal of the Acoustical Society of America, vol 98, pp 1547-1557

	$a/h = 4$			$a/h = 50$		
	$Mode\ 1$	$Mode\ 2$	$Mode\ 3$	$Mode\ 1$	$Mode\ 2$	$Mode\ 3$
$3D - Exact$	57074.5	191301	250769	618.118	15681.6	21492.8
	3D Higher order theories results - ESLM analysis					
$linear$	74105.9	196021	266337	689.867	15694.9	21507.4
$Err(\%)$	(-29.84)	(-2.47)	(-6.21)	(-11.61)	(-0.08)	(-0.07)
$parabolic$	69413.8	195860	262204	620.300	15694.9	21505.2
$Err(\%)$	(-21.62)	(-2.38)	(-4.56)	(-0.35)	(-0.08)	(-0.06)
$cubic$	58818.6	195825	259586	618.551	15694.2	21500.1
$Err(\%)$	(-3.06)	(-2.36)	(-3.52)	(-0.07)	(-0.08)	(-0.03)
	CVS and MVS results - LWM analysis					
PVD	57252.5	194840	255646	619.023	15683.4	21494.4
$Err(\%)$	(-0.31)	(-1.85)	(-1.94)	(-0.15)	(-0.01)	(-0.01)
$RMVT-1$	57056.6	194696	253955	617.996	15683.3	21493.9
$Err(\%)$	(0.03)	(-1.77)	(-1.27)	(0.02)	(-0.01)	(-0.01)
$RMVT-2$	57094.0	194697	253958	618.143	15683.3	21493.9
$Err(\%)$	(-0.03)	(-1.77)	(-1.27)	(0.00)	(-0.01)	(-0.01)

Table 1: Vibration problem for multilayered piezoelectric plate, first three modes. $\overline{\omega} = \omega/100$.

Predicting Damping in Engineered Structures

Mark S. Ewing, Associate Professor & Chair
Wanbo Liu, Graduate Research Assistant
University of Kansas Aerospace Engineering

Damping is a useful structural property whenever it is desirable to limit the amplitude of vibration. This is especially so when the amplitude of vibration is high enough to produce undesired noise or to result in structural failure through fatigue. However, predicting damped vibration response requires knowledge of the relevant *types* of damping involved and some measure of the *degree* of damping, possibly for multiple types of damping. For monolithic structure, either structural damping or fluidic damping tends to dominate. For structure which is mechanically joined, Coulomb (or, "sliding-friction" damping) tends to dominate. For structure treated with a well-engineered damping "treatment", this treatment is typically the dominant source of damping.

The problem at hand is the prediction of damping for beams and plates with and without uniform constrained layer damping (CLD). CLD involves structural elements treated with a viscoelastic damping layer which is covered by a "constraining" layer. Such 3-layer laminates are widely used to reduce vibration response. The predictive method detailed here is the Analytical Power Input Method (APIM) [1], which is based on the experimental method of determining the damping loss factor, the Power Input Method (PIM) [2]. The APIM, like any analytical method, is dependent on the measurement of material properties, especially the damping loss factors for any viscoelastic layers present.

Power Input Method

The power input method is based on measuring the ***damping loss factor***, which is the ratio of the dissipated energy to the energy stored in the structure, per radian:

$$\eta = \frac{E_D}{2 \cdot \pi \cdot E_S} \tag{1}$$

Here, E_D is the energy dissipated per cycle and E_S is the maximum strain energy. In most cases, the dissipated power is converted into heat, which cannot be easily measured. For a steady-state vibration, the dissipated power of the system, P_D, equals the input power, P_I, from the excitation. The dissipated power is the energy dissipated per cycle, that is: $P_D = \frac{1}{T} \cdot E_D = \frac{\omega}{2 \cdot \pi} \cdot E_D$, where T is the period of vibration. If the structure is driven at a single point, say via an electrodynamic shaker, the input power can be estimated from the time-averaged product of the force at the driving point $F_f(t)$ and the velocity at the driving point $V_f(t)$. That is, $P_D = P_I = \overline{F_f(t) \cdot V_f(t)}$. Usually the strain energy E_S cannot be easily measured, so it is replaced with twice the kinetic energy E_K: $E_S = 2 \cdot E_K = \int_v \rho \cdot \overline{V^2(t)}\, dv$.

Now the loss factor in terms of time-averaged expression is

$$\eta = \frac{\overline{F_f(t) \cdot V_f(t)}}{\omega \cdot \int_v \rho \cdot \overline{V^2(t)}\, dv} \tag{2}$$

To characterize the time-averaged quantities in terms of typical measurement quantities, the dissipated power is:

$$P_D = \overline{F_f(t)\cdot V_f(t)} = R_{F_fV_f}(0) = \frac{1}{\pi}\cdot\int_0^\infty \mathrm{Re}\left[S_{F_fV_f}(\omega)\right]\, d\omega = \frac{1}{\pi}\cdot\int_0^\infty \mathrm{Re}\left[Y_{ff}(\omega)\right]\cdot S_{F_fF_f}(\omega)\; d\omega \tag{3}$$

and the strain energy is:

$$E_S = \int_v \rho\cdot\overline{V^2(t)}\; dv = \int_v \rho\cdot R_{V_iV_i}(0)\; dv = \int_v \rho\cdot\frac{1}{\pi}\cdot\int_0^\infty S_{V_iV_i}(\omega)\; d\omega\; dv \tag{4}$$

where $R_{F_fV_f}(0)$ is the cross correlation between the driving point force and velocity ; $R_{V_iV_i}(0)$ is the auto-correlation of the velocity at point *i*; ρ is the density of the structure; $S_{F_fV_f}(\omega)$ is the cross power spectrum density between the driving point force and velocity; $Y_{ff}(\omega)$ is the mobility (velocity/force) of the driving point; $S_{F_fF_f}(\omega)$ is the power spectrum density of the driving point force; $S_{V_iV_i}(\omega)$ is the power spectrum density of the *i*'th point velocity.

But, practically, the kinetic energy can only be represented by a finite number of measurements, *N*, representing the response over the whole structure: $E_S \cong \sum_{i=1}^{N} m_i\cdot\frac{1}{\pi}\cdot\int_0^\infty S_{V_iV_i}(\omega)\, d\omega$. This assumes that the excitation frequency varies from zero to infinity, but in a finite frequency-band $[\omega_1,\omega_2]$, the frequency-band averaged loss factor is defined as

$$\eta(\omega_C,\Delta\omega) = \frac{\int_{\omega_1}^{\omega_2}\mathrm{Re}\left[Y_{ff}(\omega)\right]\cdot S_{F_fF_f}(\omega)\; d\omega}{\sum_{i=1}^{N} m_i\cdot\int_{\omega_1}^{\omega_2}\omega\cdot S_{V_iV_i}(\omega)\; d\omega} \tag{5}$$

where ω_C is the center frequency of the frequency-band; $\Delta\omega$ is the bandwidth; ω_1 and ω_2 are the lower and upper limits of the frequency-band. For linear systems, $S_{V_iV_i}(\omega) = \left|Y_{if}(\omega)\right|^2\cdot S_{F_fF_f}(\omega)$, where $Y_{if}(\omega)$ is the mobility (velocity/force) between the driving point *f* and the point *i*. Finally the loss factor at a frequency ω becomes

$$\eta(\omega) = \frac{\mathrm{Re}\left[Y_{ff}(\omega)\right]}{\sum_{i=1}^{N} m_i\cdot\omega\cdot\left|Y_{if}(\omega)\right|^2} \tag{6}$$

Note that each term in Equation 6 can be measured directly.

Analytical Power Input Method

The analytical estimation of loss factor differs from the experimental estimation in that the strain energy E_S can be calculated directly. The input power in Equation 3 takes an alternative form as

$$P_D = P_I = \overline{F_f(t)\cdot V_f(t)} = \overline{F_f^{\,2}(t)}\cdot\mathrm{Re}\left[Y_{ff}(\omega)\right] = \frac{1}{2}\cdot\left|F_f(\omega)\right|^2\cdot\mathrm{Re}\left[Y_{ff}(\omega)\right] \tag{7}$$

where $F_f(\omega)$ is the Fourier transform of $F_f(t)$. Thus, the loss factor can be written as

$$\eta = \frac{\frac{1}{2}\cdot\left|F_f(\omega)\right|^2\cdot\mathrm{Re}\left[Y_{ff}(\omega)\right]}{\omega\cdot E_S} \tag{8}$$

This formulation can be implemented either analytically or computationally, for instance using the finite element method. Modeling the discrete layers in a constrained layer damping treatment is easy with the finite element method—and modeling non-uniform treatment is also easy. In any case, the

frequency-dependency of the viscoelastic material properties can be taken into account directly. And, any other type of damping may be implemented rather easily.

Implementation

The PIM and the APIM have been compared with the more popular modal strain energy method [3] in the study of an aluminum plate with a uniform constrained layer damping treatment. The figure below shows predicted damping loss factor for all 3 methods. One general observation is that the power input methods are based on forced response—which involves numerous modes of vibration—whereas the modal strain energy method is based on individual mode response. As such, the APIM may be more relevant for evaluating damping in an operating environment. The difference between methods is the greatest for the "lower" modes of vibration where the modal strain energy method significantly under-predicts damping. Another observation is that the analytical and experimental implementations of the power input method only agree well in the "mid-frequency" range. Some reasons for high frequency deviations have been discovered (experimental errors), but at low frequency, the reasons are elusive.

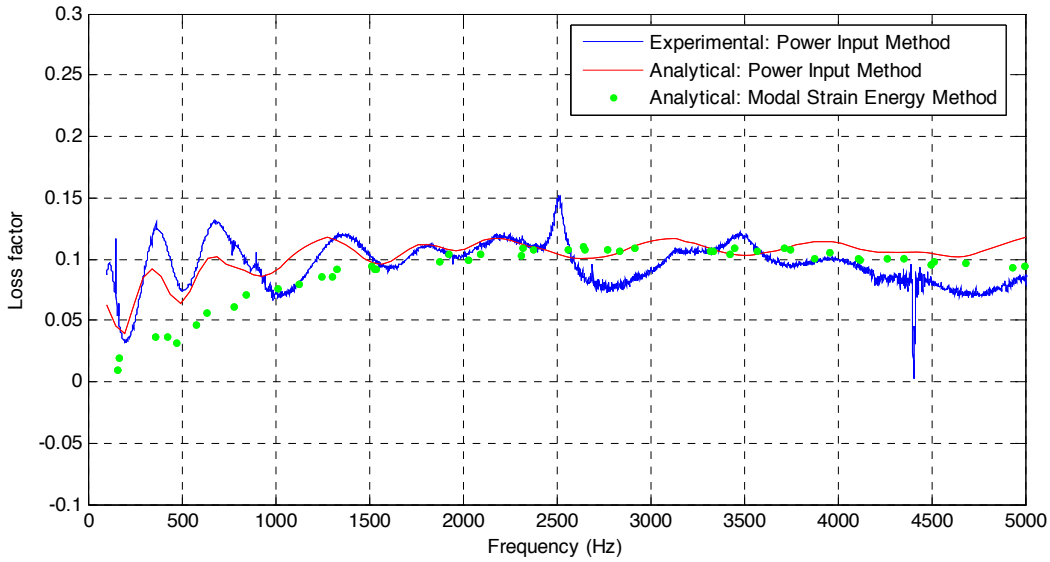

Further Discussion

The oral presentation will cover other demonstrations of the APIM on nomex-core sandwich carbon fiber beams with non-uniform constrained layer damping. Analytical formulations for the APIM for uniformly-damped beams and plates will also be discussed.

References

[1] Liu, W.B. and Ewing, M.S., Experimental and Analytical Estimation of Loss Factors by the Power Input Method, AIAA Journal, Vol 45, No 2, Feb 2007, pp 477-484.

[2] Carfagni, M. and Pierini, M., Determining the Loss Factor by the power input method (PIM), Par t 1: Numerical Investigation, Journal of Vibration and Acoustics, July 1999, Vol. 121, pp. 417-421.

[3] Johnson, C. D., Kienholz, D. A. and Rogers, L. C., "Finite element prediction of damping in beams with constrained viscoelastic layers", *Shock and Vibration Bulletin*. No. 50, 1981, Part 1, pp. 71-82.

A Critical Look at the Dirac Function and its Role in Representing Concentrated Harmonic Forces in Vibration Analysis of Structures

D. J. Gorman
Professor Emeritus, Dep't. of Mech. Eng. , University of Ottawa
Ottawa, Canada, K1N 6N5

Introduction:

Trigonometric series representations of the Dirac function are often employed to represent the amplitude of concentrated harmonic forces in the analysis of vibration of elastic structures. It is well known that such trigonometric series representations do not constitute the classic concept of the Dirac function which equals zero everywhere except in the immediate area of the concentrated force.

In this paper we look at some applications of the function in solving free vibration problems of various structures. We will be particularly interested in the rates of convergence of such solutions and the degree to which prescribed boundary conditions are actually satisfied.

Mathematical Illustrations.

We begin by solving some simple slender beam vibration problems through employment of the Dirac function. These will be problems for which the exact solutions are well known. Consider the two-span slender beam as shown in Figure 1(a). It is given simple pinned support at each outer extremity with lateral displacement, $R(\xi)$, forbidden at the junction of the spans, dimensionless distance μ along the beam. The governing differential equation pertaining to the spans is written as,

$$\frac{\partial^4 R(\xi)}{\partial \xi^4} - \beta^4 R(\xi) = 0. \tag{1}$$

where ξ equals distance along the beam divided by total beam length L,

$$\beta^4 = \frac{\rho A \omega^2 L^4}{EI} \tag{2}$$

ρA equals the mass of the beam per unit length, ω equals the circular frequency of beam vibration, and EI equals the flexural rigidity of the beam in bending. Letting subscripts 1 and 2 refer to the first and second spans, respectively, the solution for $R_1(\xi)$ is written as,

$$R_1(\xi) = A_1 \sin\beta\xi + B_1 \cos\beta\xi + C_1 \sinh\beta\xi + D_1 \cosh\beta\xi \tag{3}$$

with a similar expression for $R_2(\xi)$. A_1 , A_2 etc. are constants to be determined. Six of the constants are evaluated through enforcement of simple support at the beam outer extremities and conditions of zero lateral displacement at the intermediate support.

Finally, enforcing conditions of continuity of slope and bending moment at the support we obtain two simulteanous algebraic equations relating the remaining constants. Eigenvalues are those values of the parameter β which cause the determinant of the matrix related to these two equations to vanish.

We look next at an alternative approach to the same problem employing the Dirac function. Consider the beam of Figure 1(b). It is identical to that of Figure 1(a) except that reaction of the intermediate support on the beam is provided by a local concentrated harmonic force of dimensionless amplitude P^* . We represent this force by means of a Dirac function expanded in a sine series. The governing differential equation then becomes

$$\frac{\partial^4 R(\xi)}{\partial \xi^4} - \beta^4 R(\xi) = P^* \sum_{m=1}^{K} \sin m\pi\mu \sin m\pi\xi \tag{4}$$

The amplitude of beam vibratory displacement is expressed as,

$$R(\xi) = \sum_{m=1}^{K} E_m \sin m\pi\xi \tag{5}$$

Substituting equation 5 into equation 4 and solving for the quantity E_m we obtain for displacement at $\xi=\mu$,

$$R(\xi)_{|\xi=\mu} = P^* \sum_{m=1}^{K} \frac{\sin^2 m\pi\mu}{(m\pi)^4 - \beta^4} \tag{6}$$

The above quantity can only equal zero , with P^* not equal zero, if the summation to the right vanishes. Thus for any value of K the eigenvalue β is computed. We now look at computations related to the first mode symmetrically distributed about the intermediate support point with μ =0.5 .

In Figure 2 a plot of computed eigenvalue vs K is presented. The exact eigenvalue computed to six significant digits equals 7.85320 and is indicated by the chain–dot line in the Figure. It is seen that convergence to the exact eigenvalue is excellent. In Figure 3 a plot of the actual distribution of the driving force represented by the Dirac function is presented for a value of K equal to 41. It is seen that this distribution differs vastly from the idealized Dirac function distribution. In this paper an explanation is offered as to why in spite of this deviation excellent convergence is still obtained. This explanation relates to the fact that along the distribution to the left of the Figure adjacent half waves tend to cancel each others effect.

In a second illustrative problem (Figure 4) a driving moment is used at the beam quarter point to prevent beam rotation. This moment is applied by employing two adjacent Dirac represented forces distance ϵ apart and letting ϵ approach zero in a man ner identical to that utilized by Timoshenko for static problems. Requiring that the slope

of the beam should equal zero at the point of moment application leads to the eigenvalue equation,

$$P^* \sum_{m=1}^{K} \frac{(m\pi)^2 \cos^2 m\pi\mu}{(m\pi)^4 - \beta^4} = 0. \tag{7}$$

Here convergence is much slower as might be expected due to the quantity $(m\pi)^2$ in the numerator. This appears because in this problem we are expanding a moment rather than a force by means of the Dirac function and we must focus on the beam slope (first derrivative of displacement) rather than displacement itself. Two more orders of integration of the series are required in the first problem, greatly contributing to series convergence.

In the full paper the above illustrations are augmented by moving on to rectangular plates with point supports for the cases of both transverse and in-plane vibration.

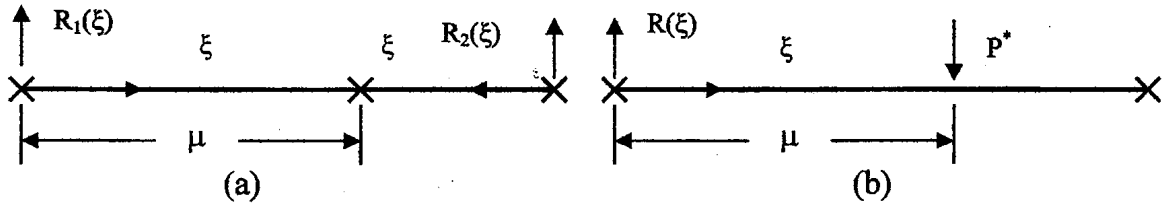

Figure 1. Two span beam

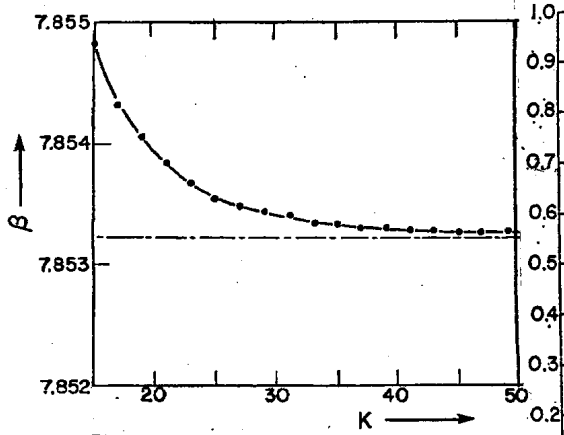

Figure 2. Eigenvalue plot.

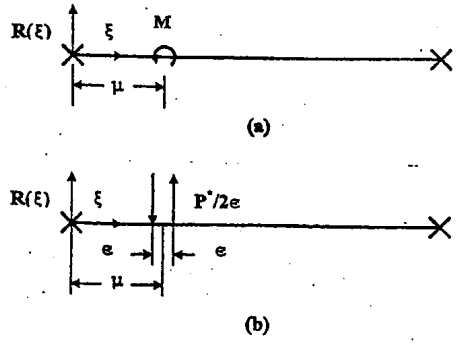

Figure 4. Moment driven beam

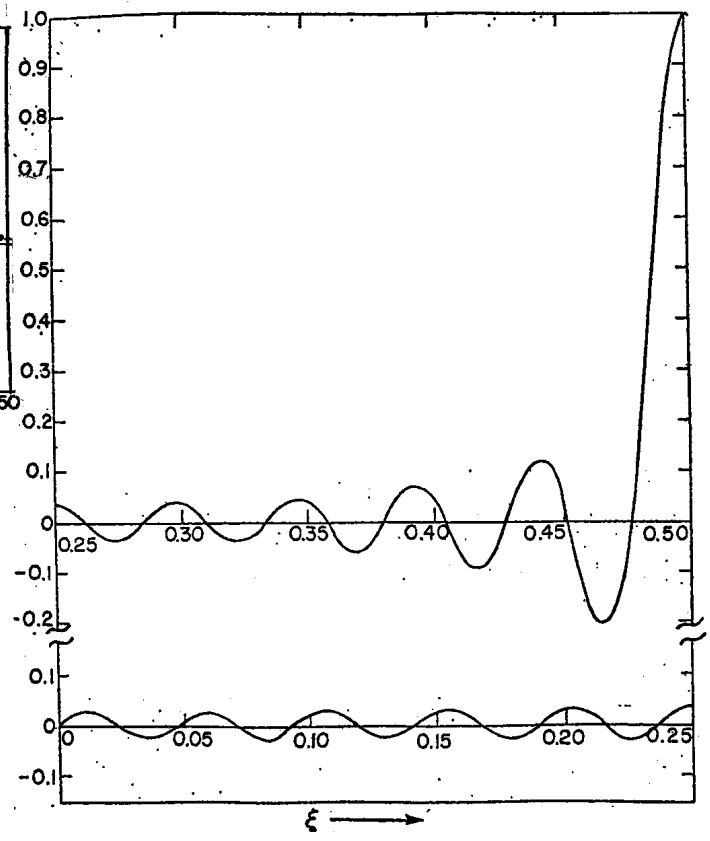

Figure 3. Dirac function plot.

Friction Induced Vibrations of a Rotating KIRCHHOFF Plate: An Excitation Mechanism of Disk Brake Squeal

Daniel Hochlenert and Peter Hagedorn
Dynamics and Vibrations Group, Technische Universität Darmstadt, Germany

Introduction

The development and optimization of new brake systems with respect to their vibration behavior in general involve costly experiments. In particular noise problems arising due to vibrations of the brake system in the audible frequency range, such as brake squeal, require time-consuming noise tests. This experimental effort can be reduced if appropriate mathematical-mechanical models are used for studying the dynamics of these brake systems. In this context, especially the mechanism generating brake squeal deserves closer attention.

The present note is devoted to the modeling of self-excited vibrations of a rotating KIRCHHOFF plate generated by friction forces. Special regard is given to an accurate formulation of the kinematics of the frictional contact in three dimensions. The contact formulation is derived in the context of a minimal disk brake model. The three dimensional contact kinematics arising in disk brakes yields essential properties of the frictional contact which cannot be observed in two dimensional models. The minimal model is then extended to a more complete disk brake model which can be used for parameter studies or a model-based active suppression of brake squeal.

Minimal disk brake model

The minimal disk brake model depicted in Figure 1 consists of a rotating annular KIRCHHOFF plate in frictional contact with idealized brake pads. The plate is fixed at its inner radius and free outside. It is driven by a torque $M_A \boldsymbol{e}_z$ such that the body fixed reference frame rotates with a constant angular velocity $\Omega \boldsymbol{e}_z$. The idealized brake pads (negligible mass) are elastically supported (stiffness k, prestress N_0) and allowed to move in the $\boldsymbol{e}_z$-direction only. The transverse displacement of the mid surface is described in polar coordinates by $w(r, \varphi, t)$. Its potential and kinetic energy are

$$U = \frac{1}{2}\, D \int_A \left(\nabla^2 w\right)^2 - 2(1-\nu)\left\{ \frac{\partial^2 w}{\partial r^2}\left(\frac{1}{r}\frac{\partial w}{\partial r} + \frac{1}{r^2}\frac{\partial^2 w}{\partial \varphi^2}\right) - \left(\frac{\partial}{\partial r}\frac{1}{r}\frac{\partial w}{\partial \varphi}\right)^2 \right\} \mathrm{d}A \tag{1}$$

and

$$T = \frac{1}{2}\, \rho h \int_A \boldsymbol{v}_{\mathrm{M}}^2 \, \mathrm{d}A, \tag{2}$$

respectively, where $\boldsymbol{v}_{\mathrm{M}}$ is the velocity of a point on the mid surface (cf. Figure 2). The equations of motion can be derived using HAMILTON's principle

$$\delta \int_{t_1}^{t_2} (T - U)\, \mathrm{d}t = -\int_{t_1}^{t_2} \delta W \, \mathrm{d}t, \tag{3}$$

where the virtual work of the contact forces acting on the plate is given by

$$\delta W = \int_A \boldsymbol{F} \cdot \delta \boldsymbol{p} \, \mathrm{d}A. \tag{4}$$

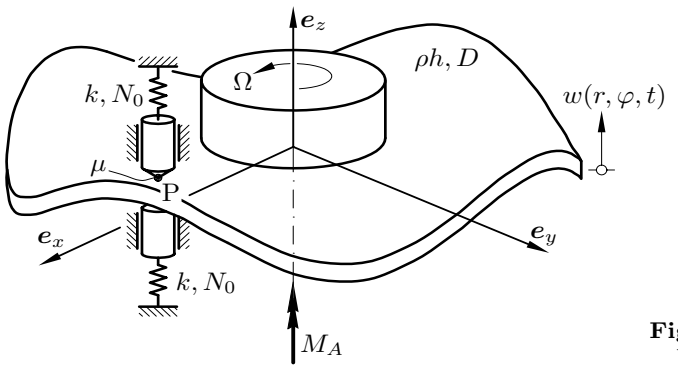

Figure 1: Rotating KIRCHHOFF plate with idealized brake pads

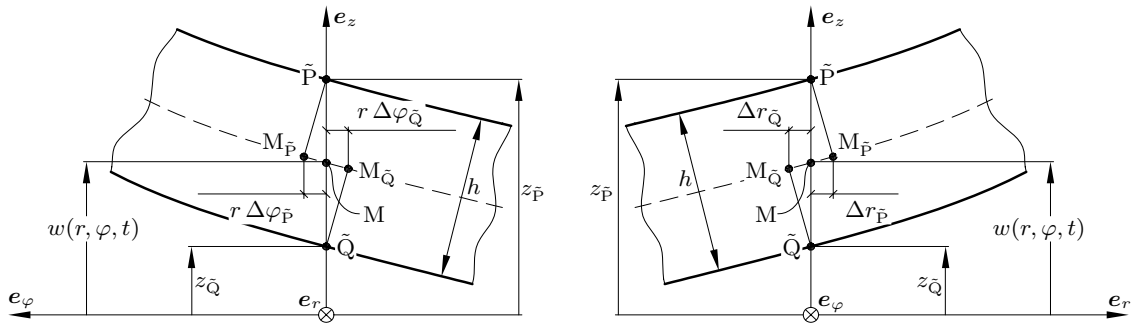

Figure 2: Contact kinematics of the KIRCHHOFF-Platte ($\boldsymbol{e}_\varphi$-$\boldsymbol{e}_z$- and $\boldsymbol{e}_r$-$\boldsymbol{e}_z$-plane)

Note that the displacements of the points of action of the contact forces have to be determined up to second order since the variation implicates a derivative with respect to $w(r,\varphi,t)$. In doing so, one has to consider the distances Δr and $r\Delta\varphi$ due to the kinematics of the KIRCHHOFF plate as shown in Figure 2. On this account it is obvious that in general the material points of the plate ($\tilde{\mathrm{P}}$ and $\tilde{\mathrm{Q}}$) in actual contact with the pads have non-vanishing velocity components in all directions, especially in the $\boldsymbol{e}_r$-direction. The contact force acting on the upper contact point P consists of a component normal to the deformed plate (normal force $\boldsymbol{N}_\mathrm{P}$) and a component in the tangential plane at the contact point (friction force $\boldsymbol{R}_\mathrm{P}$). The direction of the friction force is given by the relative velocity between the contact points of the pad and the plate. Finally, a force balance at the brake pad in $\boldsymbol{e}_z$-direction and COULOMB's law $|\boldsymbol{R}_\mathrm{P}|=\mu|\boldsymbol{N}_\mathrm{P}|$ yield the contact force at P depending on $w(r,\varphi,t)$. The contact force at the lower contact point $\tilde{\mathrm{Q}}$ can be calculated similarly such that all ingredients for HAMILTON's principle are known.

Stability analysis

The operation deflection shape of a brake disk during squeal can be approximated to a good extent by a doublet mode of a corresponding non-rotating KIRCHHOFF plate. Therefore, the energy and virtual work expressions are discretized using

$$w(r,\varphi,t) = R_{m,n}(r)\Big(c(t)\cos m\varphi + s(t)\sin m\varphi\Big), \tag{5}$$

where $R_{m,n}(r)\cos m\varphi$ and $R_{m,n}(r)\sin m\varphi$ represent a pair of orthogonal eigenmodes corresponding to one eigenfrequency close to the frequency of squeal. Excluding stick-slip at the contact points, it is possible to linearize the resulting equations of motion for small $s(t)$ and $c(t)$ to study the stability of the system. The equations of motion then read

$$\boldsymbol{M}\ddot{\boldsymbol{q}} + (\boldsymbol{D}+\boldsymbol{G})\dot{\boldsymbol{q}} + (\boldsymbol{K}+\boldsymbol{N})\boldsymbol{q} = \boldsymbol{0}, \tag{6}$$

where the matrices for the pad's position $\varphi=0$, $r=r_\mathrm{p}$ are

$$\boldsymbol{M} = \begin{bmatrix} M & 0 \\ 0 & M \end{bmatrix}, \qquad \boldsymbol{D}+\boldsymbol{G} = \begin{bmatrix} \dfrac{1}{2}\dfrac{\mu N_0 h^2}{r_\mathrm{p}\Omega}R'^2_\mathrm{p} & 2mM\Omega \\ -2mM\Omega & 0 \end{bmatrix},$$

$$\boldsymbol{K}+\boldsymbol{N} = \begin{bmatrix} \hat{k} + 2kR_\mathrm{p}^2 + N_0 h R'^2_\mathrm{p} & \mu\dfrac{\hat{N}_0}{2r_\mathrm{p}}\Big(\hat{R}_\mathrm{p} + m^2R_\mathrm{p}^2\Big) \\ -\mu k\dfrac{h}{r_\mathrm{p}}mR_\mathrm{p}^2 - \mu\dfrac{\hat{N}_0}{2r_\mathrm{p}}\hat{R}_\mathrm{p} & \hat{k} + (1+\mu^2)\dfrac{\hat{N}_0}{h}mR_\mathrm{p}^2 \end{bmatrix}, \qquad \boldsymbol{q} = \begin{bmatrix} c(t) \\ s(t) \end{bmatrix}$$

with the abbreviations

$$M = \rho h\pi\int_{r_\mathrm{i}}^{r_\mathrm{o}} rR_{m,n}^2(r)\,\mathrm{d}r, \qquad R_\mathrm{p} = R_{m,n}(r_\mathrm{p}), \qquad \hat{R}_\mathrm{p} = r_\mathrm{p}^2R'^2_\mathrm{p} - r_\mathrm{p}R_\mathrm{p}R'_\mathrm{p},$$

$$\hat{k} = (\omega_{m,n}^2 - m^2\Omega^2)M, \qquad \hat{N}_0 = mN_0\frac{h^2}{r_\mathrm{p}^2}.$$

The asymmetry of the matrix $\boldsymbol{K}$+$\boldsymbol{N}$ makes the system susceptible to self-excited vibration. The matrix $\boldsymbol{D}$+$\boldsymbol{G}$ does not only contain the expected gyroscopic terms, but also an additional linear damping term resulting from the kinematics of the plate and the frictional contact. It cannot be observed in two dimensional models, since it is due to the fact that the friction force has a component in the radial direction of the disk. The corresponding energy dissipation influences the stability of the trivial solution significantly and should not be

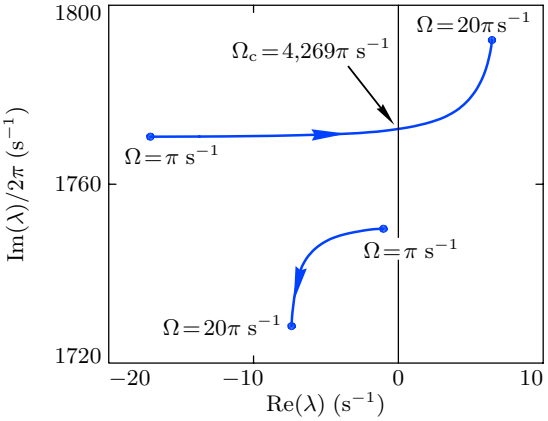

Figure 3: Root locus for varying Ω (only eigenvalues with pos. imaginary part)

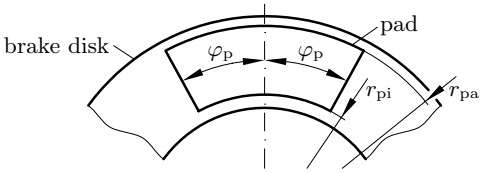

Figure 4: Geometry of the brake pad in the extended disk brake model

neglected by assuming only a circumferential direction of the friction forces. Actually it can be shown that neglecting this effect yields the instability of the trivial solution for any given set of parameters, requiring only that $\boldsymbol{K}+\boldsymbol{N}$ is not symmetric. The stability of the trivial solution can be studied using the ansatz $\boldsymbol{q}(t)=\hat{\boldsymbol{q}}e^{\lambda t}$ and solving the eigenvalue problem for λ, where a positive real part corresponds to instability. The root locus for a given set of parameters depending on the rotational speed Ω is shown in Figure 3. Above a critical speed Ω_c there exist eigenvalues with positive real part. That is to say the system shows self-excited vibration, which can be interpreted as squeal.

Extension of the minimal model

The described minimal model is now extended to a disk brake model including brake pads with finite area (cf. Figure 4), the caliper and the yoke of the brake system. Using a pointwise visco-elastic description of the pad's friction material, the contact formulation of the minimal model can be easily adapted. After discretizing the rotating Kirchhoff plate in the mentioned fashion, the extended disk brake model has a moderate number of degrees of freedom. Therefore, it is suitable for detailed parameter studies and may be used as a basis for the model based active suppression of brake squeal.

Figure 5 exemplarily points out a result of the parameter study. The two plots show the stability boundaries depending on the rotational speed of the disk for a varying pad's span angle. In the left plot the brake model is adjusted to an operation deflection shape of the disk with 3 nodal diameters and a squealing frequency of approximately 1750 Hz. The left picture corresponds to a squealing frequency of approximately 3200 Hz and 4 nodal diameters of the disk. It can be seen that the pad's span angle has a strong influence on the stability of the trivial solution. This dependency has practical relevance, especially in view of brake pads with chamfers (an usual modification to improve the brake's noise behavior) where the span angle consequently changes with the wear of the pads. From Figure 5 it can be seen that a span angle corresponding to the angle between two nodal diameters of the disk increases the region of instability and therefore the tendency to squeal of the brake system.

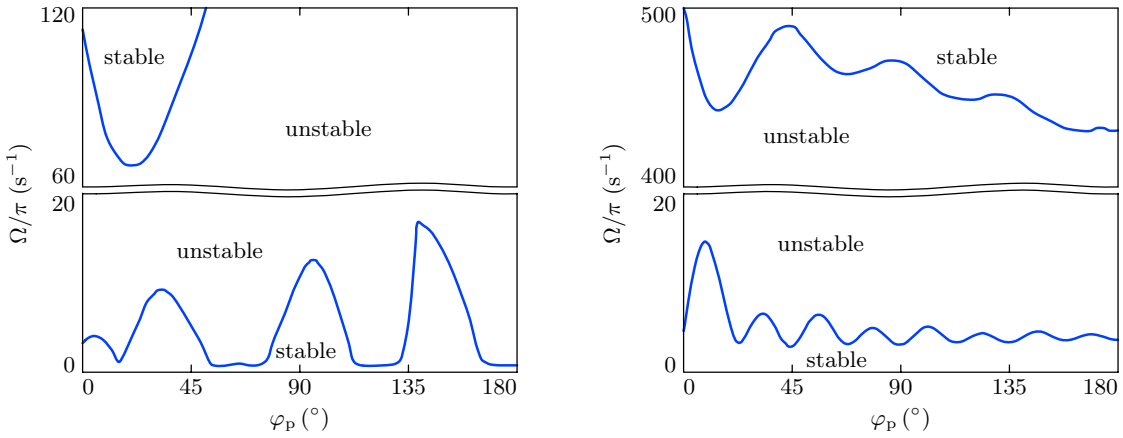

Figure 5: Regions of stability and instability depending on the rotational speed for varying span angle of the brake pad (shape functions with 3 (left) and 4 (right) nodal diameters)

Vibration of Sectorial and Skew Mindlin Plates with Corner Stress Singularities

C. S. Huang and M. J. Chang
Department of Civil Engineering, National Chiao Tung University, Hsinchu, Taiwan

INTRODUCTION

Plates in various geometric forms are commonly used in practical engineering. Stress singularities occur at the re-entrant corners of plates, for instance, at the re-entrant clamped corner of a cantilever skew plate. It is well known that the stress singularity behaviors have to be taken into account in order to perform more accurate numerical analyses.

The present work analyzes skew and sectorial Mindlin plates, where such stress singularities exist. The Ritz method, widely applied to investigate the vibrations of structural components, is used to determine the vibration frequencies and mode shapes for such plates. The admissible displacement functions used in the present work consist of two sets of functions. One is the set of traditional polynomials, and the other is the set of corner functions. The corner functions are established from the asymptotic solutions provided by Huang [1] and McGee *et al.* [2] for both moment and shear force singularities at a corner of a Mindlin plate. Hence, the corner functions not only appropriately describe the singular behaviors at the re-entrant corner, but also meet the boundary conditions around the corner.

SECORIAL PLATE

Consider a completely free sectorial plate with radius R, thickness h, density ρ, and flexural rigidity D. The stress singularities exist at the vertex when the vertex angle (α) is larger than 90^o [1, 2]. When the Ritz method is applied to find the natural frequencies and mode shapes for such a plate, the admissible functions for displacement components are assumed as the sum of two sets of functions,

$$\psi_r(r,\theta) = \Psi_{r\,p}(r,\theta) + \Psi_{r\,c}(r,\theta),\ \ \psi_\theta(r,\theta) = \Psi_{\theta\,p}(r,\theta) + \Psi_{\theta\,c}(r,\theta), \text{ and}$$

$$w(r,\theta) = W_p(r,\theta) + W_c(r,\theta),$$

where

$$\Psi_{rp}(r,\theta) = \sum_{i=2,4}^{I_1}\sum_{j=2,4}^{i} B_{ij} r^{i-1}\cos j\theta + \sum_{i=3,5}^{I_2}\sum_{j=1,3}^{i} B_{ij} r^{i-1}\cos j\theta + \sum_{i=2,4}^{I_3}\sum_{j=2,4}^{i} \widetilde{B}_{ij} r^{i-1}\sin j\theta + \sum_{i=3,5}^{I_4}\sum_{j=1,3}^{i} \widetilde{B}_{ij} r^{i-1}\sin j\theta$$

$$\Psi_{\theta p}(r,\theta) = \sum_{i=2,4}^{I_1}\sum_{j=2,4}^{i} C_{ij} r^{i-1}\cos j\theta + \sum_{i=3,5}^{I_2}\sum_{j=1,3}^{i} C_{ij} r^{i-1}\cos j\theta + \sum_{i=2,4}^{I_3}\sum_{j=2,4}^{i} \widetilde{C}_{ij} r^{i-1}\sin j\theta + \sum_{i=3,5}^{I_4}\sum_{j=1,3}^{i} \widetilde{C}_{ij} r^{i-1}\sin j\theta$$

$$W_p(r,\theta) = \sum_{i=0,2,4}^{I_5}\sum_{j=0,2,4}^{i} A_{ij} r^{i}\cos j\theta + \sum_{i=1,3}^{I_6}\sum_{j=1,3}^{i} A_{ij} r^{i}\cos j\theta + \sum_{i=2,4}^{I_7}\sum_{j=2,4}^{i} \widetilde{A}_{ij} r^{i}\sin j\theta + \sum_{i=1,3}^{I_8}\sum_{j=1,3}^{i} \widetilde{A}_{ij} r^{i}\sin j\theta$$

$$\Psi_{rc}(r,\theta)=\sum_{k=1}^{K}\left[\overline{B}_k\ \mathrm{Re}(\overline{\Psi}_{rk}(r,\theta,\lambda_k))+\hat{B}_k\ \mathrm{Im}(\overline{\Psi}_{rk}(r,\theta,\lambda_k))\right],$$

$$\Psi_{\theta c}(r,\theta)=\sum_{k=1}^{K}\left[\overline{C}_k\ \mathrm{Re}(\overline{\Psi}_{\theta k}(r,\theta,\lambda_k))+\hat{C}_k\ \mathrm{Im}(\overline{\Psi}_{\theta k}\ (r,\theta,\lambda_k))\right],\ \ W_c(r,\theta)=\sum_{l=1}^{L}\overline{A}_l\overline{W}_l(r,\theta,\lambda_k).$$

$\overline{\Psi}_{r\,k}$, $\overline{\Psi}_{\theta\,k}$ and $\overline{W}_l$ are established from the asymptotic solutions presented in Huang [1] and McGee *et al*. [2]. For simplicity, it is set that $I_1=I_3=\ I_5=I_7$ and $I_2=I_4=I_6=I_8$. Table 1 shows the convergence study for a sectorial plate with α=355°.

Table 1 Convergence of $\omega R^2\sqrt{\rho h/D}$ for a completely free sectorial plate with α=355° and h/R=0.1

mode no.	No. of corner functions	(I_{even}, I_{odd})				
		(16, 15)	(18,17)	(20,19)	(22,21)	(24,23)
1 (A)	0	5.261	5.244	5.242	5.240	5.237
	10	2.757	2.748	2.744	2.737	2.735
	20	2.741	2.739	2.735	2.731	2.730
2 (S)	0	5.345	5.301	5.297	5.296	5.294
	10	4.238	4.233	4.231	4.229	4.229
	20	4.235	4.231	4.229	4.228	4.228
3 (S)	0	8.881	8.854	8.849	8.843	8.839
	10	7.555	7.553	7.551	7.549	7.549
	20	7.554	7.552	7.550	7.548	7.548
4 (A)	0	12.02	12.00	11.99	11.98	11.98
	10	7.592	7.586	7.583	7.581	7.578
	20	7.584	7.583	7.580	7.578	7.577
5 (S)	0	12.12	12.12	12.12	12.11	12.11
	10	11.24	11.23	11.23	11.23	11.23
	20	11.23	11.23	11.23	11.23	11.23

Note: (S) and (A) denote symmetric and antisymmetric modes, respectively.

CANTILEVER SKEW PLATE

Consider a cantilever skew plate having skew angle β, spanwise length *a*, root width *b*, and tip width *c*. Following the same approach as described above and using different admissible functions that are suitable for the problem under consideration, one can obtain the accurate natural frequencies and mode shapes for the first five modes as shown in Fig.1. The parenthesized numbers are the dimensionless frequencies $\omega a^2\sqrt{\rho h/D}$.

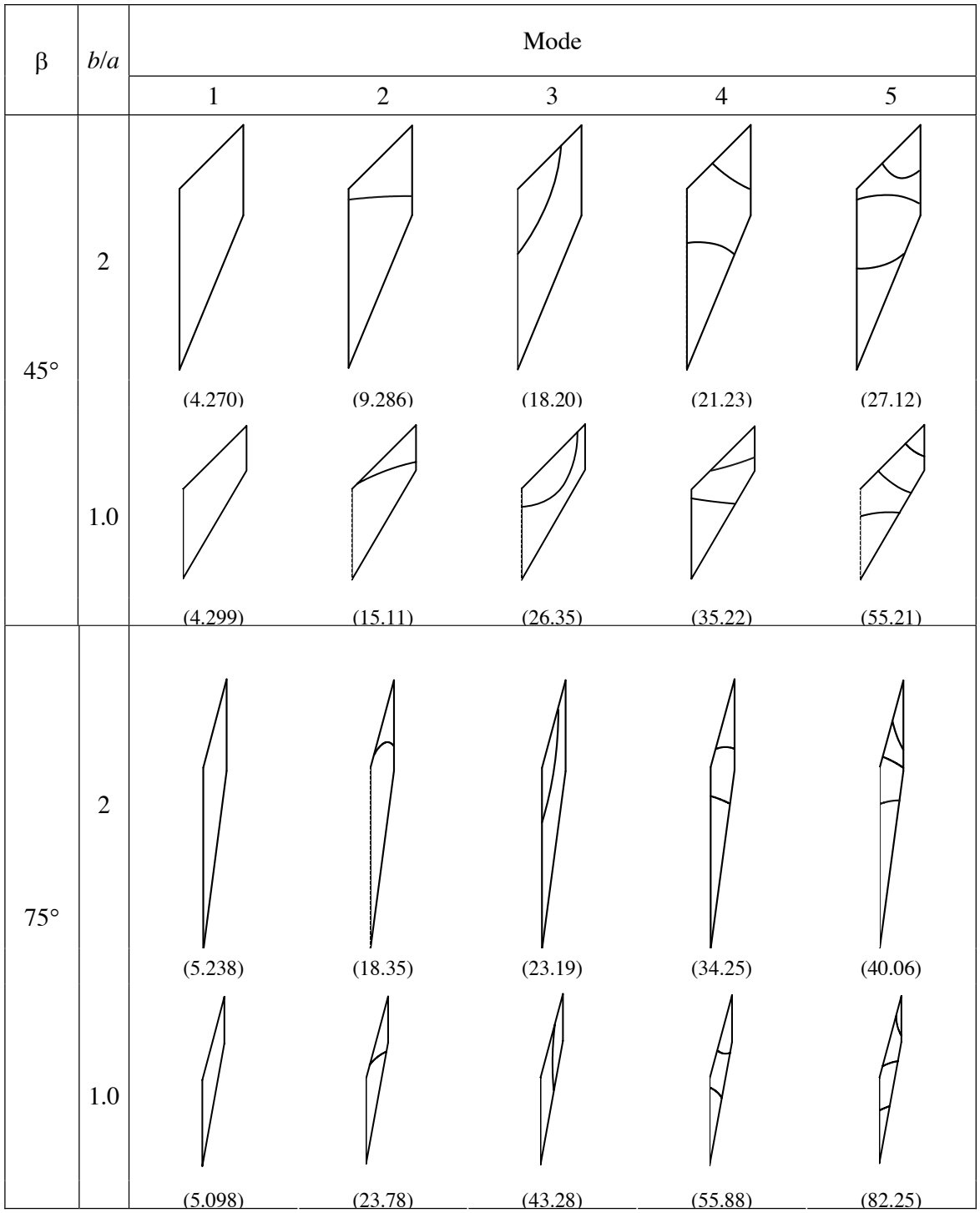

Fig. 1 Natural frequencies and nodal patterns for trapezoid plates (c/b=0.5, h/b=0.1)

REFERENCES

1. C. S. Huang, Stress singularities at angular corners in first-order shear deformation plate theory, *International Journal of Mechanical Sciences* 45 (2003) 1-20.

2. O. G. McGee, J. W. Kim and A. W. Leissa, Sharp corner functions for Mindlin plates, *Journal of Applied Mechanics* 72(1) (2005) 1-9.

Axisymmetric Vibrations of Thick Clamped Circular Plates Revisited

James R. Hutchinson
Department of Civil and Environmental Engineering
University of California, Davis CA 95616

Introduction

At the Fifth International Symposium on Vibrations of Continuous Systems, I presented a paper entitled "The Crosswise Series Superposition Method in Solid Mechanics" [1]. In the conclusion to that paper I noted that Pickett [2] had reported that he had some convergence difficulties for the problem of axial compression of circular cylinders. I also mentioned that I was having difficulty with a similar problem and would look into the matter further. I postulated that the difficulty might occur when a fixed surface is adjacent to a free surface. In looking over my past work, I discovered that I had previously solved a problem with a fixed boundary adjacent to a free surface in 1986 [3]. I decided to rerun the numbers in that problem in order to investigate convergence. The problem is particularly well suited for this purpose because there are several approximate methods with which to compare it. Mindlin [4] introduced his thick plate theory in 1951. Prior to that, in 1945 Pickett [5] developed a method for solving circular plate problems. In a 1984 paper [6] I compared the Mindlin and Pickett solutions with a crosswise series solution for the vibrations of a free circular plate. In that paper the results from all three methods were extremely close. However, in the 1986 paper [3] on clamped plates, the Pickett solution presented difficulties. In this paper I explain the difficulty and show how a better choice of boundary conditions clears up the problem.

Crosswise Series Method

In the crosswise series method, series are formed from solution forms of the governing equations. In this case the governing equations are solutions of the three dimensional equations of linear elasticity in cylindrical coordinates. For this reason I will also refer to this solution as the 3-D solution. The coefficients in the series were chosen so that the boundary condition on the axial displacement w at the outside of the plate is identically zero, and so that the shear stress on the surface of the plate is identically zero. The other two boundary conditions, of zero radial displacement u at the outside of the plate and zero normal stress on the surface of the plate are satisfied by orthogonality. This leads to an eigenvalue matrix whose order is the number of terms in the radial direction NR plus the number of terms in the axial direction NZ. As more terms in the series are chosen, the solution becomes more and more accurate. From experience it has been found that more terms should be carried in the large direction. In fact, the number of terms should be chosen roughly in proportion to the two dimensions.

All quantities in this paper are dimensionless. The radial displacement u, the axial displacement w, and the dimensions r and z are made dimensionless by dividing by the outer radius a. The natural frequency ω is made dimensionless by multiplying by the outer radius and dividing by the shear wave velocity. The distance h is the half thickness of the plate and is made dimensionless by dividing by the outer radius. In other words, h is the thickness to diameter ratio of the plate.

Pickett Method

The Pickett method also makes use of the solution forms of the 3-D elasticity equations. Instead of attempting to satisfy all boundary conditions, Pickett satisfies the equations on the surface of the plate

exactly. This leads to a characteristic equation for the wave number. Pickett showed that there were only two real roots for low frequencies. For higher frequencies additional roots emerge from the complex plane. It was shown in reference [6] that these additional real roots represented higher dispersion curves, and it was also noted that the range of applicability of the Pickett solution was limited to frequencies less than the first emergence of these higher roots. In reference [6] it was noted that the emergence occurs when ωh equals 4.3, 4.7, and 4.4 for Poisson's of 0.0, 0.3, and 0.5 respectively. In this paper I used a Poisson's ratio of 0.3 but limited the solution to $\omega h < 4.5$.

Because of only having two roots, the most that can be satisfied is two boundary conditions at $r = a$. In reference [3] I set the displacement at the center of the edge of the plate to zero ($w(a,0) = 0$) and considered four possibilities for fixing the slope: 1. Set the derivative of u with respect to z as zero. 2. Set the integral of z times u as zero. 3. Set u at the top and bottom corners as zero. 4. Set the derivative of w with respect to r as zero. These are listed in the order of edge fixity. I expected that the boundary condition 2 would give the best answers but a very strange phenomenon occurred. For those boundary conditions, there was a coalescence of the third and fourth mode natural frequencies near $h = 0.35$. In other words, the choice of boundary conditions led to a dynamic instability. In writing this paper, it occurred to me that I should have used average displacement as well as average slope to get a best answer. Thus for this paper I satisfy the displacement boundary condition by setting the integral of the axial displacement to zero and satisfy the slope boundary condition by setting the integral of z times the radial displacement to zero. This choice gives much better answers without the dynamic instability.

Mindlin Method

The Mindlin plate theory is well known and derivations are given in references [4] and [6]. The only question in the Mindlin theory is what shear coefficient is best. In reference [6] I derived a value of $5/(6 - \nu)$ for low frequencies. This is the coefficient used in this paper and can be seen to give a very close match with the 3-D and Pickett solutions.

Results

All results shown are for a Poisson's ration of 0.3. Table 1 shows how the 3-D frequencies converge as more and more terms are chosen in each series. The columns under Clamped plate are newly derived, while the columns under Free Plate are taken from reference [7]. It can be seen that the clamped plate converges at about the same rate as the free plate. The main difference is that the free plate converges monotonically from above whereas the clamped plate does not converge monotonically. This is because of the boundary conditions. A cylinder which is clamped on all boundaries also converges monotonically but from below. It can also be seen from this table that the Pickett and Mindlin solutions are reasonably close to the 3-D solution. Figures 1 and 2 give comparisons of the Pickett and Mindlin results respectively. They show the frequency as a function of the thickness of the plate for the four lowest natural frequencies as the thickness to diameter ratio goes from zero to 1. These comparisons show how good the approximate methods are in getting accurate answers, but also clearly indicate the range of applicability of these approximate solutions.

Conclusions

My previous concern about poor convergence in certain classes of problems was unfounded. The 3-D solution converges very well and provides an excellent basis for comparison of the approximate methods, both as to their accuracy and to their range of applicability.

Table 1. Convergence of frequencies for a Clamped Plate compared to a Free Plate. h = 0.1

Terms		Clamped Plate				Free Plate	
NZ	NR	MODE 1	MODE 2	MODE 3	MODE 4	MODE 1	MODE 2
4	20	0.908802	2.987344	5.632523	8.538286	0.851241	3.075969
20	100	0.908644	2.987720	5.634216	8.541349	0.832208	3.059589
40	200	0.908631	2.987701	5.634219	8.541386	0.831604	3.059075
60	400	0.908623	2.987681	5.634195	8.541366	0.831458	3.058951
120	600	0.908626	2.987692	5.634211	8.541384	0.831426	3.058924
160	800	0.908626	2.987691	5.634210	8.541384	0.831416	3.058915
200	1000	0.908626	2.987690	5.634209	8.541383	0.831412	3.058912
Mindlin		0.906389	2.982478	5.620813	8.510873	0.831368	3.057512
Pickett		0.905371	2.977832	5.615918	8.513770	0.831405	3.058997

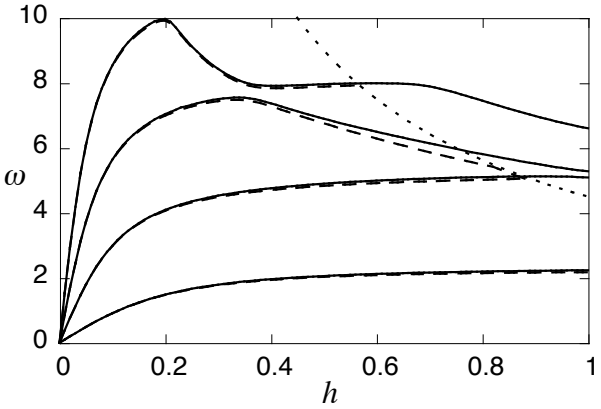

Figure 1. Frequency vs Thickness.
(——) 3-D Solution
(-----) Pickett Solution
(·····) Limit of Pickett Solution ($\omega h = 4.5$)

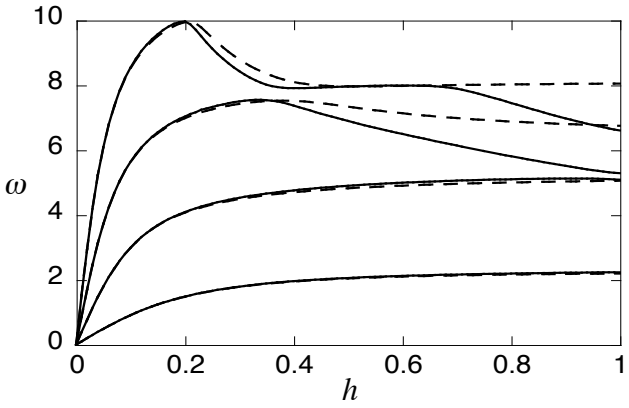

Figure 2. Frequency vs Thickness.
(——) 3-D Solution
(-----) Mindlin Solution

References

1. Hutchinson, J. R., 2005, "The Crosswise Series Superposition Method in Solid Mechanics," *Proceedings of the Fifth International Symposium on Vibrations of Continuous Systems*, Berchtesgaden, Germany July 2005, pp. 30-32.
2. Pickett, G., 1944, "Applications to the Fourier Method to Solution of Certain Boundary Problems in the theory of Elasticity," *ASME Journal of Applied Mechanics*, Vol,11, pp. A176-182.
3. Hutchinson, J. R., 1986, "On Axisymmetric Vibrations of Thick Clamped Plates," *Proceeding of the International Conference on Vibration Problems in Engineering*, Xian, China June 19-22, pp. 75-81
4. Mindlin, R. D. "Influence of Rotary Inertia and Shear on Flexural Motions of Isotropic, Elastic Plates," *ASME Journal of Applied Mechanics*, Vol.18, pp. 31-38
5. Pickett, G., 1945, "Flexural Vibrations of Unrestrained Cylinders and Disks," *Journal of Applied Physics*, Vol., pp. 820-831.
6. Hutchinson, J. R., 1984, "Vibrations of Thick Free Circular Plates, Exact versus Approximate Solutions," *ASME Journal of Applied Mechanics*, Vol.51, pp. 581-585.
7. Hutchinson, J.R., 1997, "Vibrations of Free Circular Plates Revisited," *Proceedings of the First International Symposium on Vibrations of Continuous Systems*, Estes Park, Colorado, August, pp.24-26.

Bounded Eigenvalues of Completely Free Rectangular Plates

Y. Mochida
and **S. Ilanko**
Department of Engineering, Uni. of Waikato, Hamilton, New Zealand

The vibration of the completely free rectangular plate has a long research history. Such problems were often analysed by using approximate methods, for example the Rayleigh-Ritz method, because it is difficult to find functions that simultaneously satisfy the governing differential equation and the boundary conditions of free edges. An excellent review of the literature relating to vibration analysis of plates was published by Leissa [1]. Most of these methods give upper bounds for the eigenvalues as the solution is either based on assumed shapes that effectively overconstrain the system or using the superposition [2] of exact solutions for plates with more constraints. Among the upperbound solutions, Gorman's superposition method [2,3] is very efficient and appears to give the lowest upperbound values for the natural frequencies of plates with various aspect ratios. Here, we present some lower bound results obtained using the Finite Difference Method (FDM) that are very close to the results reported by Gorman.

It is known that the finite difference method (FDM) gives lower bounds for the natural frequencies [4]. The partial differential equation governing the out-of-plane vibration of rectangular plates is [5].

$$\frac{\partial^4 W(x,y)}{\partial x^4} + 2\frac{\partial^4 W(x,y)}{\partial x^2 \partial y^2} + \frac{\partial^4 W(x,y)}{\partial y^4} - \frac{m\omega^2}{D} W(x,y) = 0 \quad (1)$$

Equation 1 was approximated in the finite difference form, in terms of the nodal displacements. The eigenvalues ($\lambda = \omega a^2 \sqrt{m/D}$) of first eight modes for different aspect ratios were computed and compared to the eigenvalues in earlier literature.

Table 1 shows the non-zero eigenvalues of completely free thin rectangular plates with aspect ratios 1.0 to 3.0 obtained by the FDM. As the plate has two axes of symmetry, the modes are classified into four categories, labelled SS, AA, SA and AS indicating that the modes are symmetric about both the x axis and y axis, antisymmetric about both axes, symmetric about the x axis and antisymmetric about the y axis, and antisymmetric about the x axis and symmetric about the y axis respectively. The natural frequencies obtained by the method of superposition [2] are also shown in Table 1. The results obtained by using the FDM exhibit excellent agreement with Gorman's results, and as expected, the FDM results are slightly lower than those obtained from the method of superposition.

Table 1. The eigenvalues and mode shapes of completely free thin rectangular plates by the FDM and the method of superposition. $\lambda = \omega a^2 \sqrt{m/D}$ $\nu = 0.3$,

	Φ = 1			1.5			2			3		
Mode	FDM	SM		FDM	SM		FDM	SM		FDM	SM	
1	13.46	13.47	AA	8.926	8.931	AA	5.358	5.366	SS	2.379	2.382	SS
2	19.57	19.60	SS	9.503	9.517	SS	6.640	6.644	AA	4.373	4.375	AA
3	24.24	24.27	SS	20.57	20.60	SA	14.60	14.62	SA	6.596	6.617	AS
4	34.75	34.80	SA	22.15	22.18	SS	14.85	14.90	AS	9.233	9.244	SA
5	34.75	34.80	AS	25.58	25.65	AS	21.97	22.00	SS	12.96	13.03	SS
6	60.90	61.09	SA	29.73	29.79	AS	25.31	25.38	AA	15.04	15.07	AA
7	60.90	61.09	AS	38.05	38.16	AA	25.96	26.00	AS	21.16	21.31	AS
8	63.56	63.69	SS	43.84	43.93	SS	29.53	29.68	SS	22.19	22.23	SS

Convergence test were carried out for all the above aspect ratios and modes and results for the fundamental frequency of a square plate are presented in Figure 1. As can be seen from the figure, both methods give results that converge as the matrix size is increased. The rate of convergence of the FDM is significantly slower than that of the superposition method but for all cases tested the convergence was from below as predicted by Weinberger [4]. The work shows that Gorman's superposition method gives excellent convergence in its results for the fundamental eigenvalues with only 20 terms [2]. These results also confirm the prediction in a recent paper [3] that Gorman's results are expected to be upper bound for a free plate. The first author generated the results for a free plate using the superposition method for various aspect ratios and numbers of terms. Thus the exact natural frequencies of a completely free plate are bracketed by the results of the FDM and the method of superposition.

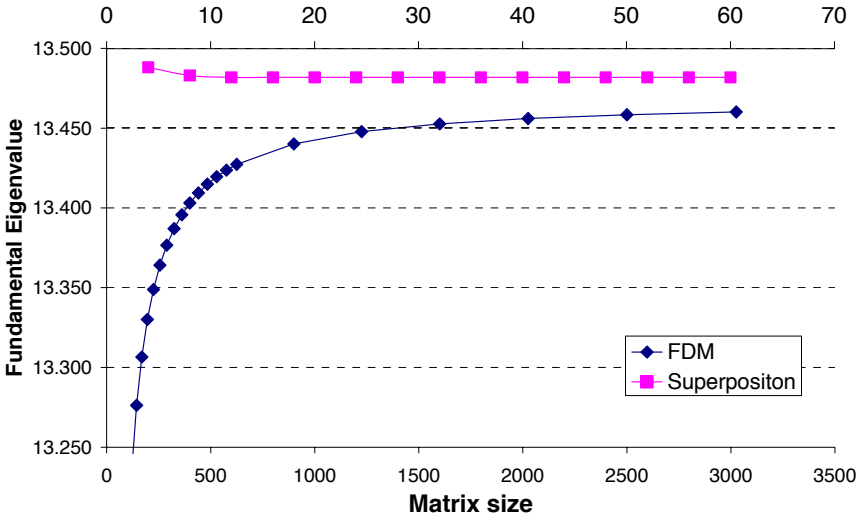

Figure 1. Fundamental natural frequencies of a square plate by the FDM and the method of superposition

In Table 2 the eigenvalues obtained by using the FDM are compared with the results published by Leissa [1]. The upper bound and lower bound results in Leissa's publication were taken from reference [6]. The present results are higher than the previously published lower bounds and very close to the upper bounds indicating these may be the best lower bound solutions available to date. The presented FDM results together with published results

by the popular upperbound methods, such as the superposition method, give an estimate of the maximum possible error in the values of the natural frequencies of completely free plates.

Table 2 Comparison of eigenvalues obtain by FDM with those in Leissa's publication [1] for the doubly antisymmetric modes of the square free plate (ν = 0.3)

Present	Liessa	
	Lower bound	Upper bound
b/a = 1		
13.46	13.092	13.474
69.04	66.508	69.576
76.95	75.146	77.411
b/a = 1.5		
8.926	8.6667	8.9351
38.05	36.651	38.294
66.50	64.844	66.965
b/a = 2		
6.640	6.4563	6.6464
25.31	24.417	25.455
58.32	56.151	59.051

REFERENCE

1. A. W. Leissa 1969 NASA SP-160. *Vibration of plates.*
2. D. J. Gorman 1978 Free vibration analysis of the completely free rectangular plate by the method of superposition, *Journal of Sound and Vibration,* 57 (3) 437-447.
3. S. Ilanko 2006 On the bounds of Gorman's superposition method of free vibration analysis, *Journal of Sound and Vibration,* 294 (1-2) 418-420
4. H. F. Weinberger 1958 Lower bounds for higher eigenvalues by finite difference methods, *Pacific Journal of Mathematics*, 8 (2) 339–368
5. D. J. Gorman 1982 *Free vibration analysis of rectangular plates*. Elsevier North Holland Inc., New York.
6. N. W. Bazley, D. W. Fox and J. T. Stadter, 1967 Upper and lower bounds for the frequencies of rectangular plates, *Journal of applied mathematics and physics,* 18 (4) 445-460

NOMENCLATURE

a plate dimension in *x* direction
b plate dimension in *y* direction
E modulus of elasticity of material
D plate flexural rigidity, $(Eh/12)/(1-\nu^2)$
m mass per unit area of plate
ω radian frequency of vibration
Φ aspect ration of half plate *b/a*
ν Poisson's ratio of material
λ $= \omega a^2 \sqrt{\rho / D}$

On Meaningless Vibration Analysis for Bodies having Elastic Constraints

Arthur Leissa
Fort Collins, Colorado, USA

There are at least scores (and probably hundreds) of published books and papers that analyze the free vibrations of bodies (e.g., beams, plates, shells) which are attached to other bodies, considering only the stiffness of the other bodies. Some of these configurations are shown in Fig. 1.

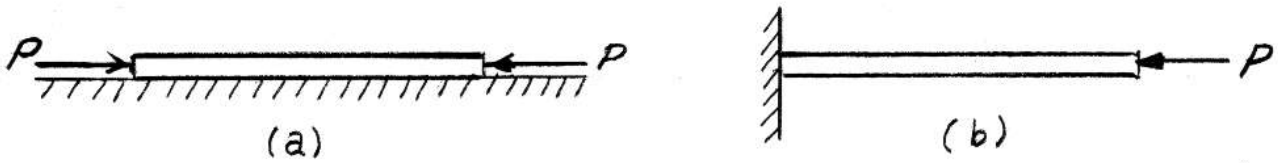

Figure 1. Examples of beams or plates with elastic constraints

Part (a) of Fig. 1 could be described as a slender beam resting upon (or better, attached to) an "elastic foundation". Axial compressive forces (P) are added to it for generality, but they need not be present. The transverse free vibrations of the beam are a long-standing, classical problem in mechanics. Indeed, no less than Timoshenko addressed this problem eighty years ago in the first edition of his famous book Vibration Problems in Engineering, by representing the foundation as having a uniformly distributed resistance kw, where w is the transverse displacement and k is the "foundation modulus". Then the differential equation of motion for the beam is

$$EI\frac{\partial^4 W}{\partial x^4} + P\frac{\partial^2 W}{\partial x^2} + KW + \rho A\frac{\partial^2 W}{\partial t^2} = 0$$

In the 4th edition of this book (Ref. 1), one finds the exact solution to this problem with P=0 displayed on pages 457-459, for arbitrary end conditions (e.g., clamped, simply supported or free).

But the elastic foundation not only has stiffness. It has mass and, hence, inertia. Or, viewing it in another way, the deformed foundation has potential energy, but it also has kinetic energy. The foundation stiffness increases the free vibration frequencies of the beam, but the foundation mass decreases them. For typical situations in the real world, the foundation mass is certainly significant. However, the writer has found no analysis in the research literature which considers this.

Figure 1(b) shows a cantilever beam. Because a perfectly rigid clamping at one end is physically impossible, some analysts replace the rigid wall by springs (translational and rotational). Reasonable values of stiffness coefficients may be determined for the stiff end structure. But how does one find equivalent masses (translational and rotational) to represent the end structure?

If the situation is static (not dynamic), with the elastic foundation of Fig. 1(a) or the elastic end constraint of Fig. 1(b), traditional analysis is reasonable. Beam deflections (and stresses) due to transverse loading may be determined straightforwardly, including the foundation or end constraint stiffnesses. If compressive axial forces (P) are also present, buckling loads may be determined. In a vibration analysis, increasing the compressive axial forces causes the beam frequencies to decrease. A zero frequency is approached as P approaches a buckling load. At the almost zero frequency, the inertia of the foundation or end constraint becomes negligible. Thus, inertia effects are less important for the lower frequencies; kinetic energy resulting from inertia is proportional to the square of the frequency.

Figure 1(a) can also represent the side view of a plate with thickness h, perhaps circular or rectangular, with free edges, resting upon (or better, attached to) an elastic foundation. Such configurations have also been studied by many in the published literature, with the resistance of the foundation considered by adding a term kw to the differential equation. Again, the inertia of the foundation, which is typically important, is ignored. Figure 1(b) can similarly be regarded as a plate of thickness h, with one edge constrained. For a non-rigid edge constraint, one must consider the inertia of the constraint, as well as its stiffness, for a proper analysis.

The comments made above apply to all dynamic systems, not only beams and plates, but also non-vibratory situations. The inertia of an elastic constraint acting along any boundary should be considered, as well as its stiffness.

Unfortunately, incorporating the inertia of an elastic constraint into an analysis is not a simple matter. The writer is currently doing this with a three-dimensional analysis of the two circular cylinders shown in Fig.2. One may regard these as a circular plate of radius R_1 and thickness h_1, resting upon a circular elastic foundation of radius R_2 and thickness h_2. The elastic modulus (E), Poisson's ratio (υ) and mass density (ρ) of each cylinder will typically be different. Furthermore, for the bottom cylinder to be a "foundation", one would designate $R_2/R_1 >> 1$ and $h_2/h_1 >> 1$. At the interface between the cylinders, any or all of the three displacement components may be made continuous.

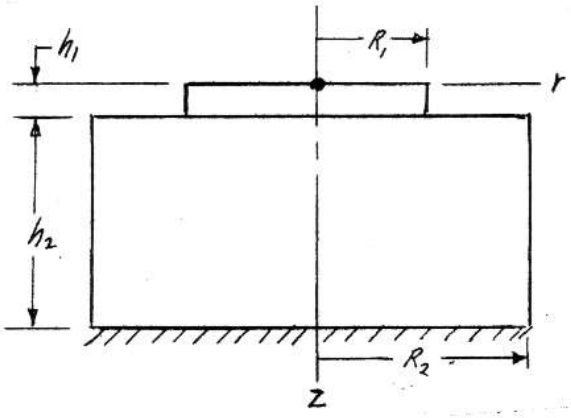

Figure 2, side view of two circular cylinders

For the upper cylinder to be a plate, $h_1/R_1 << 1$. But if $h_1/R_1 >> 1$, the configuration becomes a cantilever beam of length h_1 and circular cross-section (diameter = $2R_1$), constrained elastically at its bottom end by the foundation.

The analysis consists of using the Ritz method, with all three displacement components expressed in terms of algebraic polynomials in r and z, and cos $n\theta$ and sin $n\theta$, using the single coordinate system shown in Fig.2. This approach has worked very well for the 3-D vibration

analysis of circular cylinders (Refs. 2,3). The following difficulties have been encountered with the present problem:

1. A single coordinate system has difficulty in obtaining good convergence due to the discontinuities in dimensions and material properties at the interface.
2. The sharp corner at $z=h_1$ causes stress singularities there which cause very slow convergence with polynomial displacements. This may be alleviated if sharp corner functions (Ref. 4) are added.
3. A large foundation adds numerous frequencies to those of the plate (or beam). Identifying predominantly plate (or beam) frequencies requires additional analysis of the corresponding mode shapes.

In the presentation convergence tables of frequencies will be shown to illustrate these difficulties.

REFERENCES

1. Timoshenko, S.R; Young, D.H; Weaver, Jr., W. Vibration Problems in Engineering, 4th edition. John Wiley & Sons, 1974.

2. Leissa, A.W. and So, J., "Accurate Vibration Frequencies of Circular Cylinders from Three-Dimensional Analysis", Journal of the Acoustical Society of America, Vol. 98, No. 4, pp. 2136-2141, 1995.

3. Kang, J.-H. and Leissa, A.W., "Three-Dimensional Vibrations of Hollow Cones and Cylinders with Linear Thickness Variations", Journal of the Acoustical Society of America, Vol. 106, No. 2, pp. 748-755, 1999.

4. Huang, C.S. and Leissa, A.W., "Three-Dimensional Sharp Corner Displacement Functions for Bodies of Revolution", Journal of Applied Mechanics, Vol. 74, pp.41-46, 2007.

Symplectic Elasticity Approach for Free Vibration of Rectangular Thin Plates

C.W. Lim
Department of Building and Construction, City University of Hong Kong, Hong Kong, P.R. China

Abstract

Using a new symplectic method commonly applied by theoretical physicists, a new symplectic elasticity approach is developed for deriving exact analytical solutions to some long standing basic problems in free vibration of rectangular thin plates with any boundary conditions where exact solutions are hitherto unavailable. Employing the Hamiltonian principle with Legendre's transformation, analytical free vibration solutions could be obtained by eigenvalue analysis and expansion of eigenfunctions in both lengthwise and widthwise directions. Unlike the classical semi-inverse approaches using trigonometric, hyperbolic and/or Bessel functions where a trial amplitude function is pre-determined, this new symplectic approach is completely rational without any guess functions and yet it renders exact solutions beyond the scope of applicability of the semi-inverse approaches. In short, the symplectic approach developed in this paper presents a new approach in an area previously unaccountable in classical mechanics and the semi-analytical approach forms a limited sub domain of this new approach. Examples for plates with selected boundary conditions are solved and the exact solution is discussed. Comparison with the classical solutions shows excellent agreement. As the derivation of this new approach is fundamental, further research can be conducted not only for other types of boundary conditions, but also for thick plates as well as bending, buckling, wave propagation, etc.

1. Introduction

A symplectic group is a mathematical group and symplectic geometry was first used by Weyl [1] and the theory can be referred to Koszul and Zou [2]. The symplectic space was employed in a number of fields in physics and mathematics for many years, such as in relativity and gravitation [3], and classical and quantum mechanics [4], etc. In elasticity and Hamiltonian mechanics, the computational symplectic Hamiltonian systems including fluid dynamics was first developed by Feng and his associates [5,6]. In these papers, Feng and his associates proposed symplectic algorithms on dynamical systems. These algorithms are superior to conventional algorithms in many practical applications, such as celestial mechanics, molecular dynamics, etc. Feng's contribution in symplectic algorithm was particularly significant and important as stated in a memorial article dedicated to him by Lax [7].

Without computational algorithm [5,6], Zhong and his associates [8,9] and Lim et al. [10] developed a new analytical symplectic elasticity approach for some basic problems in solid mechanics and elasticity which have long been bottlenecks in elasticity. It is based on Hamiltonian principle with Legendre's transformation and analytical solutions could be obtained by expansion of eigenfunctions. It is rational and systematic with a clearly defined, step-by-step derivation procedure. It resolved systematically many basic problems in free vibration of rectangular thin plates previously unsolvable [11-13]. For instance, benchmark exact analytical bending solutions have been solved by Lim et al. for thin plates without two opposite sides simply supported [14] and for corner supported rectangular thin plates [15].

Based on the symplectic approach, first-known exact analytical solutions for free vibration of rectangular thin plates are presented here. Examples for thin plates with selected boundary conditions are solved and the exact solutions discussed. Comparison with the classical solutions shows excellent agreement. As the derivation of this new approach is fundamental, further research can be conducted not only for other types of boundary conditions, but also for thick plates as well as bending, buckling, wave propagation, etc.

2. Symplectic Formulation

Consider a rectangular thin plate with length $2a$ and width $2b$, the energy functional is

$$\Pi_1 = \iint \left(U - \frac{1}{2}\omega^2 \rho h w^2 \right) dxdy \tag{1}$$

where U is the strain energy, ω the vibration angular frequency, ρ the density per unit volume, h the plate thickness, and w the displacement amplitude.

From the Hellinger-Reissner variational principle [16], and denoting $\partial z/\partial x = \dot{z}$ where z is a dummy variable and the others are common notations, it can be shown that

$$\Pi_2 = \iint \left\{ V\dot{w} + M\dot{\theta} - H \right\} dxdy \tag{2}$$

where H is the Hamiltonian function. The variables are w, θ and the complementary variables are V_x, M_x or V, M briefly. These variables form a state vector $\mathbf{v} = \left\{ w \quad \theta \quad V \quad M \right\}^{\mathrm{T}}$ in the symplectic space. Performing variation on the Hamiltonian function H, we obtain

$$\dot{\mathbf{v}} = \mathbf{H}\mathbf{v} \tag{3}$$

where $\mathbf{H}$ is the Hamiltonian matrix. Upon separating the variables, the state vector can be expressed as

$$\mathbf{v}(x, y) = \xi(x)\boldsymbol{\psi}(y) \tag{4}$$

Substituting into Eq. (3) yields

$$\xi(x) = e^{\mu x} \quad \text{and} \quad \mathbf{H}\boldsymbol{\psi} = \mu\boldsymbol{\psi} \tag{5}$$

where μ is the eigenvalue and $\boldsymbol{\psi} = \left\{ \tilde{w} \quad \tilde{\theta} \quad \tilde{V} \quad \tilde{M} \right\}^{\mathrm{T}}$ is the eigenvector in which the elements are functions of y. Expressing $\boldsymbol{\psi} = \left\{ A \quad B \quad C \quad D \right\}^{\mathrm{T}} e^{\lambda y}$ and substituting into Eq. (5) yield the eigenvalues

$$\lambda_{1,2} = \pm\sqrt{\omega\sqrt{\rho h / D} - \mu^2} \quad \text{and} \quad \lambda_{3,4} = \pm\sqrt{-\omega\sqrt{\rho h / D} - \mu^2} \tag{6}$$

for nontrivial solution. The state vector can be solved by back substituting μ and $\boldsymbol{\psi}$ into Eq. (4).

For an opposite simply supported plate at $y = \pm b$, the boundary conditions are

$$M_y\big|_{y=\pm b} = 0 \quad ; \quad w\big|_{y=\pm b} = 0 \tag{7}$$

for an opposite clamped plate at $y = \pm b$, the boundary conditions are

$$w\big|_{y=\pm b} = 0 \quad ; \quad \left.\frac{\partial w}{\partial y}\right|_{y=\pm b} = 0 \tag{8}$$

and for an opposite free plate at $y = \pm b$, the boundary conditions are

$$M_y\big|_{y=\pm b} = 0 \quad ; \quad V_y\big|_{y=\pm b} = 0 \tag{9}$$

From the property of symplectic adjoint orthogonality of eigenvector and expansion of eigenvector, the state vector can be expanded as

$$\mathbf{v} = \sum^{\infty} \left[f(n) e^{\mu_n x} \boldsymbol{\psi}_{\mathbf{n}} \right] \tag{10}$$

where $f(n)$ is an unknown function depending on the boundary conditions at $x = \pm a$.

3. Examples

This example considers a rectangular plate with opposite sides clamped. The nonzero eigenvalues for symmetric vibration modes are solved first. Substituting the general solution of Eq. (3) into the clamped boundary conditions in Eq. (8) and setting the determinant to zero result in

$$\lambda_2 \cosh \lambda_1 b \sinh \lambda_2 b - \lambda_1 \sinh \lambda_1 b \cosh \lambda_2 b = 0 \tag{11}$$

which can be solved for the eigenvalue μ. The displacement can be solved as

$$w = \cosh \lambda_3 b \cosh \lambda_1 y - \cosh \lambda_1 b \cosh \lambda_3 y \tag{12}$$

Similarly for antisymmetric vibration modes, the transcendental equation is

$$\lambda_3 \sinh \lambda_1 b \cosh \lambda_3 b - \lambda_1 \cosh \lambda_1 b \sinh \lambda_3 b = 0 \tag{13}$$

and the displacement is

$$w = \sinh \lambda_3 b \sinh \lambda_1 y - \sinh \lambda_1 b \sinh \lambda_3 y \tag{14}$$

The next example considers a rectangular plate with opposite sides free. The nonzero eigenvalues for symmetric vibration modes are solved first. Substituting the general solution of Eq. (3) into the free boundary conditions in Eq. (9) and setting the determinant to zero result in the following transcendental equation

$$\lambda_2 \left(\lambda_2^2 - \upsilon\mu^2 + 2\mu^2\right)\left(\lambda_1^2 + \upsilon\mu^2\right) \sinh \lambda_2 b \cosh \lambda_1 b - \lambda_1 \left(\lambda_1^2 - \upsilon\mu^2 + 2\mu^2\right)\left(\lambda_2^2 + \upsilon\mu^2\right) \sinh \lambda_1 b \cosh \lambda_2 b = 0 \tag{15}$$

which can be solved for the eigenvalue μ. The displacement can be solved as

$$w = \left(\upsilon\mu^2 + \lambda_3^2\right) \cosh \lambda_3 b \cosh \lambda_1 y - \left(\upsilon\mu^2 + \lambda_1^2\right) \cosh \lambda_1 b \cosh \lambda_3 y \tag{16}$$

Similarly, for antisymmetric vibration modes, the transcendental equation is

$$\lambda_3 \left(\lambda_3^2 - \upsilon\mu^2 + 2\mu^2\right)\left(\lambda_1^2 + \upsilon\mu^2\right) \sinh \lambda_1 b \cosh \lambda_3 b - \lambda_1 \left(\lambda_1^2 - \upsilon\mu^2 + 2\mu^2\right)\left(\lambda_3^2 + \upsilon\mu^2\right) \cosh \lambda_1 b \sinh \lambda_3 b = 0 \tag{17}$$

and the displacement can be solved accordingly.

4. Conclusions

In this paper, a new symplectic elasticity approach has been presented. Analytical benchmarks for free vibration of rectangular thin plates have been presented for some cases where analytical solutions have been hitherto unavailable. For example, the paper presents analytical solutions for free vibration of completely free rectangular thin plates in which all natural and geometric boundary conditions are satisfied. The new approach has very high potential for exact plate bending solutions.

References

[1] Weyl, H., 1939. The Classical Groups, Their Invariants and Representations, Princeton University Press.
[2] Koszul, J., Zou, Y., 1986. Theory of Symplectic Geometry, Beijing: Science Press. (in Chinese)
[3] Kauderer, M., 1994. Symplectic Matrices, First Order Systems and Special Relativity, World Scientific Publishing.
[4] De Gosson, M.A., 2001. The Principles of Newtonian and Quantum Mechanics, World Scientific Publishing.
[5] Feng, K., 1985. On difference scheme and symplectic geometry, In K. Feng, (Ed.), Proc. Beijing Symp Differential Geometry and Diifferential Equations, Beijing, Science Press, 42-58.
[6] Feng, K., 1986. Difference schemes for Hamiltonian formalism and symplectic geometry, J. Computational Mathematics, 4(3), 279-289.
[7] Lax, P., 1993. Feng Kang, SIAM News, 26(11).
[8] Zhong, W., 1991. Plane elasticity problem in strip domain and Hamiltonian system, Journal of Dalian University of Technology, 31(4), 373-384. (in Chinese)
[9] Yao, W., Zhong, W., Lim, C.W., 2007. Symplectic Elasticity, submitted to World Scientific Publishing.
[10] Lim, C.W., S. Cui and Yao, W.A., On new symplectic elasticity approach for exact bending solutions of rectangular thin plates with two opposite sides simply supported, International Journal of Solids and Structures, in press, 2007.
[11] Leissa, A.W., 1969. Vibration of Plates, NASA SP-160.
[12] Leissa, A.W., 1973. The free vibration of rectangular plates, Journal of Sound and Vibration, 31, 257-293.
[13] Timoshenko, S.P., Woinowsky-krieger, S., 1970. Theory of Plates and Shells, Mcgraw-hill International editions.
[14] Lim, C.W. and S. Cui, On new symplectic elasticity approach for exact bending solutions of rectangular thin plates without two opposite sides simply supported, in preparation, 2007.
[15] Lim, C.W., S. Cui and Yao, W.A., Exact symplectic solutions for bending of corner supported rectangular thin plates, in preparation, 2007.
[16] Hu, Haichang., 1981. Variational Principle of Elasticity and Its Application, Beijing: Science Press. (in Chinese)

Acknowledgement

The work described in this paper was supported by a grant from Research Grants Council of the Hong Kong Special Administrative Region (Project No. 9041145).

A Theory of Stability of a Moving Oscillator on an Infinitely Long, Flexibly Supported Beam

Andrei V. Metrikine
Delft University of Technology, The Netherlands

In the mid-1980s, Denisov *et. al.* [1] and Bogacz *et. al.* [2] have shown that a linear oscillator that moves along an infinitely long, straight beam on a viscous-elastic foundation can be unstable. The instability implies that the initial transverse deflection of the moving oscillator grows in time until the contact between the oscillator and the beam is broken.

During the last ten years, a number of papers have been published [3-6], in which the instability of various moving objects on one-, two- and three-dimensional elastic structures has been considered. The interest in the subject is driven by the massive introduction of high-speed trains, whose stability at high-speeds greatly depends on dynamic interaction between the train wheels and the rails.

In the present work, the above-described instability phenomenon is first introduced by analyzing the natural frequencies of a two-mass oscillator that moves along a flexibly supported Euler-Bernoulli beam as shown in Figure 1(a).

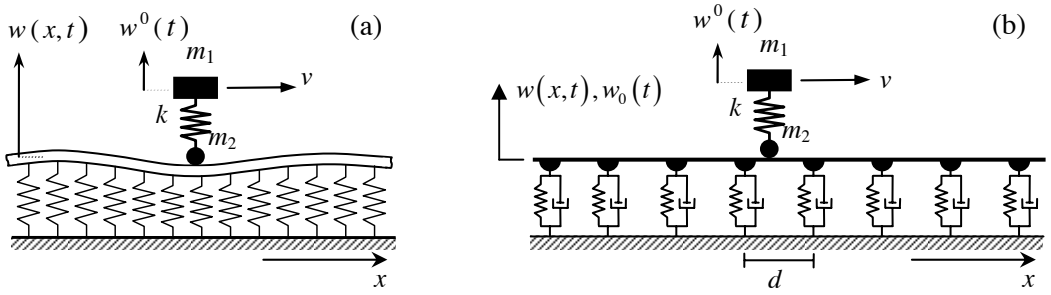

Figure 1. Moving oscillator on (a) continuously supported beam, (b) periodically supported string.

The natural frequencies of the oscillator can be real or complex, depending on the velocity of the oscillator and the system parameters. The imaginary part of the complex frequencies can be either negative or positive corresponding to decaying or growing (unstable) vibration, respectively. The complex natural frequencies occur because of the energy input by a force that maintains uniform motion of the oscillator along the beam and because of radiation damping associated with flexural waves that the vibrating oscillator generates in the beam.

To explain the different possible types of natural vibration of the oscillator, the energy and momentum variation in the system are studied on the basis of the following equations [7,8]:

$$\frac{dE^0}{dt} + \left(S - ve\right)\Big|_{x=vt-0}^{x=vt+0} = Rv, \qquad \frac{dP^0}{dt} + \left(F - vp\right)\Big|_{x=vt-0}^{x=vt+0} = R, \tag{1}$$

where E^0 and P^0 are the energy and the longitudinal component of the momentum of the oscillator, v is the oscillator's velocity, R is an external force that maintains the uniform motion of the oscillator along the beam, S and e are the energy flux through a cross-section of the beam and the linear energy density of the supported beam, and F and p are the flux and density of the wave momentum.

Using the energy and momentum variation laws given by Eq. (1), it is shown that the three regimes of natural vibration of the oscillator (harmonic, decaying and growing) are one-to-one related to the possible regimes of wave generation in the beam. Harmonic oscillations occur if the vibrating oscillator does not generate evanescent (not propagating) waves in the beam. Decaying and growing oscillations occur when the oscillator generates propagating waves in the beam. These waves can be either "normal Doppler waves" or "anomalous Doppler waves" according to the terminology introduced in [9]. Reaction of the former waves decreases the energy of the oscillator, whereas that of the latter increases it. It should be noted that the anomalous Doppler waves may be generated by the oscillator only if it moves at a velocity higher than the minimum phase speed of flexural waves in the beam. Therefore, the oscillator, when moving on a homogeneous system, may become unstable only if its velocity is high enough.

The above analysis of the energy variation of the oscillator shows that the energy increase in the unstable regime is due to the force that maintains the oscillator's motion along the beam. This force is essentially horizontal (directed along the beam), and, therefore, the work of this force may strongly depend on the description of longitudinal dynamics of the beam (friction in the contact, longitudinal vibrations, etc.). To check this, coupled transversal-longitudinal vibrations of the beam are considered, taking into account friction in the contact and longitudinal stiffness of the beam's elastic foundation. It is shown that due to the contact friction, a non-negligible axial compression and axial tension occur in front of and behind the oscillator, respectively (the compression and tension interchange their locations if a driving wheel of the train's locomotive is modeled by the oscillator). These axial forces strongly depend on the velocity of the oscillator. The higher the velocity of the oscillator and/or the higher the longitudinal stiffness of the beam's foundation, the stronger is the effect of friction in the contact on the stability of the oscillator.

If a beam on elastic foundation as shown in Figure 1(a) would be considered as a realistic model for the railway track, the instability of a train would be predicted to occur at train velocities higher than 2000 kilometers per hour, which is unreachable for high-speed trains (unless vacuum would be created in a tunnel in which the trains would run). However, the beam on elastic foundation is totally unacceptable as a model of railway tracks for high-speed trains. The main drawback of this model is that it does not account for dependence of the stiffness of the railway track's subsoil on the frequency and wavelength of vibration of the rails. To show the effect of this dependence, a three-dimensional model is considered of a railway track that consists of a beam on a viscous-elastic half-space. It is shown that the instability may occur as soon as the oscillator's (train's) velocity would exceed the Rayleigh wave velocity in the half-space. This velocity can be as low as 200 kilometers per hour if the railway track is built on soft subsoil, which is currently the case in some parts of Sweden, the Netherlands and China. Therefore, the instability phenomenon is of practical significance.

All models discussed above are homogeneous in the direction of motion of the oscillator. One may wonder whether a certain inhomogeneity of the model would influence the instability phenomenon. This question has a strong engineering background because nearly all railway tracks and overhead catenary lines for trains (the instability may occur also in the course of interaction of a

current collector of a train with the overhead contact wire) are periodically inhomogeneous along their length. It can be anticipated that the periodical inhomogeneity can influence the instability phenomenon strongly because the anomalous Doppler waves can be generated in inhomogeneous systems at any speed of the oscillator [9]. Another, probably more "mechanical", reason for anticipating a significant effect of the periodical inhomogeneity on the system stability can be formulated as follows. The parameters of a periodically-inhomogeneous elastic system at the contact point with the moving oscillator vary periodically in time provided that the oscillator's velocity is constant. The period of this variation equals d/v, where d is the spatial period of inhomogeneity and v is the oscillator's velocity. Obviously, one may expect parametric resonance if one of the natural frequencies of the oscillator on the elastic system equals $nd/2v$.

To explore the effect of the periodical inhomogeneity, the stability is studied of the moving oscillator on a string supported by periodically spaced discrete supports as shown in Figure 1(b). This model mimics simplistically the dynamic interaction of an overhead power line and the current collector of a train. It is shown that, as expected, parametric instability zones exist in the parameter space of the system. The size of these zones strongly depends on the stiffness and viscous damping in the supports of the string. The stiffer the supports, the wider are the zones. The effect of the damping is ambiguous. The higher-order zones become narrower as the damping increases, whereas the main zone widens. The latter effect can be explained by the fact that a higher damping in the supports increases their dynamic stiffness thereby causing a larger energy input into the system by the force that maintains the uniform motion of the oscillator along the string.

References

1. G.G. Denisov, E.K. Kugusheva, V.V. Novikov, On the problem of the stability of one-dimensional unbounded elastic systems. *Journal of Applied Mathematics and Mechanics* 49 (1985) 533-537.
2. R. Bogacz, S. Nowakowski, K. Popp, On the stability of a Timoshenko beam on elastic foundation under a moving spring-mass system. *Acta Mecanica* 61 (1986) 117-127.
3. A.V. Metrikine, H.A. Dieterman, Instability of vibrations of a mass moving uniformly along an axially compressed beam on a visco-elastic foundation, *Journal of Sound and Vibration* 201(5) (1997) 567-576.
4. A.V. Kononov AV, R. de Borst R, Instability analysis of vibrations of a uniformly moving mass in one and two-dimensional elastic systems. *European Journal of Mechanics A-Solids* 21 (2002) 151-165.
5. D.Y. Zheng, S.C. Fan, Instability of vibration of a moving-train-and-rail coupling system *Journal of Sound And Vibration* 255 (2002) 243-259.
6. A.V. Metrikine, S.N. Verichev, J. Blaauwendraad, Stability of a two-mass oscillator moving on a beam supported by a visco-elastic half-space, *International Journal of Solids and Structures* 42 (2005) 1187-1207.
7. A.I. Vesnitskii, L.E. Kaplan, G.A. Utkin, The laws of variation of energy and momentum for one-dimensional systems with moving mountings and loads, *PMM Journal of Applied Mathematics and Mechanics* 47 (1983) 692-695.
8. A.V. Metrikine, Unstable lateral oscillations of an object moving uniformly along an elastic guide as a result of an anomalous Doppler effect, *Acoustical Physics* 40 (1994) 85-89.
9. V.L. Ginzburg, *Theoretical Physics and Astrophysics,* Pergamon, Oxford, 1979.

Experiments on Chaotic Vibrations of a Post-buckled Rectangular Plate under Compression Normal to Clamped Edges

Ken-ichi NAGAI, Shinichi MARUYAMA, Masaki KUROSAWA and Takao YAMAGUCHI
Department of Mechanical System Engineering, Gunma University,
1-5-1 Tenjin-cho, Kiryu, Gunma 376-8515, JAPAN
nagai@eng.gunma-u.ac.jp

1. Introduction Experimental results are presented on chaotic vibrations of a thin rectangular plate subjected to periodic lateral excitation. The plate is clamped at opposite edges and is simply supported at the other edges. The plate is buckled by an in-plane elastic constraint at the clamped edges. Chaotic responses are examined with the Poincaré projections and the Lyapunov exponents. Contribution of vibration modes to the chaotic responses of the plate is inspected with the Karhunen-Loève transformation.

2. Test Plate and Test Procedure As shown in Fig.1, a phosphor-bronze plate with thickness h=0.24 mm, square form of length a=140 mm is clamped at opposite edges. The other edges are simply-supported by adhesive flexible films. The plate is initially compressed to the post-buckled configuration with the elastic spring in the in-plane direction normal to the clamped edges. In the figure, the coordinate system is defined by the x-axis along the simply-supported edge, the y-axis along the clamped edge and z-axis perpendicular to the mid-plane of the plate. In the experiment, first, the restoring force and the linear natural frequencies of the post-buckled plate are examined. Next, the plate is excited laterally with an electromagnetic exciter. The plate is subjected to gravitational acceleration g and periodic acceleration $a_d \cos 2\pi f t$, where f is the exciting frequency and a_d is the peak amplitude of acceleration. Dynamic responses of the plate are measured with multiple laser displacement sensors and recorded for the data analysis. Chaotic responses are inspected with the frequency response curves, the Fourier spectra, the Poincaré projections and the maximum Lyapunov exponents. Finally, the chaotic responses on the multiple positions of the plate are measured. Mode contribution to the chaos is discussed with the K-L transformation.

3. Results and Discussion The results of the experiment are arranged with the following non-dimensional notations.

$$[\xi, \eta] = [x, y] / a,\ w = W / h,\ n_x = N_x / N_{cr},\ [p_s, p_d] = [g, a_d]\, \rho a^4 / D,\ q_s = Q_s a^2 / Dh,$$
$$[\omega, \omega_{mn}] = [f, f_{mn}]\, (2\pi / \Omega_0),\ \tau = \Omega_0 t \qquad (1)$$

where $\Omega_0 = a^{-2}\sqrt{D/\rho h}$ is the coefficient corresponding to lateral vibration of the plate. Notation $D = Eh^3 / \{12(1-\nu^2)\}$ is the bending rigidity of the plate, where E is Young's modulus and ν is Poisson's ratio. In Eq. (1), ξ and η are the non-dimensional coordinates, w is the lateral displacement normalized by the plate thickness h. The symbol n_x is the non-dimensional stress resultant, normalized by the buckling resultant N_{cr}, acting on the cross section perpendicular to the x-direction. Notations p_s and p_d are the non-dimensional load intensities related to the gravitational acceleration g and the periodic peak acceleration a_d, respectively. When the restoring force of the plate is examined, static deflection under the static concentrated force Q_s is measured. Notation q_s is the non-dimensional force. Notations ω and τ are the nondimensional exciting frequency and the time, respectively. In the experiment, the static load intensity by the gravity p_s and the amplitude of periodic excitation p_d are chosen as $p_s = 337$ and $p_d = 688$, respectively.

Figure 2 shows the static deflection w of the plate under the concentrated force q_s loaded at the center $\xi = 0.5$ and $\eta = 0.5$. The deflections at four points are detected. When the force increases from the stable equilibrium position to the positive z direction, the plate deflections show the characteristics of a hardening spring. As the force is loaded to the negative z direction, the spring characteristics change to the softening-and-hardening type. When the force q_s is close to q_s = -30, the gradients of the

curves of the force decrease to zero-value. Consequently, the large-amplitude of lateral deformation appears in the plate. Table 1 shows the linear natural frequencies ω_{mn} where m and n denote the half-wave numbers of the vibration modes along the x-axis and the y-axis, respectively. In the table, the lowest natural frequency ω_{11}=34.9 is close to one third of the natural frequency ω_{13} =101 of the mode with two nodal lines along the x-axis. This relation implies the possibility of the existence of internal resonance.

Nonlinear response curves of the plate are presented in Fig. 3. The amplitude of response at the position $\xi = 0.6$ and $\eta = 0.4$ is shown with the root mean square value. The resonance response is denoted by the symbol (m, n; p) with the mode of vibration (m, n) and the type of resonance p. For example, $p = 1$ and $p = 1/2$ represent the principal resonance and the sub-harmonic resonance of 1/2 order, respectively. The large amplitude response (1, 1; 1) is generated from the principal resonance of the lowest mode of vibration. The nonlinear response exhibits the characteristics of a softening-and-hardening spring. A chaotic response is denoted with the symbol C(m, n; p), where indices m and n represent a predominant mode of vibration generated in the chaos and index p is the type of resonance. For example, C(1, 1; 1/2) denotes the chaotic response of the fundamental mode generated from the sub-harmonic resonance of 1/2 order. C(m, n; p: i, j; q) represents the chaotic response involving the response of internal resonance. In Fig. 4, the time progress, the Fourier spectrum and the Poincaré projection of the chaotic response C(1,1;2/3) are shown, at the exciting frequency ω=41.6. The time progress of the response w is presented by the number of excitation period τ_e. In Fig. 4(b), broad band spectrum is observed. Dominant peaks of the spectrum correspond to the ultra-sub harmonic resonance of order 2/3 with the lowest mode of vibration. In Fig. 4(c), the Poincaré projection shows the distinct figure in the space of deflection and velocity. When the exciting frequency ranges from ω=50.9 to ω=57.0 and from ω=58.5 to ω=67.7, as shown in Fig. 5, the predominant chaotic response of the type C(1,1;1/2) prevails in a relatively wide range of frequency. Furthermore, as shown in Fig.6, when the exciting frequency increases to ω=66.8, the chaotic response of the type C(1,1;1/2) is dominated by the internal resonance condition of $3\omega_{11} \approx \omega_{13}$. Irregular amplitude modulation of chaotic response is observed. Consequently, the chaotic response C(1,1;1/2:1,3;3/2) involves both the sub-harmonic component of order 1/2 with the lowest mode of vibration (1,1) and the ultra-sub harmonic component of order 3/2 with the mode of vibration (1,3). Figure 7 shows the maximum Lyapunov exponents λ_{max} related to the embedding dimension e of the chaotic responses. The maximum Lyapunov exponent λ_{max}=1.3 is obtained in the chaotic response C(1,1;2/3) at ω=41.6, while λ_{max}=1.4 in the response C(1,1;1/2) at ω=54.3. The chaotic response C(1,1;1/2:1,3;3/2) related with the internal resonance at ω=66.8 shows the exponent within λ_{max}=0.2 and λ_{max}=0.4. The maximum Lyapunov exponents converge to the positive constants, then these responses are confirmed as chaos.

The Karhunen-Loève transformation can estimate the contribution of vibration modes to the chaotic response of the post-buckled plate. The chaotic time progresses of deflection are measured simultaneously at six positions of the plate. Applying the K-L transformation to the data of the chaotic response of C(1,1;2/3) at ω=41.6, the contribution ratio and related modal pattern are shown in Fig. 8. The lowest mode (1,1) has the largest contribution ratio μ_1=87%. The second larger contribution ratio of μ_2=7% corresponds to the mode (1,2), while the third one μ_3=3% is related with the higher modes (1,3) and (3,1). For the other chaotic responses, including the former one, the contribution ratios and the corresponding modal patterns are shown in table 2. The chaotic response of C(1,1;1/2) is generated close to the natural frequency of the mode (1,2). Thus, the contribution ratio of the second mode (1,2) increases to μ_2=17% compared with the contribution ratio μ_1=70% of the lowest mode (1,1). In the chaotic response C(1,1;1/2:1,3;3/2) with the type of internal resonance, the lowest mode of vibration(1,1) and the degenerated mode combined with (1,3) and (3,1) are generated simultaneously with the contribution ratio μ_1=77% and μ_2=16%. The corresponding modal patterns are shown in Fig. 9.

4. Conclusion Precise experimental results are presented on chaotic vibrations of a post-buckled plate clamped at opposite edges. Chaotic responses are generated from the sub-harmonic resonance of 1/2 order and from the ultra-sub harmonic resonance of 2/3 orders with the lowest mode of vibration. In the specific region of the latter one, the chaotic response is dominated by the internal resonance. In the chaotic responses, the lowest mode of vibration and the mode with the nodal lines perpendicular to the clamped edges are predominantly induced.

References

(1) Nagai, K., Maruyama, S., Oya, M. and Yamaguchi, T., "Chaotic oscillations of a shallow cylindrical shell with a concentrated mass under periodic excitation," Computers and Structures Vol.82,(2004),pp.2607-2619.

(2) Yamaguchi, T. and Nagai, K., "Chaotic vibration of a cylindrical shell-panel with an in-plane elastic-support at boundary," Nonlinear Dynamics Vol.13,(1997), pp.259-277.

(3) Azeez, M.F. and Vakakis, A.F., "Proper orthogonal decomposition (POD) of a class of vibroimpact oscillations," Journal of Sound and Vibration Vol.240, No.5, (2001), pp.859-889.

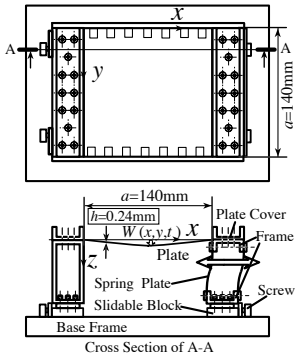

Fig.1 Plate and fixture

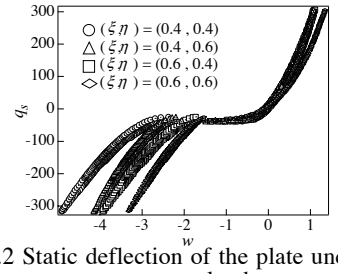

Fig.2 Static deflection of the plate under concentrate load

Table.1 Natural frequencies and Natural modes of vibration

Mode i	Mode (m,n)	Modal pattern (ξ, η)	Experimental results ω_{mn}	Experimental results f_{mn} [Hz]
1	(1,1)		34.9	61.2
2	(1,2)		55.6	97.5
3	(2,1)		70.7	123.8
4	(2,2)		82.8	145.0
5	(1,3)		101.0	177.0
6	(3,1)		109.8	192.4

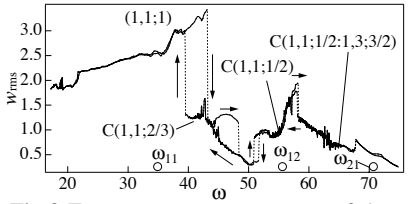

Fig.3 Frequency response curve of the plate (n_x=1.5)

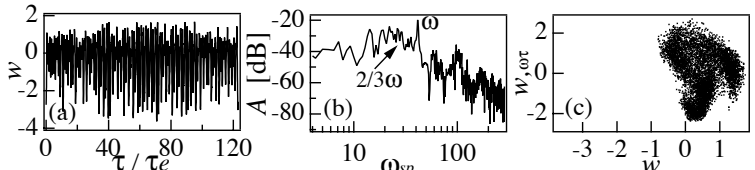

Fig.4 Chaotic response (p_d=688, ω=41.6, C(1,1;2/3))

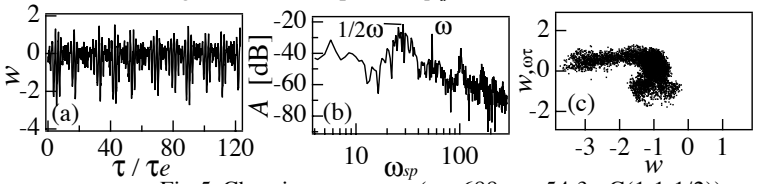

Fig.5 Chaotic response (p_d=688, ω=54.3, C(1,1;1/2))

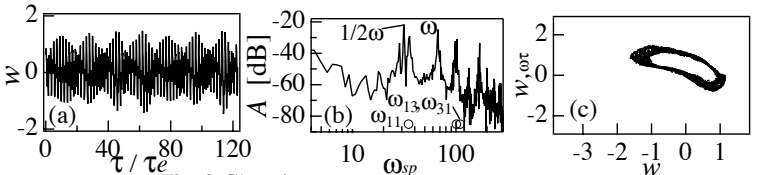

Fig.6 Chaotic response (p_d=688, ω=66.8, C(1,1;1/2:1,3;3/2))

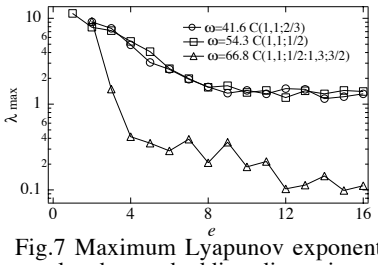

Fig.7 Maximum Lyapunov exponent related to embedding dimension

Table.2 Contribution ratio of principal components

Type of response	Mode (m,n)	Contribution Ratio [%]
C(1,1;2/3)	(1,1)	86.7
	(1,2)	6.78
C(1,1;1/2)	(1,1)	69.5
	(1,2)	17.3
C(1,1;1/2 :1,3;3/2)	(1,1)	76.8
	(1,3)(3,1)	15.9

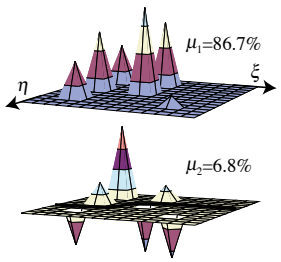

Fig.8 Modal pattern obtained by Karhunen-Loève transformation (p_d=688, ω=41.6, C(1,1;2/3))

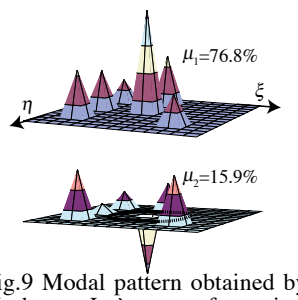

Fig.9 Modal pattern obtained by Karhunen-Loève transformation (p_d=688, ω=66.8, C(1,1;1/2:1,3;3/2))

FREE VIBRATION OF SHALLOW SHELLS WITH GENERAL SURFACES EXPRESSED BY A CUBIC POLYONOMIAL FUNCTION

Yoshihiro Narita and Daisuke Narita

Department of Mechanical Engineering, Hokkaido University, Sapporo, 060-8628 Japan

e-mail: ynarita@eng.hokudai.ac.jp

1. Introduction

This study proposes an analytical method to deal with the free vibration of shallow shells with generally curved surfaces expressed by cubic polynomial functions. Such shell structures with variable curvature are recently found in automobile and other design-oriented structural applications. In the analysis an interpolating function of the third order is introduced to represent the required surface shape and the corresponding curvature is derived as a linear function of the position. The obtained curvature is substituted into the total potential energy of the shell, and the analytical procedure is shown to derive a frequency equation by the Ritz method. Numerical examples demonstrate that the vibration of shallow shells with various curved surfaces can be analyzed by the present method, and the effects of varying the coefficients in the cubic function for geometric expression are clarified on the natural frequencies and mode shapes. Although there have been some papers on shallow shells with slightly non-uniform curvature [1.2], very little has been done on shallow shells with general curvature given by polynomial functions.

2. Vibration Analysis

A rectangle-like shallow shell whose planform has a dimension of $a \times b$ (h: thickness) is considered, as shown in Fig.1, and the height (shell height) of the shell middle-plane from the xy plane is interpolated in the third polynomial as

$$\phi(x,y)=c_0+c_{10}x+c_{01}y+c_{20}x^2+c_{11}xy+c_{02}y^2+c_{30}x^3+c_{21}x^2y+c_{12}xy^2+c_{03}y^3 \quad (1)$$

where c_0, c_{10} … c_{03} are unknown coefficients to be determined by interpolating with the representative points of shell geometry.

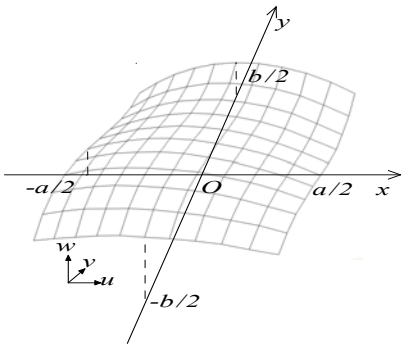

Fig.1 Example of shallow shell with general cubic surface

Based on an assumption $(\partial\varphi/\partial x)^2=(\partial\varphi/\partial y)^2=0$ where the slope of the shell geometry is relatively small, the curvatures are obtained by differentiating Eq.(1) twice as

$$\frac{1}{R_x}=2(c_{20}+3c_{30}x+c_{21}y),\quad \frac{1}{R_y}=2(c_{02}+c_{12}x+3c_{03}y),\quad \frac{1}{R_{xy}}=c_{11}+2c_{21}x+2c_{12}y \quad (2)$$

Equation (2) indicates that the curvatures vary in linear fashion. The coefficients c_0, c_{10} and c_{01} are not included in the curvatures and those of (c_{20} and c_{30}) and (c_{02} and c_{03}) appear only in $1/R_x$ and $1/R_y$, respectively. The twisting curvature is generated by c_{11}, c_{21} and c_{12} in the terms of products of x and y in Eq.(1). In the Donnell-type thin shell theory, the relations between the middle-plane displacements (u, v and w) and the strains (ε_x, ε_y and γ_{xy}) are given by

$$\varepsilon_x = \frac{\partial u}{\partial x} + \frac{w}{R_x} \quad , \quad \varepsilon_y = \frac{\partial v}{\partial y} + \frac{w}{R_y} \quad , \quad \gamma_{xy} = \frac{\partial u}{\partial y} + \frac{\partial v}{\partial x} + \frac{2w}{R_{xy}} \tag{3}$$

The difference between the present and conventional shell analyses is characterized by the fact that the curvatures in Eqs.(3) are not constant but linear functions of the coordinate (*x,y*).

In using the Ritz method, one has to evaluate the strain energy $V = V_s + V_{bs} + V_b$, where V_s is the energy caused by the in-plane motion, V_{bs} is the energy by the coupling and V_b is the energy by out-of-plane motion.

$$V_s = \frac{1}{2}\iint \{\varepsilon\}^T [A]\{\varepsilon\}\, dxdy, \;\; V_{bs} = \frac{1}{2}\iint \left(\{\kappa\}^T [B]\{\varepsilon\} + \{\varepsilon\}^T [B]\{\kappa\} \right) dxdy, \;\; V_b = \frac{1}{2}\iint \{\kappa\}^T [D]\{\kappa\}\, dxdy \tag{4}$$

where $\{\varepsilon\}$ and $\{\kappa\}$ are the strain and curvature vectors, and the stiffness matrices are given here for the isotropic materials. The kinetic energy for the shell is also defined.

Next, the displacement functions are assumed by the double series form as

$$u(\xi,\eta,t) = \sum_{i=0}^{M-1}\sum_{j=0}^{N-1} P_{ij} X_i(\xi) Y_j(\eta) \sin\omega t, \;\; v(\xi,\eta,t) = \sum_{k=0}^{M-1}\sum_{l=0}^{N-1} Q_{kl} X_k(\xi) Y_l(\eta) \sin\omega t, \;\; w(\xi,\eta,t) = \sum_{m=0}^{M-1}\sum_{n=0}^{N-1} R_{mn} X_m(\xi) Y_n(\eta) \sin\omega t \tag{5}$$

where P_{ij}, Q_{kl} and R_{mn} are unknown coefficients , and $X_i(\xi)$, $Y_j(\eta)$,… and $Y_n(\eta)$ are the functions that satisfy the geometrical boundary conditions. After the equations are rewritten by using the non-dimensional quantities, the displacements (5) are substituted into the functional $L=T_{max}- V_{max}$ in terms of the maximum strain and kinetic energies. Then an eigenvalue equation is derived by the minimizing process $\partial L/\partial P_{ij} = \partial L/\partial Q_{kl} = \partial L/\partial R_{mn}$.

3. Numerical Results and Discussions

The variable curvatures for $1/R_x$, $1/R_y$ and $1/R_{xy}$ are described by Eq.(2). The coefficients c_{ij} (i,j=0,1,2,3) are arbitrary, and the number of combinations will be innumerable even when the coefficients are made discrete numbers. In the examples, the standard shape of the present shallow shell is set up for reference purposes. This is a model of bonnet (hood) of an automobile, as shown in Fig.2, denoted by NUC (Non-Uniform Curvature) model. The NUC model has a shape of height

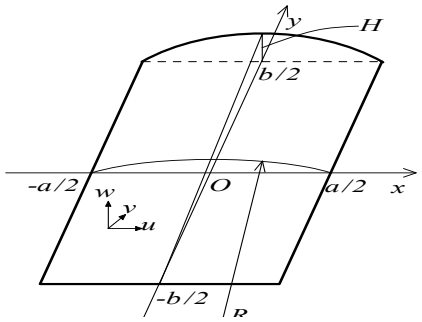

Fig.2 NUC model

$$\phi(-a/2, y) = \phi(a/2, y) = \phi(x, -b/2) = 0, \;\; \phi(0, b/2) = H \tag{7}$$

The material is isotropic (Poisson's ratio ν=0.3), and the frequency parameter is made non-dimensional with the representative length and Young's modulus as $\Omega = \omega a^2(\rho h/D)^{1/2}$ with $D = Eh^3/12(1-\nu^2)$. The NUC model here has the thickness of h/a=0.01 and the aspect ratio of square planform (a/b=1). The frequency parameters and vibration mode shapes are calculated to study effects of varying the coefficient values in the curvatures (2) for the simply supported shallow shells.

Figure 3 presents contour plots of the mode shapes for the lowest four modes with the frequency parameter Ω_1, Ω_2, Ω_3 and Ω_4. The corresponding shell geometry before deformation is illustrated in each row. The mark "×" represents the maximum displacement point and the thin lines denote the displacement contour lines. The thick lines represent the nodal lines (i.e., lines of zero displacement). In Fig.3(a), the result for a NUC model is given

with the coefficients c_{00}=0.03157, c_{01}=0.0635, c_{20}=-0.127 and c_{21}=-0.254 in Eq.(1), where the maximum height is the same as a cylindrical shell with a/R_x=0.5, and is used as a base for comparison. When the number of a half wave is used to describe the mode shapes, the first mode (Ω_1) is the (1,1) mode, the second (Ω_2) is the (2,1) mode, the third (Ω_3) is the (1,2) mode and the fourth (Ω_4) is the (2,2) mode. Because of the curvature on the surface, the nodal line becomes rather distorted, like U-shape in the third mode, in the *y* direction but still symmetric about the *y* axis. In the following study, the coefficients not used in the present NUC model are slightly shifted (± 0.05) to observe effects caused by varying the coefficients.

In (b) c_{11}=0.05, since c_{11} is a coefficient of the *xy* term that gives the constant twist, the mode shapes are skewed slightly. In (c), the c_{02} is a coefficient of the y^2 term that gives the linear curvature only in $1/R_y$, and all the mode shapes are symmetric about the *y* axis. The present method is thus capable of analyzing the vibration of shallow shells with linearly changing curvatures for $1/R_x$, $1/R_y$ and $1/R_{xy}$ and also with arbitrary boundary conditions. These advantages offer the analytical tool for parametric study, which is indispensable in optimization of shell geometry.

References

[1] Fan, S.C. and Luah, M.H., *J. Sound Vibr.*, (1995), vol.179, pp.763-776.
[2] Hu, X.X. and Tsuji, T., *J. Sound Vibr.*, (1999), vol.219, pp.63-88.

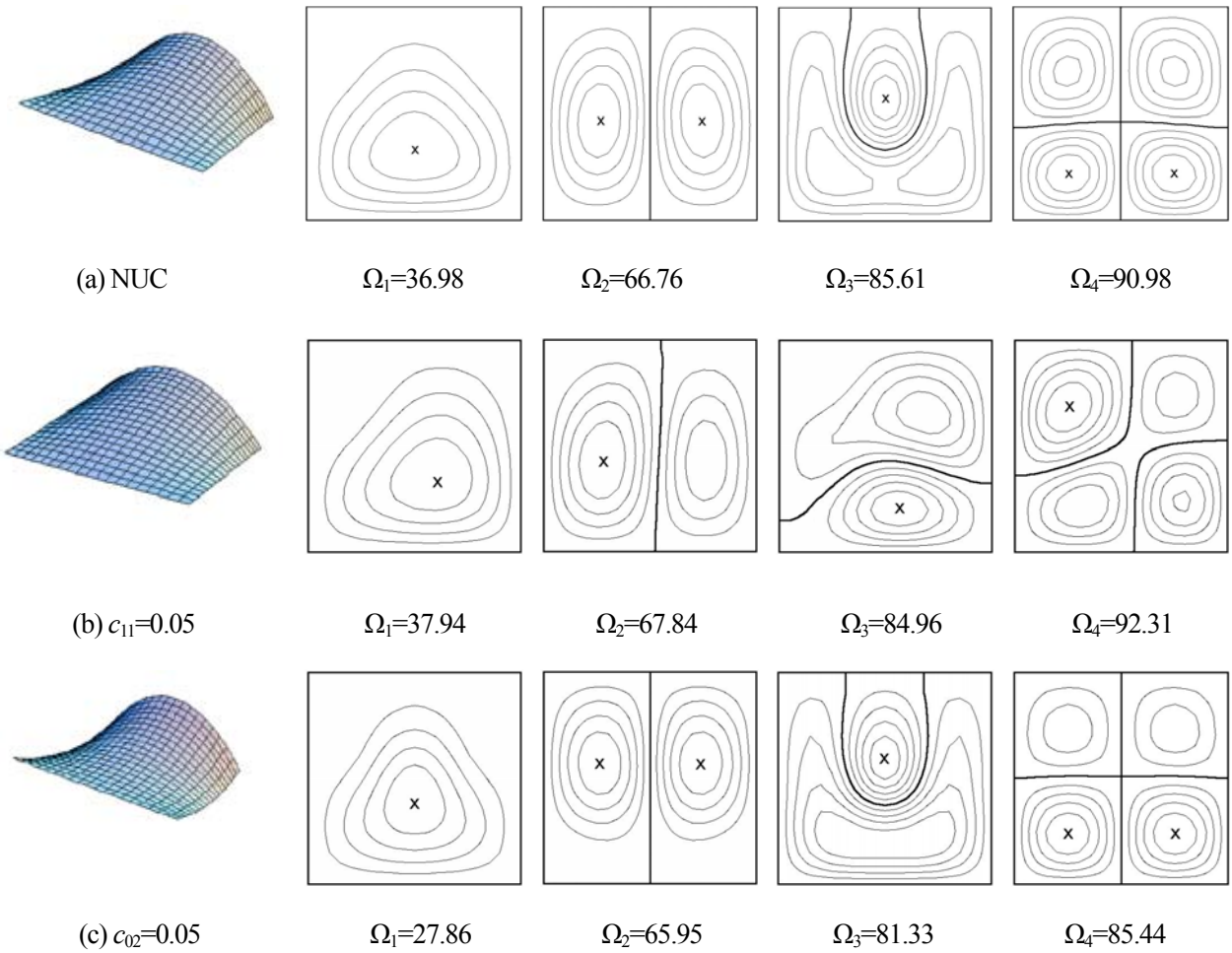

Fig.3 Mode shapes and frequency parameters for simply supported shallow shells with various curvatures.

Resonant Vibration of Planetary Gears Having an Elastic Continuum Ring Gear Excited by Mesh Stiffness Fluctuations

Xionghua Wu and Robert G. Parker
Department of Mechanical Engineering
Ohio State University

In order to maximize the power density and improve load sharing among the planets, planetary gears used in numerous industries are designed to have thin rims, and this leads to elastic deflection of the gear bodies, especially the ring gear [1-3].

The parametric instability of planetary gears having elastic continuum ring gears is analytically investigated based on a hybrid continuous-discrete model. Mesh stiffness variations of the sun-planet and ring-planet meshes caused by the changing number of teeth in contact are the source of parametric instability. The natural frequencies of the time invariant system are either distinct or degenerate with multiplicity two, which indicates three types of combination instabilities: distinct-distinct, distinct-degenerate and degenerate-degenerate instabilities. By using the structured modal properties of planetary gears, the instability boundaries are obtained as simple expressions in terms of mesh parameters through the method of multiple scales. Instability existence rules for in-phase and sequentially phased planet tooth meshes are also discovered. For in-phase planet meshes, instability existence depends only on the type of gear mesh deformation. For sequentially phased planet meshes, the number of teeth on the sun (or the ring) and the type of gear mesh deformation govern the instability existence. The instability boundaries are validated numerically.

This work derives the parametric instability boundaries as simple expressions in the system parameters. We show that some mode types cannot combine to create combination instabilities, and general instability existence rules are obtained for equally spaced planets. By adjusting the tooth numbers, contact ratios, and mesh phase one can neutralize (or suppress) certain types of instabilities, such as all the primary instabilities of any two rotational modes.

1 MATHEMATICAL FORMULATION

Figure 1 shows the elastic-discrete model of a planetary gear. The ring gear is modeled as a thin elastic body. The sun, carrier and planets are treated as rigid bodies with two translational and one rotational DOF. N is the number of planets. The motion of the ring is separated into two parts: the rigid body motion (x_r, y_r, u_r) and the elastic tangential deformation $v(\theta,t)$, which is related to the elastic radial deflection by $w(\theta,t) = -\partial v(\theta,t)/\partial\theta$. The displacement of the system $\mathbf{a}$ is the combination of the elastic deformation of the ring $v(\theta,t)$ and the discrete body deflections $\mathbf{q}$ as

$$\mathbf{a}^T = [v, \mathbf{q}^T] \tag{1}$$

The bearings and supports of the sun, carrier, ring, and planets are modeled as two perpendicular springs with equal stiffness. The sun-planet and ring-planet tooth meshes are modeled as springs with time-varying stiffnesses that fluctuate as the number of teeth in contact at the mesh changes. The amplitude of the stiffness fluctuation relative to the mean stiffness is ε. c_s and c_r are contact ratios of the sun-planet and ring-planet meshes, and Ω is the mesh frequency.

The dimensionless equation of motion for the time-varying system is

$$M\ddot{\mathbf{a}} + K(t)\mathbf{a} = 0 \tag{2}$$

where M and $K(t)$ are extended inertia and stiffness operators that combine the ring PDE with the ODEs for the discrete elements. M and $K(t)$ are self-adjoint with the inner product $<\mathbf{a}^1, \mathbf{a}^2> = \int_0^{2\pi} v^1\overline{v}^2 d\theta + (\mathbf{q}^1)^T\overline{\mathbf{q}}^2$, where the overbar denotes complex conjugation.

The method of multiple scales is used with the introduction of the slow time $\tau = \varepsilon t$, yielding

$$\mathbf{a} = \mathbf{a}_0(t,\tau) + \varepsilon \mathbf{a}_1(t,\tau) + O(\varepsilon^2), \quad \mathbf{a}_0 = \begin{bmatrix} v_0 \\ \mathbf{q}_0 \end{bmatrix}, \quad \mathbf{a}_1 = \begin{bmatrix} v_1 \\ \mathbf{q}_1 \end{bmatrix} \tag{3}$$

$$M\frac{\partial^2 \mathbf{a}_0}{\partial t^2} + K_0 \mathbf{a}_0 = \mathbf{0} \tag{4}$$

$$M\frac{\partial^2 \mathbf{a}_1}{\partial t^2} + K_0 \mathbf{a}_1 = -2M\frac{\partial^2 \mathbf{a}_0}{\partial t \partial \tau} - 2\sum_{L=1}^{\infty}(K_{v1}^{(L)} \sin L\Omega t + K_{v2}^{(L)} \cos L\Omega t)\mathbf{a}_0 \tag{5}$$

The general solution for the time-invariant system (4) is $\mathbf{a}_0 = \sum_{s=1}^{\infty} c_s(\tau)\mathbf{Y}_\mathbf{s}(\theta)e^{i\omega_s t} + c.c.$, where $\mathbf{Y}_\mathbf{s}(\theta)$ are the eigenfunctions in extended variable form [3] and $c.c.$ refers to the complex conjugate of preceding terms. The multiplicity of the natural frequencies are summarized as: (i) Rotational and purely ring modes have distinct natural frequencies; (ii) Translational modes are degenerate with multiplicity two; and (iii) Planet modes exist when the number of planets $N > 3$; if the number of planets is odd, all the planet modes are degenerate with multiplicity two, otherwise, the planet modes may be either degenerate with multiplicity two or distinct. Therefore, all natural frequencies of planetary gears with an elastic ring gear are either distinct or degenerate with multiplicity two.

When a harmonic of the mesh frequency is close to the sum of two natural frequencies secular terms exist in (5), which leads to sum type parametric instability. This condition is

$$L\Omega = \omega_p + \omega_q + \varepsilon\sigma \tag{6}$$

When the harmonic of mesh frequency is close to the difference of two natural frequencies, such as $L\Omega = \omega_p - \omega_q + \varepsilon\sigma$, one can show that difference type parametric instabilities are not possible. The instability boundaries are derived for the cases where ω_p and ω_q are distinct, one distinct and one degenerate, and both degenerate. These expressions simplify considerably based on the modal properties of planetary gears.

Equal planet spacing requires $(z_s + z_r)/N$ to be an integer, where z_s and z_r are the tooth numbers of the sun and ring. Equal planet spacing has only two possible phase conditions: in-phase and sequentially phased. When z_s and z_r are not each integer multiples of *N*, the sun-planet meshes are sequentially phased, as are the ring-planet meshes; otherwise, all the sun-planet meshes are in-phase and all the ring-planet meshes are in-phase.

Further analysis taking advantage of the special modal properties of planetary gears with an elastic continuum ring gear leads to compact expressions for the parametric instability boundaries. In particular, many instabilities can be completely suppressed by appropriate parameter selection.

Selected results are summarized as follows:

- The combination and single mode instabilities associated with a purely ring mode always vanish for either in-phase or sequentially phased meshes.
- For in-phase planet meshes, one can state a key rule governing the existence or elimination of parametric instabilities: If two modes have the same type of gear mesh deformation (as captured by the mode type index T_p) their combination instability exists, otherwise their combination instability vanishes. Consequently, all distinct-degenerate instabilities vanish for in-phase planet meshes.
- For the two cases of distinct-distinct combination instability that do not vanish for in-phase meshes, the instability boundaries are

$$\varepsilon^2\Lambda_{pq}^{(L)} = \frac{4N^2}{L^2\pi^2}\Big[\mu^2(\delta_{s1}^{[p]}\delta_{s1}^{[q]})^2\sin^2(L\pi c_s) + \varepsilon^2(\delta_{r1}^{[p]}\delta_{r1}^{[q]})^2\sin^2(L\pi c_r) + 2\mu\varepsilon\delta_{s1}^{[p]}\delta_{r1}^{[p]}\delta_{s1}^{[q]}\delta_{r1}^{[q]}\sin(L\pi c_s)\sin(L\pi c_r)\cos L\pi(c_r + 2\gamma_{sr} - c_s)\Big] \tag{7}$$

where the δ quantities are modal mesh deflections. When both Lc_s and Lc_r are integers, all potential instabilities driven by the L^{th} harmonic of mesh frequency vanish. When neither of Lc_s, Lc_r are integers, a minimum instability region can be achieved by adjusting c_s, c_r and γ_{sr} in the third term of (7) such that this term is negative with large absolute value comparable to the sum of the first two terms. The width of the instabilities region of two distinct modes is proportional to the number of planets *N* and inversely proportional to *L*.

- Similar closed-form expressions can be derived for other modes and sequential mesh phasing.
- The foregoing closed-form expressions for the instability boundaries are compared to the numerical solution from Floquet theory. Figure 2 shows the instability boundaries for a planetary gear with four in-phase planet meshes. Some instability regions appear to be predicted by only the numerical solution; this is because the figure shows only the primary and secondary instabilities from the analytical solution, and the unmatched instability regions are tertiary or higher order instabilities. Single mode instabilities such as $\omega_5, \omega_7, 2\omega_5, 2\omega_7$ always exist. As predicted by analysis, combination instabilities exist only for modes with the same type of gear mesh deformation such as $\omega_1 + \omega_5$ (two translational modes), $\omega_3 + \omega_7$ (two rotational modes) or $(\omega_4 + \omega_9)/2$ (two planet modes).
- The instability existence rule for sequentially phased meshes is: If $[Lz_s \pm (T_p \pm T_q)]/N \neq$ integer, the instability vanishes; otherwise, the instability exists.

REFERENCES

1. A. Kahraman, A. A. Kharazi, and M. Umrani, A Deformable Body Dynamic Analysis of Planetary Gears with Thin Rims, Journal of Sound and Vibration, 262 (2003), 752-768.
2. T. Hidaka, Y. Terauchi, and K. Nagamura, Dynamic Behavior of Planetary Gear (7th Report), Bulletin of the JSME, 22 (1979), 1142-1149.
3. X. Wu and R. G. Parker, Modal Properties of Planetary Gears with an Elastic Continuum Ring Gear, ASME Journal of Applied Mechanics, Submitted (2006).

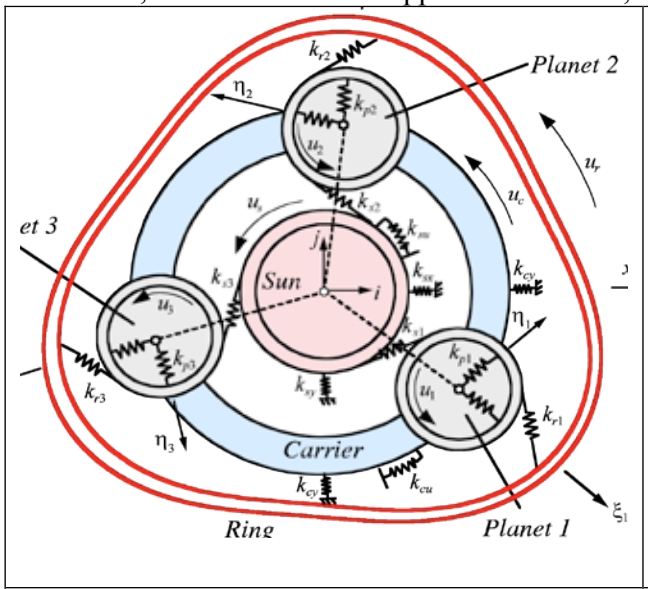

Figure 1: Planetary gear model

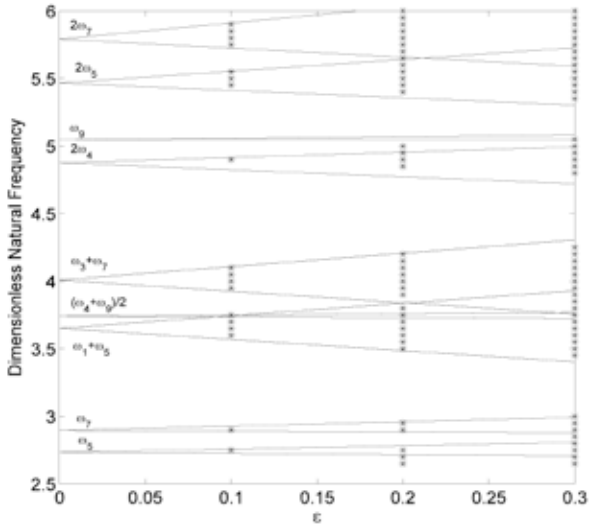

Figure 2: Instability regions for in-phase meshes.

Dynamics of Circular Cylindrical Shells

Francesco Pellicano
Dept. Mech. Civ. Eng., Univ. Modena and Reggio Emilia, Modena, 41100 Italy.
francesco.pellicano@unimore.it

Abstract
In the present paper linear and nonlinear vibrations of circular cylindrical shells having different boundary conditions are analyzed by means of the Sanders-Koiter theory. Displacement fields are expanded in a mixed double series based on harmonic functions and Chebyshev polynomials. Simply supported boundary conditions are analyzed, as well as connection with rigid bodies; in the latter case experiments are carried out. Comparisons with experiments and finite element analyses show that the technique is computationally efficient and accurate in modelling linear vibrations of shells with different boundary conditions. An application to large amplitude of vibration shows that the technique is effective also in the case of nonlinear vibration: comparisons with the literature confirm the accuracy of the approach.

INTRODUCTION

The continuous growing of the commercial use of Space facilities leads to the development of new and more efficient aerospace vehicles; therefore, new and accurate studies on light-weight, thin-walled structures are needed.
The literature on the vibration of shells is extremely wide, the reader can refer to Leissa [1] or Amabili and Païdoussis [2]. Refs. [3-6] are strictly related to the present theory: shell like structures are analyzed by means of different kinds of expansions based on orthogonal polynomials.
In the present paper, linear and nonlinear vibrations of circular cylindrical shells are analyzed. Sanders-Koiter theory is considered for shell modelling; displacement fields are expanded by means of a double mixed series: harmonic functions for the circumferential variable; Chebyshev polynomials for the longitudinal variable. Then Lagrange equations are considered to obtain an ordinary differential equation system, from potential and kinetic energies and the virtual work of external forces. A shell, clamped at the base and connected to a rigid body, is analyzed experimentally, analytically (present theory) and using standard finite elements models. Nonlinear vibrations, due to large amplitude of vibration, are analyzed in the case of simply supported shells; the present theory is compared with the literature.

MODELLING

The Sanders-Koiter theory is used in the present work, see Refs. [1,2,7,8]; an energy approach based on Lagrange equations is considered for deriving the equations of motion both in linear and nonlinear vibrations, details are not reported for the sake of brevity.

Linear vibration: modal analysis.

The modal shape is expanded in a double series, in terms of Chebyshev polynomials $T_m^*(\eta)$, and harmonic functions:

$$U(\eta,\theta)=\sum_{m=0}^{M_U}\sum_{n=0}^{N}\tilde{U}_{m,n}T_m^*(\eta)\cos n\theta\,,\; V(\eta,\theta)=\sum_{m=0}^{M_V}\sum_{n=0}^{N}\tilde{V}_{m,n}T_m^*(\eta)\sin n\theta\,,\; W(\eta,\theta)=\sum_{m=0}^{M_W}\sum_{n=0}^{N}\tilde{W}_{m,n}T_m^*(\eta)\cos n\theta \qquad (1)$$

where $T_m^*(\eta)=T_m(2\eta-1)$ and $T_m(\cdot)$ is the m-th order Chebyshev polynomial [9].
Expansion (1) does not satisfy any particular boundary condition; geometric boundary conditions are satisfied by suitably choosing some of the coefficients $\tilde{U}_{m,n}$, $\tilde{V}_{m,n}$, $\tilde{W}_{m,n}$ of the equation (1).

Nonlinear analysis

In the nonlinear analysis, displacements fields $u(x,\theta,t)$, $v(x,\theta,t)$ and $w(x,\theta,t)$ are expanded by using linear mode shapes obtained in the previous section:

$$u(x,\theta,t)=\sum_{j=1}^{N_{\max}} U^{(j)}(x,\theta)\, f_{u,j}(t) \quad v(x,\theta,t)=\sum_{j=1}^{N_{\max}} V^{(j)}(x,\theta)\, f_{v,j}(t) \quad w(x,\theta,t)=\sum_{j=1}^{N_{\max}} W^{(j)}(x,\theta)\, f_{w,j}(t) \qquad (2)$$

Expansion (2) satisfies the boundary conditions and modal shapes $U^{(j)}(x,\theta)$, $V^{(j)}(x,\theta)$, $W^{(j)}(x,\theta)$, are known functions expressed in terms of polynomials and harmonic functions.

NUMERICAL RESULTS

Linear analysis

Numerical analyses are carried out on a circular cylindrical shell made of P.E.T. material (Polyethylene terephthalate), clamped at the base and rigidly connected to a disk on the top, see Figure 1. The shell characteristics are: length L=0.096m, radius R=0.044m, thickness h=0.3×10^{-3}m, mass density ρ=1366 kg/m^3; Poisson ratio ν=0.4.; Young modulus E = 4.6 10^9 N/m^2. The disk: mass m=0.82 kg, moment of inertia along axes orthogonal to the cylinder axis J_y=J_z=7.55×10^{-4} kg/m^2, position of the disk center of mass with respect to the shell top h_G=0.01684 m. Experiments are carried out using seismic excitation from the base, excitation on the shell or excitation from the disk. In Figure 2 the fifth mode (seven nodal diameters) is shown as an example: experiments give 816Hz, the present theory predicts 802Hz and a finite element analysis gives 802Hz; the error is about 1.7%. For the first seven modes (95-1070Hz) the error is below 5%. Similar results are obtained for simply supported and clamped-clamped shells.

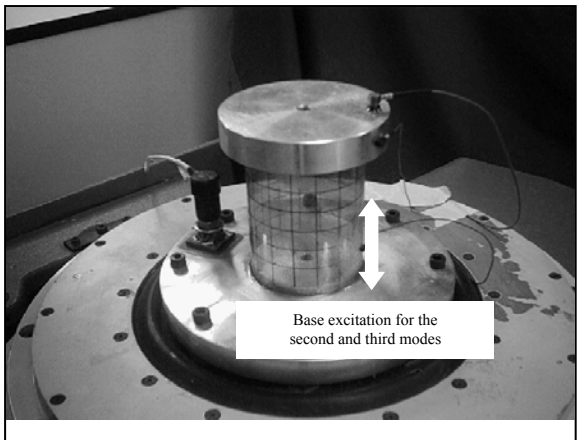

Figure 1. Experimental setup.

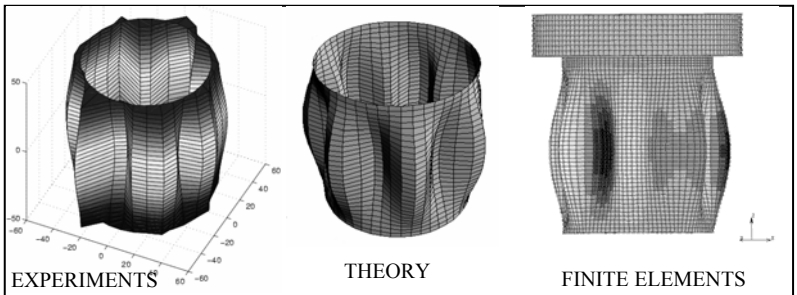

Figure 2. Mode shape comparisons:

Nonlinear analysis

Experiments carried out with the setup of Figure 1 shows that important nonlinear phenomena appears when the shell is excited seismically and the first breathing mode is in resonance. Such phenomenon is currently under investigation both theoretically and experimentally. In order to carry out a theoretical analysis an approach able to handle both complex boundary conditions and large amplitude of vibrations is needed.

As intermediate step of the present research, a simply supported steel made shell is considered, the geometrical and physical parameters are: L =0.2 m; R = 0.1m; h = 0.247×10^{-3}m; ρ = 2796kg/m^3; ν = 0.31; E=71.02×10^{9}N/m^2.

Large amplitude of oscillations are analyzed for Case A shell; such geometry was deeply investigated in the past, see Refs. [10-12]. The shell is excited by means of a pressure acting on the surface with modal distribution $q_r = f_{1,6}\sin(\eta)\cos(6\theta)\cos(\Omega t)$ the amplitude is $f_{1,6} = 0.0012h^2\rho\omega_{1,6}^2$ and frequency close to the (k=1,n=6) mode frequency: $\Omega\cong\omega_{1,6}$=2π×553.3 rad/s; the modal damping ratio considered in the calculations is 0.0005.

The response is slightly softening as confirmed by

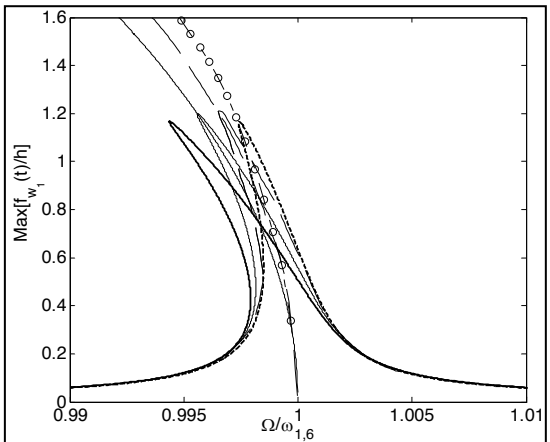

Figure 3. Nonlinear response. '▬ ▬'present theory; '–○–' Ref. [10]; '— —' Ref. [11]; '—' Ref. [12]; '▬' Ref. [13].

comparisons with Refs. [10-13]: the present model shows nonlinearity very close to Ref. [10], Refs.[11-13] predict larger nonlinear softening behaviour. It is to note that in Refs. [12,13] Donnell's nonlinear shallow shell theory is considered: this theory is less accurate than Sanders-Koiter theory, the static condensation of in-plane displacements and simplified kinematics reduce the accuracy; generally the Donnell's nonlinear shallow shell theory magnifies the softening behaviour.
It is worthwhile to stress that, in the past, several theoretical and numerical studies failed in predicting the softening response, as correct nonlinear behaviour. It is to be noted that often, spurious hardening behaviours were found. Recently, it was clarified that circular cylindrical shells generally show a softening behaviour [13]: only very short or very thick shells can have hardening behaviour. Therefore, the analysis presented in Figure 3 is an important benchmark for evaluating the accuracy of the method.

CONCLUSIONS

In this work both theoretical and experimental analyses have been carried out on shells vibration. The approach developed for solving the initial PDE is a general framework that allows to respect boundary conditions in a systematic way and to analyze large amplitude nonlinear vibrations with good accuracy. The final goal of the research is to understand complex nonlinear phenomena that appear when circular cylindrical shells are seismically excited.

References

1. A.W. Leissa, *Vibration of Shells*, NASA SP-288. Washington, DC: Gov. Print. Office. Now available from The Acoustical Society of America, 1993.
2. M. Amabili, M.P. Païdoussis, Review of studies on geometrically nonlinear vibrations and dynamics of circular cylindrical shells and panels, with and without fluid-structure interaction. *Applied Mechanics Reviews,* **56** (2003) 349-381.
3. D. Zhou, Y.K. Cheung, S.H. Lo, F.T.K. Au, 3D vibration analysis of solid and hollow circular cylinders via Chebyshev–Ritz method, *Computer Methods Appl. Mechanics Engineering*, **192 (**2003) 1575–1589.
4. K. P. Soldatos, A. Messina, Vibration Studies of cross-ply laminated shear deformable circular cylinders on the basis of orthogonal polynomials, *Journal of Sound and Vibration*, **218**(2) (1998) 219-243.
5. A. H. Nayfeh, H. N. Arafat, Nonlinear Dynamics of Closed Spherical Shells, *Proceedings of DETC2005 ASME 2005 Int. Design Eng. Technical Conferences & Computers and Information in Engineering Conference, September 2005, Long Beach, California USA*, paper N. DETC2005-85409.
6. V. A. Trotsenko and Yu. V. Trotsenko, Methods for calculation of free vibrations of a cylindrical shell with attached rigid body. *Nonlinear Oscillations*, **7**(2) (2004) 262-284.
7. Y.V. Trotsenko, Frequencies and modes of vibration of a cylindrical shell with attached rigid body, *Journal of Sound and Vibration*, **292** (2006) 535-551.
8. N. Yamaki, *Elastic Stability of Circular Cylindrical Shells*, North-Holland, Amsterdam, 1984.
9. M. A. Snyder, *Chebyshev methods in numerical approximation*, Prentice-Hall, London, 1966.
10. M. Ganapathi and T. K. Varadan, Large Amplitude Vibrations of Circular Cylindrical Shells, *Journal of Sound and Vibration*, **192**(1) (1996) 1-14.
11. J. C. Chen and C. D. Babcock, Nonlinear Vibration of Cylindrical Shells, *AIAA Journal*, **13**(7) (1975) 868-876.
12. M. Amabili, F. Pellicano and A. F. Vakakis, Nonlinear Vibrations and Multiple Resonances of Fluid Filled Circular Shells; Part 1: Equation of Motion and Numerical Results, *Journal of Vibration and Acoustics,* **122**(1) (2000) 346-354.
13. F. Pellicano, M. Amabili and M.P. Païdoussis, Effect of the Geometry on the Non-Linear Vibration of Circular Cylindrical Shells, *International Journal of Nonlinear Mechanics*, **37 (**2002) 1181-1198.

Oscillation of a sheet of falling water

Yuichi SATO
Department of Mechanical Engineering
Saitama University
Saitama, Saitama, Japan
ysato@mech.saitama-u.ac.jp

A water sheet flowing over a weir sometimes oscillates as shown in Fig. 1. Such water sheet oscillation, sometimes called nappe oscillation, causes windowpanes in the neighborhood to vibrate and even the weir itself in some cases. Since nappe oscillation is generally considered to be due to the pressure variation behind a water sheet, spoilers are set to suppress oscillation in the crosswise direction to divide a sheet of water into several parts. The mechanism of nappe oscillation, however, is not fully understood. Oscillation still occurs. We study the relation between oscillation of a falling water sheet and pressure variation behind the water sheet experimentally and theoretically. Consequently, falling motion of a disturbed water sheet and pressure variation behind the sheet form a positive feedback loop, which is a cause of water sheet oscillation.

Fig.1 Oscillation of a sheet of falling water

Figure 2 shows an experimental apparatus. Water in an upper reservoir falls down to a lower reservoir through a slit or an outlet of the upper reservoir, 300 mm in length and a_N =1.3 mm or 3.1 mm in width. To form a water sheet expanding full width we set two acrylic plates at both ends. Behind the water sheet, we set a rear board as shown in Fig. 2. The distance b from the undisturbed water sheet to the rear board is changed to 300, 200, or 95 mm. Water depth d of the upper reservoir is set 150, 200, or 250 mm, which is kept constant during the experiment. The falling distance h is varied from 470 to 620 mm. As the falling distance h is increased, the velocity of the lower part of the sheet increases due to gravity and water sheet oscillation occurs, which is stopped by rupturing the water sheet. The air chamber is not enclosed completely but there are some narrow gaps.

Behavior of a falling water sheet is monitored by a movie camera. Pressure variation in the air chamber is also measured. Figure 3 shows the behavior of an oscillating water sheet for one cycle with corresponding pressure variation. In each figure, an air chamber is located on the right side of the sheet. A triangular mark denotes the location of an anti node of the sheet. From the photographs, we note that the undulating water sheet travels downward and is accelerated by gravity with time. By dropping ink into water in the upper reservoir, water falling speed was measured, which was almost the same as the falling speed of an anti node, that is, phase velocity. Pressure in the air chamber varies periodically with the same frequency f, as that of water sheet oscillation. Pressure reaches a maximum when the bottom part of the

sheet approaches a leftmost position as shown in Fig. 3(a) whereas minimum when a rightmost as shown in Fig.3(e). Further, the pressure changes rapidly around these extrema. A falling water sheet shows similar characteristics for other conditions.

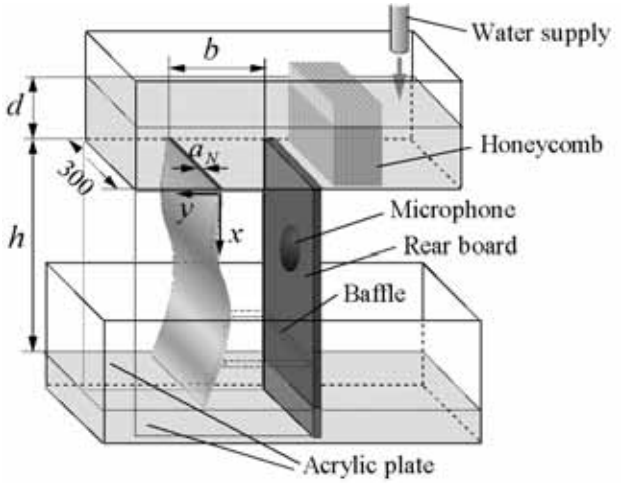

Fig.2 Experimental apparatus

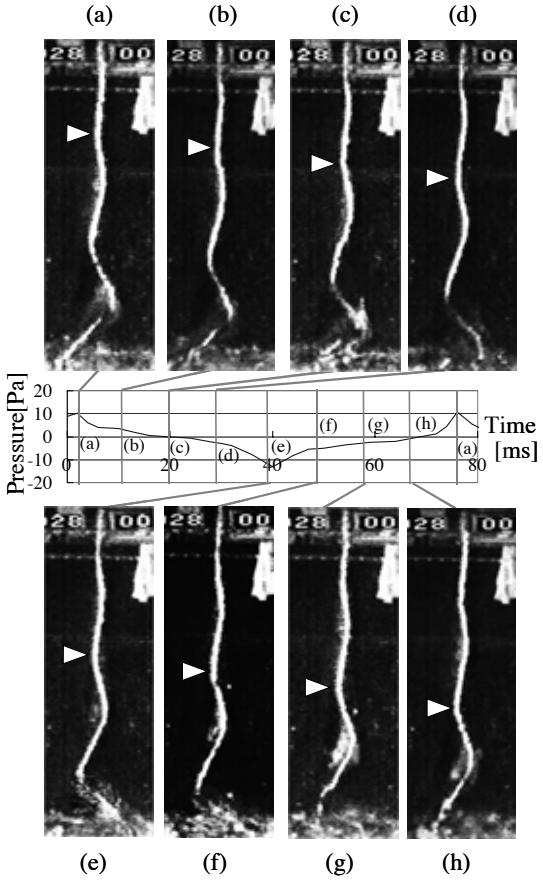

Fig.3 Relation between pressures in the air chamber and water sheet configurations

(a_N =1.3 mm, b=300 mm, d=250 mm, h=621 mm, f=13 Hz)

Since experimental observation shows that the pressure in an air chamber varies periodically with the same frequency as that of water sheet vibration, there should be an interaction between sheet vibration and pressure variation. For simplicity, we assume that the motion of a water sheet is uniform in the crosswise direction, that is, in the z-direction as

shown in Fig. 2. The air pressure p_0 in front of a water sheet is kept constant while the pressure behind the sheet is $p_0+\Delta p$ when it vibrates. Since the size of the air chamber behind the sheet is much smaller than the wave length of sound, Δp is assumed constant throughout the chamber. The velocity is assumed constant across the sheet, that is, in y direction since it is very thin. Then the equation of motion(see Figure 4) for the sheet is given as,

$$\left.\begin{aligned} &\frac{\partial u}{\partial t}+u\frac{\partial u}{\partial x}=g-\frac{\Delta p}{\rho_w a}\frac{\partial \eta}{\partial x} \\ &\frac{\partial v}{\partial t}+u\frac{\partial v}{\partial x}=\frac{\Delta p}{\rho_w a} \end{aligned}\right\} \tag{1}$$

where u and v are the flow velocities in x and y directions, respectively, and $h(x, t)$ the water sheet displacement, ρ_w water density, and $a(x, t)$ water sheet thickness. Between η and v is

$$v=\frac{\partial \eta}{\partial t}+u\frac{\partial \eta}{\partial x} \tag{2}$$

The boundary conditions at x=0 are

$$u=u_N,\ \ v=0,\ \ \eta=0. \tag{3}$$

Since the flow rate q_N for a unit width is constant, we get

$$au=a_N u_N=q_N=\text{const.} \tag{4}$$

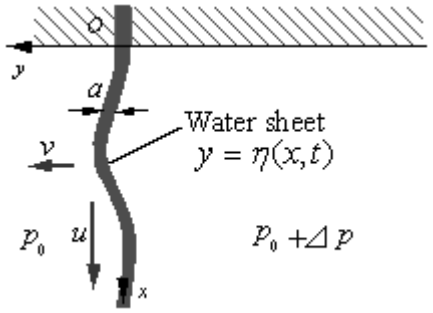

Fig. 4 Analytical model

We assume that the sheet velocities, displacement, water sheet thickness and pressure behind the sheet are expanded in a series in ε in the following forms:

$$\left.\begin{aligned} u&=u_0(x)+\varepsilon u_1(x,t)+\cdots \\ v&=\quad\ \varepsilon v_1(x,t)+\cdots \\ \eta&=\quad\ \varepsilon \eta_1(x,t)+\cdots \\ a&=a_0(x)+\varepsilon a_1(x,t)+\cdots \\ \Delta p&=\quad\ \varepsilon p_1(t)+\cdots \end{aligned}\right\} \tag{5}$$

where subscript 0 denotes the equilibrium condition and subscript 1 denotes the perturbed condition. Substitution of equations (4) and (5) into (1) yields

$$u_0=\sqrt{2gx+u_N^{\,2}},\ u_1=0 \tag{6}$$

$$\frac{\partial^2 \eta_1}{\partial t^2}+2u_0(x)\frac{\partial^2 \eta_1}{\partial t\partial x}+u_0(x)^2\frac{\partial^2 \eta_1}{\partial x^2}=\frac{u_0(x)p_1}{\rho_w q_N} \tag{7}$$

Solving this equation and calculating the work done by water sheet, we obtain the following conclusions.

We observed that the frequency of air pressure variation in a chamber behind a water sheet is the same as that of the sheet oscillation. Considering this observed result, we analyze the characteristic of a falling water sheet that performs small oscillation. Consequently, water sheet oscillation occurs when W_{total} is positive. W_{total} is the difference between the work done by a water sheet on the air in a chamber behind the sheet and the work done by air pressure in the chamber on the sheet. Water sheet oscillation is induced by the potential energy due to gravity. When S(=water sheet frequency times falling time) is close to an integer plus 0.23-0.24, sheet oscillation occurs. Placing a baffle at a quarter of wavelength above the water surface of the lower reservoir prevents water sheet oscillation. There are multiple modes of water sheet oscillation for a particular condition. Some appear more frequently while others less frequently. The mechanism of selecting a particular mode is not well understood and is a problem to be solved.

VIBRATION ANALYSIS OF OPEN SHELLS OF REVOLUTION

Anand V. Singh* and Selvakumar Kandasamy
Department of Mechanical and Materials Engineering
The University of Western Ontario
London, Ontario, N6A 5B9
Canada

* Corresponding author: Tel: + 1 519 661 2111 (extn. 88321); fax: + 1 519 661 3020.
E-mail: avsingh@eng.uwo.ca

Free vibration and transient response analyses of open circular cylindrical shells subjected to various boundary conditions have been investigated recently by the authors of this paper [1, 2]. They have used the polynomial-type method for the free vibration solution and state-space method in conjunction with Runge-Kutta integration algorithm for the forced vibration. Specifically, they have successfully applied the method to skewed (supported on non-rectangular boundary) open cylindrical shells [1]. The work is further continued towards the same for the open shells of revolution such as conical and spherical shells.

Equations are developed using the first order shear deformable shell theory, wherein the displacement components in the meridional (ϕ) and circumferential (θ) directions vary linearly along the thickness.

$$\begin{aligned} u'(\phi,\theta,z) &= u(\phi,\theta) + z\psi_1(\phi,\theta) \\ v'(\phi,\theta,z) &= v(\phi,\theta) + z\psi_2(\phi,\theta) \\ w'(\phi,\theta,z) &= w(\phi,\theta) \end{aligned} \tag{1}$$

where, u', v', and w' denote the components of displacements along ϕ, θ, and z for any point within the shell and z is the distance measured from the middle surface of the shell. Similarly, u, v, and w denote the middle surface displacements and the symbols ψ_1 and ψ_2 correspond to the components of the rotation of the normal to the middle surface of the shell in ϕ and θ directions respectively. Also, one should note that the transverse displacement component does not vary along the thickness. A shear correction factor of (5/6) is used so that the formulation is consistent with the parabolic distribution of the transverse shear stresses.

The energy functional which is the basis of the formulation and derivation of the equation of motion is deduced from the following strain-displacement relations in curvilinear coordinates from the general theory of elasticity [3].

$$\varepsilon'_{\phi\phi} = \left(1+\frac{z}{R_\phi}\right)^{-1}\left(\frac{1}{R_\phi}\frac{\partial u'}{\partial \phi}+\frac{w'}{R_\phi}\right)$$

$$\varepsilon'_{\theta\theta} = \left(1+\frac{z}{R_\theta}\right)^{-1}\left(\frac{1}{R_\theta \sin\phi}\frac{\partial v'}{\partial \theta}+\cot\phi\frac{u'}{R_\phi}+\frac{w'}{R_\theta}\right)$$

$$\varepsilon'_{\phi\theta} = \left(1+\frac{z}{R_\phi}\right)^{-1}\left(\frac{1}{R_\phi}\frac{\partial v'}{\partial \phi}\right)+\left(1+\frac{z}{R_\theta}\right)^{-1}\left(\frac{1}{R_\theta \sin\phi}\frac{\partial u'}{\partial \theta}-\cot\phi\frac{v'}{R_\phi}\right) \qquad (2)$$

$$\varepsilon'_{\theta z} = \frac{\partial v'}{\partial z}+\left(1+\frac{z}{R_\theta}\right)^{-1}\left(\frac{1}{R_\theta \sin\phi}\frac{\partial w'}{\partial \theta}-\frac{v'}{R_\theta}\right)$$

$$\varepsilon'_{\phi z} = \frac{\partial u'}{\partial z}+\left(1+\frac{z}{R_\phi}\right)^{-1}\left(\frac{1}{R_\phi}\frac{\partial w'}{\partial \phi}-\frac{u'}{R_\phi}\right)$$

Equation (1) is first substituted in the strain-displacement equation (2) and then into the strain and kinetic energy expressions to obtain the stiffness and mass matrices of the shell structure. The derivation is further carried out using a modified version of the Rayleigh-Ritz method, where the geometry of the shell and the displacement fields are expressed in terms of polynomials. This is done by using two different sets of grid points on the middle surface of the shell, one for surface coordinates and the other for displacement components respectively. The number of points in the first case depends upon the complexity of the edges forming the geometry and these points are termed here for convenience as the geometric nodes. Similarly, the number of grid points for the displacement components governs the order of the polynomials and in turn determines the accuracy of the results, i.e. increased number of points renders converged results. The above said polynomials are expressed in natural coordinates, ξ and η, in the following manner along the middle surface of the shell.

$$\phi(\xi,\eta) = \sum_{j=1}^{q} N_j(\xi,\eta)\phi_j \text{ and } \theta(\xi,\eta) = \sum_{j=1}^{q} N_j(\xi,\eta)\theta_j \qquad (3)$$

where $N_j(\xi,\eta)$ is known as the "*geometric shape function*" corresponding to the *j-th* geometric node, and q is the number of geometric nodes chosen to accurately represent the shell model. The next step in the process is to define the displacement fields, also in terms of ξ and η coordinates, for each of u, v, w, ψ_1 and ψ_2. To achieve this, a set of grid points, other than the one used in equation (3) for geometric nodes, is considered. It can be easily found that the expression for the displacement field has the same form as that used for the geometric shape function. The difference here is that displacement shape functions are created using a relatively high order interpolating function. Only the displacement component u is given in the following for simplicity and the other four are defined by replacing u by the respective displacement components.

$$u = \sum_{j=1}^{p} u_j N_j(\xi,\eta) \qquad (4)$$

In the above, $p = (p_1+1)\times(p_2+1)$, p_1 = order of the polynomial in ξ, similarly p_2 = order of the polynomial in η and $N_j(\xi,\eta)$ corresponds to the *u-displacement u_j of the j-th displacement node*. With the help of equations (1 – 4), the energy functional comprising strain energy, kinetic energy, and the work done by the applied load in the case of forced vibration is established and the matrix equation of motion is obtained by the Hamilton Method in which the variation is taken on the displacements $(u_j, v_j, w_j, \psi_1, \psi_2)$. Terms associated with ψ_1 and ψ_2 are retained in the

kinetic energy expression and hence the effect of the rotary inertia is included in the formulation along with the transverse shear deformation.

Presently, the work is in progress and computer program is being developed in C++ with the objective that one program produces results for the cylindrical, conical and spherical shell panels. This is achieved by selecting appropriate coordinate system and the radii of curvatures for a particular type of shell of revolution. Natural frequencies and mode shapes will be calculated for above said three types of open shells and validated by comparing with results available in the literature. A convergence study with regards to the order of the polynomials used for the displacement fields will be performed to gain the confidence in the results. The program will also be expanded to the transient vibration analysis of the shell panels and both linear and geometrically nonlinear cases will be considered. For transient vibration analysis the well known Newmark's integration method will be used.

References

[1] S. Kandasamy, and A. V. Singh, 2006, Free vibration analysis of skewed open circular cylindrical shells, Journal of Sound and Vibration, 290, 1111–1118.
[2] S. Kandasamy, and A. V. Singh, 2006, Transient vibration analysis of open circular cylindrical shells, ASME Journal of Vibration and Acoustics, 128, 366-374.
[3] A. S. Saada, 1993, Elasticity: Theory and Applications, 2nd Edition, Krieger Publishing Company, Florida.

On Bending-Torsional Flutter of a Cantilever with Tip Fluid Jet

Jörg Wauer and Francis C. Moon
Institut für Technische Mechanik, Universität Karlsruhe (TH), Germany
and Cornell University, Ithaca, NY, U.S.A

Introduction

From the 1950s to the 1970s, stability problems of structural members subjected to follower forces attracted very much attention. Meanwhile it seems to be clear (see [4], for instance) that many of such problems are academic and structural members subjected to fluid flow loading belong to the few representatives of non-conservative mechanical systems of practical relevance.

A special type of this problem class is a cantilevered bar subjected to a transverse follower force of fluid jet, which during the early 1970s (see [5,8], for example) was studied in many details. The investigations were based on linear models taking into consideration some pre-deformation due to the time-independent loading or on a simplified geometrically non-linear theory. In addition, the treatment was focused on a special arrangement producing the follower force of fluid jet. Since i) a consistent geometrically nonlinear theory of elasticity for such problems is available now (see [6,9] where the academic problem of a cantilever subjected to follower tip moment was treated) and ii) other specifications of tip jets are interesting to be discussed, the described problem is re-considered here.

In a first step, a sufficiently consistent formulation of the governing boundary value problem is presented, where two different mechanisms of fluid jet loads are discussed. The corresponding variational equations are derived next where a non-dimensional notation is introduced. This non-dimensional formulation is the key to recognizing the important parameters influencing the stability behavior and the flutter load, in particular qualitatively but also quantitatively.

Physical Model

Consider a slender beam of length L and mass per unit length $\mu_S = \rho A$ (ρ mass density, A cross-sectional area) with narrow rectangular cross-section (thickness $h \ll$ height H) so that the smaller of the bending stiffnesses EI_2 and the torsional stiffness GI_T are much smaller than the other bending stiffness EI_1, see Fig 1a. All data are assumed to be constant. One end of the beam is rigidly fixed and there is introduced a Cartesian reference frame $\{O\boldsymbol{e}_X\boldsymbol{e}_Y\boldsymbol{e}_Z\}$ with origin O coinciding with the centroid $S(Z=0)$ of the cross-sectional area, where the unit base vectors $\boldsymbol{e}_X, \boldsymbol{e}_Y$ correspond with the symmetry axes of that cross-section and $\boldsymbol{e}_Z$ is directed along the non-deformed bar axis. Due to the deformations (displacements u, v, w and a torsional angle φ), the centroid $S(Z)$ of a general cross-section located at the position $Z\boldsymbol{e}_Z$ displaces to s with a corresponding changed orientation denoted by the body-fixed reference frame $\{o\boldsymbol{e}_x\boldsymbol{e}_y\boldsymbol{e}_z\}$ with origin o coinciding with location s of the deformed cross-sectional centroid, where $\boldsymbol{e}_z$, $\boldsymbol{e}_y$ correspond with the symmetry axes of the actual cross-section (which itself remains undeformed) and $\boldsymbol{e}_z$ is the outside normal of that cross-section.

Two layouts of follower fluid jet load are considered, see Fig. 1b and c. The first one is that intro-

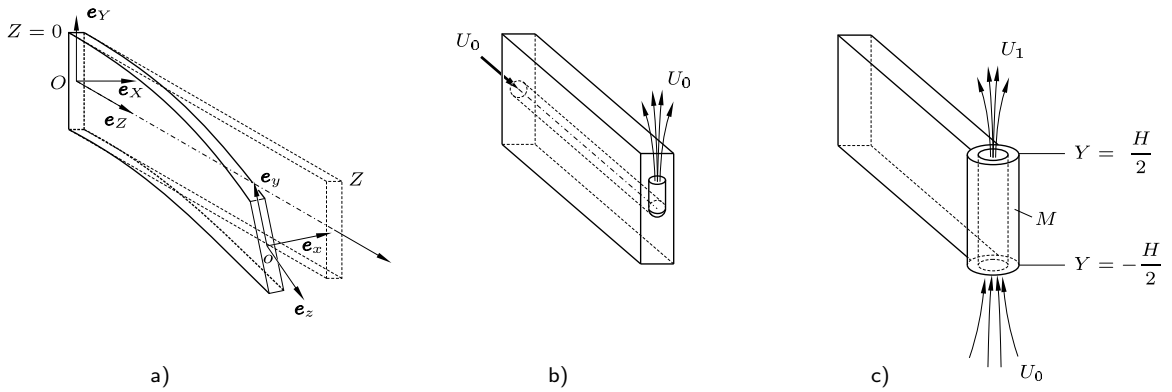

Figure 1. Bar Model, Coordinate Systems and Layouts of Fluid Jet Load.

duced by [5] and [8]. In this case, the bar has a uniform circular bore of certain suitable diameter along

the Z-axis (in un-deformed state), through which an incompressible fluid (e. g., water) at constant speed U_0 is flowing. A nozzle is connected at the free end of the beam with the hole such that the fluid leaves the system in the deformed state at the centroid $s(Z = L)$ in the form of a jet following the end cross-section in its actual state shooting into the $\boldsymbol{e}_y(Z = L)$-direction.

The second specification is geared to that one suggested by Como [2] and Wohlhart [10] here also at the tip end. To make their academic follower force practicable, a slender rigid attachment of mass M and length H with a central hole as a model of a jet engine is appropriately fixed at the end cross-section along $\boldsymbol{e}_y(Z = L)$ where air is coming in with speed U_0 at $Y = -H/2$ and exhaust gas is leaving with larger speed $U_1 > U_0$ (neglecting the fuel mass rate against the air flow rate) at $Y = H/2$ so that a transverse follower propulsion in the $-\boldsymbol{e}_y$-direction results.

Formulation

The governing boundary value problems are derived based on the assumptions as follows: The fluid is inviscid. Rotary inertia and shear deformation of the beam are neglected as well as gravity effects. Then, HAMILTON's principle

$$\delta \int_{t_0}^{t_1} (T - V)\,\mathrm{d}t + \int_{t_0}^{t_1} W_{\mathrm{virt}}\,\mathrm{d}t = 0$$

will be applied where T is the kinetic energy of the open system to be considered, V is the corresponding potential energy and W_{virt} contains the virtual work of all non-conservative forces and the contributions of mass transport over the open boundaries.

Independently from the two follower force realizations, there are the energy contributions

$$T_{\mathrm{S}} = \frac{1}{2}\int_0^L \mu_{\mathrm{S}}(u_{,t}^2 + v_{,t}^2 + k_{\mathrm{S}}^2\varphi_{,t}^2)\,\mathrm{d}Z, \quad k_{\mathrm{S}}^2 = \frac{I_1 + I_2}{A}$$

and

$$V_{\mathrm{S}} = \frac{1}{2}\int_0^L \left[EI_2u_{,ZZ}^2 + EI_1(-v_{,ZZ} + \varphi u_{,ZZ})^2 + GI_T\varphi_{,Z}^2\right]\,\mathrm{d}Z$$

of the structural member together with its virtual work term

$$\begin{aligned} W_{\mathrm{virt,S}} \;=\; & -d_{\mathrm{e}}\int_0^L \mu_{\mathrm{S}}(u_{,t}\delta u + v_{,t}\delta v + k_S^2\varphi_{,t}\delta\varphi)\,\mathrm{d}Z \\ & - d_{\mathrm{i}}\int_0^L (EI_2u_{,ZZt}\delta u_{,ZZ} + EI_1v_{,ZZt}\delta v_{,ZZ} + GI_T\varphi_{,Zt}\delta\varphi_{,Z})\,\mathrm{d}Z \end{aligned} \tag{1}$$

characterizing external and internal damping in a linear formulation which is sufficient.

Two alternative fluid flow contributions to kinetic energy and virtual work representing the distinct follower force concepts have to be added. In case 1 where fluid flows through the central hole of the bar and leaves at the nozzle following the end cross-section into $\boldsymbol{e}_y(L)$-direction (here in such a form that the fluid speed within the nozzle remains unchanged), there is an additional kinetic energy

$$T_{\mathrm{F}}^{(1)} = \frac{1}{2}\int_0^L \mu_{\mathrm{F}}\left[u_{,t}^2 + v_{,t}^2 + 2U_0(u_{,t}u_{,Z} + v_{,t}v_{,Z})\right]\,\mathrm{d}Z$$

and a work term

$$W_{\mathrm{virt,F}}^{(1)} = -\mu_F U_0\Big[(u_{,t} - U_0\varphi)\delta u + (v_{,t} + U_0)\delta v\Big]_{Z=L}.$$

If the shortening of the bar were to be taken into consideration, a supplement would occur that would not significantly modify the stability analysis.

In case 2 (assuming that the fluid mass within the attached engine is negligible compared to M) the kinetic energy of the jet engine

$$T^{(2)} = \frac{1}{2}\Big[M(u_{,t}^2 + v_{,t}^2) + \frac{MH^2}{12}\varphi_{,t}^2\Big]_{Z=L}$$

and the contribution of the fluid jet

$$W_{\mathrm{virt,F}}^{(2)} = \mu_F\Big\{U_0\Big[(u_{,t} - U_0\varphi)\delta u + (v_{,t} + U_0)\delta v\Big] - U_1\Big[(u_{,t} - U_1\varphi)\delta u + (v_{,t} + U_1)\delta v\Big]\Big\}_{Z=L}$$

have to be added. Also in this case, the shortening of the bar end (together with the inclination angle $v_{,Z}(Z = L)$) can easily be taken into account.

It is straightforward now to evaluate HAMILTON's principle for both cases to get the respective governing boundary value problems.

It will be mentioned that, for a consistent post buckling analysis or the examination of interacting oscillations in both lateral directions of the beam, a geometrically nonlinear theory of elasticity to the cubic order (see [1], for instance) or a nonlinear elastica theory (see [3,7], for instance) should be applied.

Evaluation and Results

In a first step, the steady deformation state is determined which is for both follower force realizations a pure time-independent bending about the stiffer of the two main inertia lateral axes without torsion:

$$u_0(Z,t), \varphi_0(Z,t) \equiv 0, \quad v_0(Z,t) = v_0(Z) \text{ where}$$
$$EI_1 v_{0,ZZ} = -\mu_F U_0^2 (L - Z) \text{ (case 1) or } EI_1 v_{0,ZZ} = -\mu_F (U_1^2 - U_0^2)(L - Z) \text{ (case 2).}$$

Taking now solutions of the form

$$u(Z,t) = u_0 + \Delta u(Z,t), \quad v(Z,t) = v_0 + \Delta v(Z,t), \quad \varphi(Z,t) = \varphi_0 + \Delta\varphi(Z,t)$$

and substituting them into the governing nonlinear boundary value problems, we get – linearizing in the Δ-quantities – the variational equations as the starting point for the stability analysis. As expected the coupled boundary value problem in Δu and $\Delta\varphi$ constitute the lateral buckling problem while the other decoupled one in Δv describes simple damped oscillations.

Introducing non-dimensional variables and parameters, it becomes obvious that besides two characteristic damping coefficients D_e and D_i the stiffness ratio $GI_T/(EI_2)$ together with the slenderness $(k_S/L)^2$ may drastically influence the eigenvalues as a function of the load parameter $\mu_F U_0^2 L^2/\sqrt{GI_T EI_2}$ (case 1) or $\mu_F (U_1^2 - U_0^2) L^2/\sqrt{GI_T EI_2}$ (case 2). The stability behavior will be discussed in detail where, in particular, some qualitative results not given in [5,8] will be presented.

Acknowledgement *The first co-author is grateful to Professor F. C. Moon who invited him for a sabbatical stay at Cornell University, NY, U.S.A. where some of the work originated.*

References

1. Botz, M., *Zur Dynamik von Mehrkörpersystemen mit elastischen Balken*, Diss. TU Darmstadt, Germany, 1992.
2. Como, M., Lateral Buckling of a Cantilever Subjected to a Transverse Follower Force, *Int. J. Solids Structures*, Vol. 2, 515–523, 1966.
3. Cusumano, J. P., and Moon, F. C., Chaotic Non-planar Vibrations of the Thin Elastica, Part I and II, *J. Sound Vibration*, Vol. 179, 185–208 and 209–226, 1995.
4. Elishakoff, I., Controversy Associated with the So-called "Follower Forces": Critical Overview, *Applied Mechanics Reviews*, Vol. 58, 117–142, 2005.
5. Kalmbach, C. F., Dowell, E. H., and Moon, F. C., The Suppression of a Dynamic Instability of an Elastic Body Using Feedback Control, *Int. J. Solids Structures*, Vol. 10, 361–381, 1974.
6. Meyer, A., Tan, H., and Wauer, J., Die Wirkung äußerer und innerer Dämpfung auf die Stabilität des Prandtlschen Kragträgers unter mitgehender Momentenbelastung, *Ing.-Archiv*, Vol. 54, 205–219, 1984.
7. Plaut, R. H., Postbuckling and Vibration of End-supported Elastica Pipes Conveying Fluid and Columns Under Follower Loads, *J. Sound Vibration*, Vol. 289, 264–277, 2006.
8. Prasad, S. N., and Herrmann, G., Stability of a Cantilevered Bar Subjected to a Transverse Follower Force of Fluid Jet, *Ing.-Archiv*, Vol. 39, 341–356, 1970.
9. Wauer, J., Der Prandtlsche Kragträger unter konservativer und nichtkonservativer Momentenbelastung, *ZAMP*, Vol. 29, 334–340, 1978.
10. Wohlhart, K., Dynamische Kippstabilität eines Plattenstreifens unter Folgelast, *Z. Flugwissenschaft*, Vol. 19, 291–298, 1971.

Biographical Sketches of Participants

Eberhard W. Brommundt
Institut für Dynamik und Schwingungen
Technische Universität Braunschweig
PF 3329, D-38023 Braunschweig, Germany
E.Brommundt@tu-bs.de

Biographical sketch

Education:

1952 – 1955 Polytechnic School of Engineering, Mannheim, Germany: Mechanical Engineer
1957 – 1962 Technische Hochschule Darmstadt: Mathematics

Industrial experience

1955 – 1957 Brown, Boveri & Cie, Mannheim; Steam Turbines (strength, vibrations)

University degrees (all TH Darmstadt)

1962	Dipl.- Math.
1966	Dr. rer. nat.
1968	Habilitation for Mechanics

Academic occupations

1962 – 1968	Research Assistant at the Institute of Mechanics and Vibrations, TH Darmstadt
1968/69	Visiting Assistant Professor, Department of Aerospace Engineering and Mechanics, University of Minneapolis, Minn.
1969/70	Docent of Mechanics, TH Darmstadt
1970 – 2000	Professor of Mechanics, Institute of Technical Mechanics, Technical University Braunschweig
since 2000	Professor emeritus, Institute of Dynamics and Vibrations, TU Braunschweig

Fields of Interest:

Basic as well as applied problems from dynamics, linear & nonlinear oscillations, stability of motion, self-excitation

Applications from

Rotor dynamics, Rail-wheel dynamics, Stability of fluid centrifugals, Drill-string dynamics

Recent Publications:

E. Brommundt: Friction, friction lock, self-excitation: considerations on Painlevé's paradox (in German). Int. J. Non-Lin. Mech. 38 (2003), 691-703.
E. Brommundt: High-order sub-harmonic synchronization in a rotor system with a gear coupling. Technische Mechanik, 24 (2004), 242-253
E. Brommundt, E. Krämer: Instability and self-excitation caused by a gear coupling in a simple rotor system. Forsch. Ingenieurwes. 70 (2006), 25-37
E. Brommundt: Stabilization of a rotor with internal friction by a helical damper strip. Machine Dynamics Problems (ISSN 0239-7730) 29 (2006), 21-46

Biosketch of Erasmo Carrera

After earning two degrees (Aeronautics, 1986 and Aerospace Engineering, 1988) in the Politecnico di Torino, Erasmo Carrera received his PhD degree in Aerospace Engineering in 1991, at the Politecnico di Milano – Politecnico di Torino – Universitá di Pisa. He began working as a Researcher at the Department of Aerospace of Politecnico di Torino in 1992 holding courses on Missiles and Aerospace Structure Design, Plates and Shells, Finite Element Method and since 2000 is associate Professor of Aerospace Structures and Aeroelasticity. He visited twice the Institute für Statik und Dynamik, Universität Stuttgart, the first time as a PhD student (six months in 1991) and then as visiting Scientist under GKKS Grant (18 months in 1995-96). In the Summer of '96 he was Visiting Professor at ESM Dept of Virginia Tech. In the period May-July 2004 he has been visiting professor at SUPEMCA, Paris, France. His main research topics are: composite materials, finite elements, plates and shells, vibrations, postbuckling and stability by FEM, smart structures, thermal stress, aeroelasticity, multibody dynamics, multifield problems, design and analysis of non classical lifting systems and inflatable structures. He his an author of more than one hundred articles on these topics, many of which have been published in international journals. He serves as a referee for dozens journals such as *Applied Mechanics Reviews* , AIAA Journal, *Journal of Sound and Vibration* , *International Journal of Solids and Structures* and *International Journal for Numerical Methods in Engineering* a and as contributing editor for *Mechanics of Advanced Materials and Structures*.

1

Stuart M. Dickinson

Professor Emeritus
The University of Western Ontario
London, Ontario, Canada

The above served an engineering apprenticeship with Ford Motor Company, Dagenham, UK, before attending the University of Nottingham, where he obtained both his B.Sc. and Ph.D. in Mechanical Engineering. He then spent three years as a lecturer at the University of Liverpool before immigrating to Canada in 1969 to take up a faculty position at The University of Western Ontario, becoming Professor Emeritus upon his early retirement in 1997. Whilst at Western, he had the opportunity of spending sabbatical leaves at the Institute of Sound and Vibration Research, Southampton, UK, the University of Canterbury, Christchurch, New Zealand, and Monash University, Melbourne, Australia.

His research and teaching interests have mainly been in the vibration of beams, plates and shells, with brief excursions into acoustics. Most of his research was of a theoretical or numerical nature, primarily employing "classical" approaches, although some experimental work was conducted and, in the early years, some work was done on the development of finite element methods.

His recreational interests, shared with his wife Rosemary, include curling (a little like lawn bowling on ice), badminton and dinghy sailing. He has also been learning to play the euphonium (half size tuba), and participates in a band program run at the university.

Mark S. Ewing
University of Kansas

I grew up interested in science and mathematics, largely due to my fascination with the U.S. spacecraft I used to watch launch from Cape Canaveral—when I lived in nearby Orlando, Florida. I received my BS in Engineering Mechanics from the U.S. Air Force Academy, then began a 20-year career in the Air Force. I served for four years in turbine engine stress and durability analysis where I was an "early" user of finite element analysis for hot, rotating turbomachinery. I then served a two-year assignment in turbine engine maintenance and support, which was less technical, but eye-opening. During these early years—in my spare time—I earned an MS in Mechanical Engineering from Ohio State University.

With an MS in hand, I returned to the Air Force Academy to serve on the faculty as an Assistant Professor. After two years, I returned to Ohio State to complete a PhD. As a student of Art Leissa's, I focused on the combined bending, torsion and axial vibrations of "stubby" beams, thereby establishing my interest in the vibrations of continuous systems.

After returning to and teaching at the Academy for six years, I was assigned to the Air Force Flight Dynamics Lab, where I worked on two interesting projects. The first was the development of a structural design algorithm capable of, among other things, "maximizing" the separation of two natural frequencies. The utility of this endeavor was to allow the design of aircraft wings for which the bending and torsional natural frequencies are sufficiently separated (in frequency) to avoid flutter. The other interesting project was the analysis of the effect of convected aerodynamic loads on a missile.

I am now on the Aerospace Engineering faculty at the University of Kansas. My current research interests are in structural acoustics, which is a topic of increasing interest to aircraft manufacturers. In recent years, I have focused on the ability to analyze—and design—structural damping for built-up fuselage structures. All the test articles I've used to validate my work through experimentation are simple structural elements, namely beams and plates.

I have a great love of the outdoors, and of the mountains in particular. When Art Leissa asked me to help organize the first International Symposium on Vibrations of Continuous Systems, and he told me he wanted to meet in the mountains, I was really excited. I look forward to attending the Symposium this year after missing the last two.

Daniel Gorman
Dep,t of Mech. Eng
The University of Ottawa, Ottawa Canada

Took my graduate studies at the Department of Mechanical and Aertospace Engineering, Syracuse University. Subsequently returned to Atomic Energy of Canada Limited. Worked on R and D projects for five years. Principal work related to studies of flow induced vibration of nuclear reactor fuel and nuclear steam generator U-Tubes. Continued with same research after joining the University of Ottawa. Subsequently broadened field to vibration studies of beams and plates. Currently conduct plate vibration research as Professor Emeritus with a special interest in rectangular plate in-plane vibration. Also conduct development work on a remote operated window cleaner for high-rise buildings.

Peter Hagedorn
Darmstadt University of Technology

I received most of my education in Sao Paulo, Brazil, where I obtained a degree in mechanical engineering and later a doctor's degree (in 1966) at the Escola Politecnica da Universidade de Sao Paulo. Later I did my 'Habilitation' (similar to a D.Sc. degree) at Karlsruhe in Germany. My main professional interests are vibrations and stability of discrete and continuous systems (such as beams, plates and cables), and vibration control. While my early work was more analytical (e.g. the converse of the Lagrange-Dirichlet theorem, differential games, etc.), during the last 20 years I have worked more and more also with problems related to industrial applications, including experimental work, the emphasis however usually being on producing practical mathematical models.

Recently I have been working with piezoelectric ultrasonic travelling wave motors, wind excited vibrations of overhead transmission lines (including cfd calculations), and with the dynamics and active noise control in disk brakes. I am the author of several books on linear and nonlinear vibrations as well as a three volume German textbook on elementary statics, strength of materials and dynamics. Recently I also organized several workshops dealing with the question of how we should teach engineering mechanics to our students today.

I have been a visiting professor and research fellow at Stanford, Berkeley, Paris, Irbid (Jordan), Rio de Janeiro and Christchurch (New Zealand). My personal hobbies are travelling, photography and hiking (mainly day hikes).

Daniel Hochlenert

Dynamics and Vibrations Group, Technische Universität Darmstadt

I was born on March 21st 1978 in Frankfurt am Main, Germany.

In 1997 I finished high-school (Abitur) and did civilian service for 13 months. In October 1998 I started the studies of industrial engineering / mechanical engineering at Darmstadt University of Technology.

After finishing my preliminary diploma in 2001 I switched to the studies of applied mechanics with the main focus on dynamics. I continued my studies in the fall semester 2001 and the spring semester 2002 at the University of California at Berkeley.

In Juli 2003 I started as a Ph.D. student at Darmstadt University of Technology in the group of Professor Hagedorn. In October 2006 I finished my dissertation with the title „Self-excited vibration in disk brakes: mathematical modeling and active suppression of disk brake squeal“.

My hobbies are cycling (road and mountain bike), skat and cooking.

Chiung-Shiann Huang
National Chiao Tung University

Chiung-Shiann Huang's current position is a Professor in the Department of Civil Engineering, National Chiao Tung University, Taiwan. He received his Ph. D in 1991 at the Department of Engineering Mechanics at the Ohio State University. After that, he spent nine months as a postdoctoral research associate in the Department of Civil Engineering at the Ohio State University. The doctoral and postdoctoral research dealt with the use of singular corner stress functions to permit accurate solutions for free vibration frequencies of thin plates having sharp corners.

In 1992, he went back Taiwan and joined the research staff at the National Center for Research on Earthquake Engineering (NCREE). In addition to continue his serious interests on computational mechanics, he began to study the system identification of structures from monitoring earthquake responses of structures and the responses from various tests in field, such as ambient vibration test and forced vibration test.

After having stayed in NCREE for nine years, he joined the faculty of the Civil Engineering Department at National Chiao Tung University in 2000. His current main interests are dynamic and stability analysis of curved beams, vibrations of thick plates with stress singularities, system identification using time series, neural network, and wavelet transform.

James R. Hutchinson

Jim was born in San Francisco Ca. He graduated from Stanford University with a BS in Mechanical Engineering in 1954. Upon graduation he went to work for Westinghouse's Atomic Power Division in Pittsburgh Pa. While working at Westinghouse he earned his masters in Mathematics in 1958. He then went to work for Lockheed Missiles and Space Division in Palo Alto Ca. While working at Lockheed he went back to Stanford as a part time student, earning his Ph.D. in Engineering Mechanics in 1963. He stayed on at Lockheed for another year before taking an academic position at the University of California, Davis. He was at Davis until his retirement January 1 1993.

His interest in vibrations began while he was working at Lockheed. His primary responsibility at Lockheed was in missile vibrations. When he arrived at Davis he was asked to teach the graduate course in Mechanical Vibrations. Many of his students were from Agricultural Engineering. They were interested in shaking fruit and nuts from trees. Of course, the solution methods were the same whether the vibrating body was a missile or a tree, and a number of cooperative projects took place on the study of tree vibrations. His early interest in continuum vibration also had its roots in missile applications.

Jim loves to sing and was very active in the Davis Comic Opera Company that mainly produced the works of Gilbert and Sullivan. Unfortunately, the Davis Comic Opera Company ended its existence this year after 30 years of entertaining the people of Davis and the surrounding communities. He is still singing with the University Chorus, and this year had the privilege of singing the Mozart Requiem in December, Beethoven's 9th Symphony in March, and the opera Carmen in May. Jim is also a home-brewer and has dabbled in photography, stained glass, auto mechanics, and lately web design.

He is presently chair of the Yolo County Juvenile Justice / Delinquency Prevention Commission. He does volunteer work with Citizens Who Care (a local non-profit agency dedicated to helping the elderly). He has become an avid golfer but still enjoys doing some research on topics of his own choosing.

Jim and his wife Pat celebrated their 50th wedding anniversary last summer by taking their family on a cruise to Alaska

Sinniah Ilanko
The University of Waikato
Te Whare Wananga o Waikato

e-mail: < Ilanko@Waikato.ac.nz>
www URLs: < http://www.mech.canterbury.ac.nz/people/ilanko.shtml>
<http://www.geocities.com/ilanko/vibration.htm >
<http://www.geocities.com/ilanko/eng.html >

Ilanko was born in the north of Sri Lanka (Jaffna) in1957, and according to the common Tamil practice, he does not have/use a family name. Ilanko is his given name and Sinniah is his late father's given name.

He graduated from the University of Manchester (U.K) with a BSc in civil engineering and also obtained an MSc from the same university under the supervision of Dr S.C. Tillman. His move to England at an early age was the result of his late brother Senthinathan's foresight on the Sri Lankan political situation. After working as an assistant lecturer at the University of Peradeniya in Sri Lanka for about two years, he commenced doctoral studies at the University of Western Ontario under the supervision of Professor S.M. Dickinson. Soon after completing his PhD, he worked as a postdoctoral fellow at the UWO for about six months until he joined the University of Canterbury in 1986. He continued his academic career at Canterbury for nearly 20 years, in various positions, as lecturer, senior lecturer and associate professor until he joined the University of Waikato in 2006. He has also served as the Head of Mechanical Engineering Department at Canterbury for a year (2001-2202) and worked as a visiting professor at the Annamalai University (India) and Technical University of Hamburg-Harburg during his study leaves. In 1997, he was awarded the Erskine Fellowship and visited several universities in Australia, Canada, Singapore and the U.K.

His research areas include vibration and stability of continuous systems, numerical modelling and adaptive mechanisms. He is also interested in computer-aided learning and has developed and used several interactive lectures and tutorials for teaching Mechanics of Materials and Vibration, as well as computer tutorials and games for learning/teaching Tamil language. He maintains a "vibration resources homepage" (see the second URL above), which at present contains some interactive simulation programs for calculating natural frequencies and modes of some structural elements.

He is married to Krshnanandi and they have two daughters, Kavitha and Tehnuka. Ilanko's birth family is scattered across the globe (Australia, Canada, New Zealand, the U.K. and the U.S.A.) because of the civil war in Sri Lanka.

Arthur W. Leissa
Colorado State University

After earning two degrees in mechanical engineering, with a strong interest in machine design, I decided to seek better understanding of stress and deformation of bodies, so I got my Ph.D. in engineering mechanics (from Ohio State University in 1958). My dissertation research was in the theory of elasticity. I then stayed on as a faculty member.

Working part-time for two aircraft companies (Boeing and North American Aviation) made me very interested in vibrations. In 1965 I approached NASA to support me with research funds to collect the literature of the world in plate and shell vibrations, and summarize it in two monographs. They did, and the two books were published in 1969 and 1973. They were out of print for a long time. But in 1993 they were reprinted by The Acoustical Society of America and are currently available from them.

After gaining considerable knowledge in writing the two books, I continued to do extensive research on vibrations of continuous systems, including laminated composites turbomachinery blades, and three-dimensional problems. More than 100 published papers, and most of the 40 dissertations I supervised, have been in this field. But 14 years ago I agreed to become the Editor-in-Chief of Applied Mechanics Reviews, so I then had less time available for research.

I have always intended to update the "Vibration of Plates" monograph. Indeed, more than 20 years ago I had a graduate student collect the more recent literature. This consisted of 1500 additional references dealing with free vibrations. But I never could find the time needed to undertake the writing.

Many of my former Ph.D. advisees have wanted to collaborate with me on further research in vibrations, and several of them are doing so now, including ones abroad. This is an ideal situation for me---better than having graduate students! They know what they are doing, and why.

In June of 2001 I formally retired from Ohio State University after having been on its faculty for 45 years. In July, 2002 Trudi and I moved to Fort Collins, Colorado, approximately 60 miles north of Denver, and close to the mountains. I am now an Adjunct Professor in the Department of Mechanical Engineering of Colorado State University. Having no serious responsibilities there, I continue my editorial functions with AMR, and still collaborate with others on research..

My serious interest in the mountains began as a boy, reading books about Mallory and Irvine on Everest, and others. In 1961 when I could first afford it (with a family) I began climbing mountains, which I pursued strongly for decades. Now being 75, I can no longer climb them, but I still enjoy greatly being in the mountains---hiking, skiing and snowshoeing.. They restore one's vitality and one's peace. I am happy to be able to share this feeling, to some extent, with the Symposium participants.

Biographical Sketch of Chee W. Lim

I graduated with a B.Eng. degree in Mechanical Engineering (Aeronautics) from University of Technology, Malaysia in 1989. I was conferred a M.Eng. degree in Mechanical Engineering from National University of Singapore in 1992 for the research in hydrodynamic stability of potential and boundary layer flows over periodically supported compliant surfaces. The research was an attempt to model and understand the mechanism and responses of flows over the skin of a dolphin and the ability of a flexible skin to stabilize boundary layer flows. Subsequently, I pursued research in vibration of isotropic and laminated plates and shells and was awarded a PhD degree in Mechanical Engineering from Nanyang Technological University, Singapore in 1995.

I continued research as a postdoctoral fellow at Department of Civil Engineering, The University of Queensland, Australia from 1995 to 1997, and as a research fellow at Department of Mechanical Engineering, The University of Hong Kong from 1998 to early 2000. I joined Department of Building and Construction, City University of Hong Kong as an assistant professor in 2000 and was promoted to associate professorship in 2003.

My main research interests are in developing new models and applications of plate and shell structures including flow-structures interaction in advanced engineering fields such as smart piezoelectric structures, micro-electro-mechanical systems (MEMS) and nanomechanics. Recently, I have much interest in a new subject symplectic elasticity which bridges physics (including quantum mechanics and electromagnetism), control and applied mechanics.

I am married to Moi P. Choo, have a daughter Qin Y. Lim, twelve, and a son Ying H. Lim, now eight.

Name: Andrei V. Metrikine
Title: PhD, Dr.Sc. (physics and mathematics)
Affiliation: Delft University of Technology,
Faculty of Civil Engineering and Geosciences
Address: Stevinweg 1, 2628 CN Delft, The Netherlands
Phone: +31 15 2784749
Fax: +31 15 2785767
E-mail: A.Metrikine@tudelft.nl
Web: http://www.mechanics.citg.tudelft.nl/

Short Biography.

Andrei has graduated from the faculty of radio-physics of the State University of Nizhniy Novgorod, Russia in 1989. After graduation he became a junior researcher at the Mechanical Engineering Institute of RAS (Russian Academy of Sciences). In 1992 he received his PhD degree in the field of Theoretical Mechanics from the State Technical University of St. Petersburg, Russia. After that he was a researcher, senior researcher and leading researcher at the Mechanical Engineering Institute of RAS. In 1994-1996 Andrei was a post-doctoral researcher at Delft University of Technology and then, in 1996 - 1997, a Humboldt's Foundation fellow in the Institute for Mechanics of the Hannover University, Germany. In 1998 he has received his Dr.Sc. (Doctor of Sciences) degree in the field of Mechanics of Solids from the Institute for Problems in Mechanical Engineering RAS, St.Petersburg, Russia.

Since 1999 Andrei is a member of staff of the Structural Mechanics Section of the Faculty of Civil Engineering and Geosciences of Delft University of technology, the Netherlands. Currently, he is an associate professor and the head of Wave Mechanics research group.

In 2006 Andrei has been appointed as an associate European editor of the Journal of Sound and Vibration.

Ken-ichi Nagai
Gunma University

Ken is a professor of the Department of Mechanical System Engineering in Graduate School of Engineering, Gunma University.

He was born in Fukushima north-east of Japan. He graduated from the national college of technology in Fukushima. During the student, he received deep impression from the book "Mechanics" by Den Hartog. At the time, he wanted to devote himself to research and education. He received his B. Eng. in 1970 from Ibaraki University. He obtained M. Eng. and Dr. Eng. in 1972 and 1976 from Tohoku University, respectively.

Since 1976, he has been taking an academic position in Gunma University. From 1990 to 1991, he was a visiting fellow at Cornell University in U. S. A., Technische Hochshule Darmstadt in Germany and Polish Academy of Sciences in Poland.

He is a Fellow of the Japan Society of Mechanical Engineers and is the chairman of the Division of Dynamics, Measurement and Control in JSME. He organized the Technical Section on Nonlinear Vibration under the division. He has been a consultant to ministry, local government and automobile industry.

He is now devoted in the research filed of nonlinear vibration, dynamic stability and chaotic oscillations of structure such as beam, arch, plate and shell.

Recently, he published the book of "Dynamic system Analysis-Energy Approaches from Structural Vibration to Chaos-".

His personal interests include hiking and drinking a little. He feels spiritual happiness as walking in fields and facing to new phenomena of chaotic vibration.

Yoshi (Yoshihiro Narita)

Hokkaido University, Sapporo, Japan

Hello, everyone! I am Yoshi (Yoshihiro) Narita of Hokkaido University, Sapporo, Japan. I moved to HU three year and three months ago (An academic year starts in April, and Prime Minister Shinzo Abe tries to change so that half of the students start in September). I had spent twenty-four years at Hokkaido Institute of Technology.

I enjoy the blessed surroundings at HU because of less teaching duties and many more graduate students who are capable of doing excellent research works. Our laboratory, with my two colleagues, has five PhD students and eleven Master course students in addition to seven senior undergraduate students. We expect one Korean sabbatical visitor and foreign students soon. I wish I had more time with them. This summer, I will run a conference called APVC2007 (Asian Pacific Vibration Conference) on the HU campus, and after this ISVCS, I will fly back to give a finishing touch to the preparation of APVC.

I started my research on vibration of continuous systems when I was a graduate student under adviser Prof.Irie of HU in 1976, and continued it when I had a chance to study one year in 1978-1979 under Prof.Leissa at the Ohio State University. In these days when researchers change their topics more frequently, one may say, it is incredible that I have kept the same topic thirty years. But somehow, I love the research in the area of continuous systems. Recently, I combine the vibration and buckling of plates and shells with optimization.

On a personal note, I have a wife and three children (a male HU student of 22 year old, a high-school girl of 17 old and a junior-high-school boy of 14 old). They used to come with me in early ISVCS's, but the children are now busy with their own schedules. I am happy only with the fact that they are healthy and still stay with me and my wife in Sapporo.

I am also happy that I could join all the ISVCS's, including ISVCS-I(Estes Park, USA), II(Grindelwald, Switzerland), III(Grand Teton, USA), IV(Keswick, UK) and V(Berchtesgarden, Germany). These are full of good memories. In the present ISVCS, I look forward to meeting old and new friends in the research community of applied mechanics.

Let's enjoy!

Robert G. Parker

Department of Mechanical Engineering
Ohio State University

I have been a faculty member in the Ohio State Mechanical Engineering Department since 1995. My graduate study was all at the University of California, Berkeley. Between my M.S. and Ph.D. degrees, I worked in the Structural Dynamics Department at The Aerospace Corporation in Los Angeles and spent one year as a visiting researcher at the University of Sydney. I spent one summer conducting research at the University of Tokyo under the NSF Japan Program and another as a NASA Faculty Fellow at Glenn Research Center. In 2005, I spent my sabbatical as 7.5 months in the Wind Energy Department at Risoe National Lab in Denmark and six weeks at the University of Technology, Sydney.

My research interests are the vibration and stability of high-speed mechanical systems. Current projects investigate the linear and nonlinear dynamics of multi-mesh gears and automotive belt drives. A particular focus is planetary gear dynamics with application to helicopter, automobile, wind turbine, and aircraft engine transmissions. Planetary gears are a fascinating research topic because of the complex tooth meshing at the multiple meshes, where the teeth act as discrete, time-varying, nonlinear stiffnesses. Elastic continuum vibrations of the ring gear couple the sun, planet, and carrier motions to form a hybrid discrete-continuum system. With ARO support, we built a major test stand (24 ft x 12 ft, 32,000 lb) to measure the dynamic motions of the planetary gear components at operating conditions. The belt drive problem examines the coupled vibration of the continuous, moving belt span with multiple discrete accessory pulleys. The concerns are noise, belt slip, fatigue, and, in some cases, belts jumping off pulleys.

I received the Army Research Office Young Investigator Award. This award led to the Presidential Early Career Award for Scientists and Engineers, which was presented at the White House. Both of these are associated with the planetary gear research. In 1999, I received the National Science Foundation CAREER Award for the high-speed belt drive and disk-spindle system projects. I am a Fellow of the American Association for the Advancement of Science and received ASME's Gustus Larson Award for outstanding achievement within 20 years of the BS degree. I am currently an Associate Editor for the ASME Journal of Vibration and Acoustics.

My wife, Bethann, and I have three kids (10, 8, and 5) who will join us in Squaw Valley. When time permits, we enjoy travel and most outdoor activities and look forward to the hikes and conference activities in Squaw Valley. We enjoy cooking, live theater, and recently are developing an interest in gardening. I am an avid tennis and squash player. Another hobby of mine is brewing beer.

Biography
of Francesco Pellicano

Francesco Pellicano was born in Rome, Italy on July 19, 1966. He received a M.S. degree in Aeronautical Engineering in 1992 and Ph.D. in Theoretical and Applied Mechanics in 1996, both at the University of Rome "La Sapienza", Dept. of Mechanics and Aeronautics.

He was Researcher at the University of Modena and Reggio Emilia, Faculty of Engineering, Dept. of Mechanical and Civil Engineering, 1996-2003.

He is currently Associate Professor at the same University since January 2004.

He was involved in investigations concerning: nonlinear vibrations of structures; nonlinear normal modes; axially moving systems; nonlinear vibration of shells with fluid structure interaction; gears modeling; non-smooth dynamics; Chaos; Nonlinear Time Series Analysis; Forecasting Methods in Oceanography.

He cooperated with Prof. Vestroni, Prof. Sestieri and Prof. Mastroddi of the University of Rome "La Sapienza" and with with: Prof. Païdoussis (Mc Gill Univ. Canada); Prof. Vakakis (Univ. of Illinois at Urbana Champaign; recently National Technical Univ. of Athens, Greece); Prof. Amabili (Univ. of Parma, Italy).

The teaching activity regards: Vibrations of Discrete and Continuous Systems; Signal Processing; Machine Theory and Machinery.

He was coordinator of an international NATO CLG-Grant project on Nonlinear Dynamics of Shells with Fluid Structure Interaction and was the local coordinator of an Italian project on Shells Vibrations.

His research activity regards also industrial problems, he cooperated for research and consultancies with several companies about: vehicle stability; experimental vibrations; clutch instabilities and failures.

He was reviewer for the following international journals: SIAM Journal of Applied Mathematics, Nonlinear Dynamics, ASME Journal of Vibration and Acoustics, J. of Solids and Structures; J. of Sound and Vibration, Computer Methods in applied Mechanics and Engineering, Int. J. of Systems Science; and reviewer for the foundations: FCAR (Fonds pour la Formation de Chercheurs et l' Aide à la Recherche) Québec, CANADA; Natural Science and Engineering Research Council of Canada.

He is in the international advisory editorial board of the journal: *Communications in Nonlinear Science and Numerical Simulation, Elsevier.*

He published a Book, more than 30 Journal papers and more than 50 conference papers.

Yuichi Sato
Saitama University

I received my B. E., M. E., and D. E. in Mechanical Engineering from Tokyo Institute of Technology in 1973, 1975, and 1978, respectively. In those days, my research topics were concerned with dynamic characteristic of fluid lubricated bearings, such as unstable phenomena called oil-whirl, whirl onset and pneumatic hammer in a gas bearing.

After my D. E. graduation I worked for Toshiba Corporation for some years. Then I got a position at Saitama University as an associate professor and became a full professor in 1994. My interests gradually shifted to vibrations coupled with structures and fluid, especially self-excited vibrations. Now I study the oscillation of a falling water sheet flowing over a dam and friction induced vibration of a long flexible shaft.

Wolfgang Seemann

Wolfgang Seemann studied mechanical engineering at the University of Karlsruhe from 1980 to 1985. After civil service he got a PhD also from the University of Karlsruhe, with a thesis on ‘Wave propagation in rotating or prestressed cylinders’ in 1991. In 1992 he left Karlsruhe to join the group of Prof. Peter Hagedorn to work as a postdoc. In 1998 he was appointed as Professor of Machine Dynamics at the University of Kaiserslautern. In 2003 he was appointed as professor in the Institute of Applied Mechanics of the University of Karlsruhe.

Anand V. Singh
The University of Western Ontario

Anand graduated in 1968 with B. Sc. Eng. (First Class with Distinction) in Mechanical Engineering from Bihar Institute of Technology Sindri, India. He then came to Canada and completed M.A.SC (1971) and Ph.D.(1975) degrees from the University of Ottawa. After working with the Department of National Defence of Canada as a Defence Scientist and later with Ontario Hydro as a Design Engineer, he joined the University of Western Ontario in December 1984 as an assistant professor. Currently, he is a professor in the Department of Mechanical and Materials Engineering. Over the years he has taught: Dynamics, Kinematics and Dynamics of Machinery, Machine Component Design, Mechanical Vibrations, Modern Control Theory, Finite Element Methods, Theory of Plates and Shells.

Research work during the period of his graduate studies dealt with the free vibration analysis of sandwich spherical shell using classical closed form solution methods. Solutions were obtained in terms of the Legendre Polynomials of complex and real orders. He continued working in the area of vibrations of plates and shells, but switched to numerical methods such as, the Rayleigh-Ritz and finite element methods. Now he is totally involved with the field of computational solid mechanics including plates and shells. His research activities include random vibrations, geometrically nonlinear analysis, laminated and sandwich constructions, embedded piezo-electric materials, and visco-elastic materials.

Anand is married to Bimla and together they have two children, Bidhi (son) and Shikha (daughter), who are now independent and currently reside in Michigan, USA. Bimla and Anand like to work in the garden, construct structures in the back yard, go for a walk, travel and enjoy life to the fullest. Currently, he is in the middle of renovating the basement that involves building a bath from scratch, framing walls and ceiling, dry-walling, and other physically rigorous jobs under her supervision.

Gottfried Spelsberg-Korspeter
Technische Universität Darmstadt

On August 13th 1978 I was born in Dortmund Germany.

I grew up in Dortmund, Düsseldorf and Ludwigsburg where I finished high-school (Abitur) in 1998. After completion of the compulsory military service I started studying at TU Darmstadt in 1999.

In 2001 I finished my preliminary diploma in industrial engineering and in mechanical engineering and decided to pursue my mechanical interests in the applied mechanics department with main focus on dynamics. Taking part in an exchange program of the industrial engineering department I spend the fall semester 2002 and the spring semester 2003 at the University of Illinois at Urbana Champaign where I mainly worked in the area of operations research.

In 2004 I finished my masters degree in applied mechanics with a thesis related to mechanical modelling of ultrasonic motors and went back to the University of Illinois to write my master thesis in industrial engineering again in the area of operations research. After completion I joined the research group of Professor Hagedorn in January 2005. The topic of my Ph.D. dissertation is about self excited vibrations in gyroscopic systems.

My hobbies are hiking, climbing and other sports.

Biographical sketch

Jörg Wauer

I am a Professor of Technical Mechanics at the University of Karlsruhe, Germany, in the Department of Mechanical Engineering, holding this position since 1977. I apprenticed as a mechanic and studied mechanical engineering at the Engineering College of Kaiserslautern and the University of Karlsruhe. I received my Ing.-Grad. and Dipl.-Ing degree in 1964 from the Engineering College of Kaiserslautern and in 1969 from the University of Karlsruhe, respectively. At the University of Karlsruhe, I was promoted to Dr.-Ing. in 1972 and Docent habil. in 1976. My industrial experience includes positions as a mechanic specialist and design engineer.

Structural dynamics and dynamics of machines are my principal research interests but during the last fifteen years, I extended this work to multi-field problems as dynamic fluid-structure interaction or vibrations of thermo-elastic and piezoelectric solids. I have authored or co-authored approximately 150 scientific papers concerning the mentioned topics, and I am a co-author of a book on mathematical methods in engineering mechanics. Together with my colleague W. Seemann, in 2005 we lectorated the translation of the 3-volume book “Engineering Mechanics” by Hibbeler into German with significant adaptations and enlargements.

Teaching is the other part of my activities at the university. I gave courses in all undergraduate mechanics topics, and I taught and I am still teaching many advanced mechanics courses for graduate students as structural dynamics, dynamics of machines, measurement of mechanical vibrations, mathematical methods in engineering vibrations, stability of elastic structural members, and presently, dynamics of mechatronic systems.

As the principal adviser, I promoted sixteen students to their Dr.-Ing. degree and two of them also to his habilitation. I am a member of GAMM and EUROMECH, I am active in several committees and work as a reviewer for several mechanics journals. In 2004 I received an honorary doctor degree from the Technical University of Sofia, Bulgaria.

Besides all these scientific activities, from 1994 until 2002, I held an important position in administration of my faculty at the University of Karlsruhe: I was the so-called Studiendekan responsible for all our actual reform work in the curriculum of the study of Mechanical Engineering at the University of Karlsruhe. In addition, from 1999 until 2001, I chaired one of the University councils in Karlsruhe. Since 2000, I am a member of a nationwide committee for accrediting of Bachelor’s and Master’s studies in Engineering Sciences.

May 2007